Non-ionotropic NMDA receptor signaling in
structural plasticity of dendritic spines and schizophrenia

By

DEBORAH K. PARK
DISSERTATION

Submitted in partial satisfaction of the requirements for the degree of

DOCTOR OF PHILOSOPHY

in

Pharmacology and Toxicology

in the

OFFICE OF GRADUATE STUDIES

of the

UNIVERSITY OF CALIFORNIA

DAVIS

Approved:

Dr. Karen Zito, Chair

Dr. Johannes Hell

Dr. John Gray

Dr. Jie Zheng

Committee in Charge

2021

Abstract

The crucial ability to remember and learn from past experiences depends on dynamic rewiring of neural circuitry in response to environmental stimuli. This reshaping of synaptic connectivity occurs through a combination of strengthening and weakening of structural units on neuronal branches called dendritic spines where majority of excitatory connections occur. Long-term potentiation (LTP) of synapses allow for strengthening and growth of dendritic spines, whereas long-term depression (LTD) of synapse instead lead to weakening and shrinkage of spines. The molecular signaling pathway that mediates both LTP and LTD associated changes of spine volume is initiated through the activation of *N*-methyl-D-aspartate receptors (NMDARs). Ion flux through the receptor pore is a crucial factor for induction of LTP and spine growth, whereas emerging studies point to an ion flux-independent signaling of NMDARs in mediating LTD and spine shrinkage. Driven by glutamate binding to the receptor, non-ionotropic NMDAR signaling involves conformational change of the receptor that then requires the activity of p38 MAPK to drive synaptic weakening and shrinkage.

Because non-ionotropic NMDAR signaling is activated through glutamate binding to the receptor and results in shrinkage and elimination of dendritic spines, this function of NMDARs may play a role in the development of schizophrenia. Associated with decreased spine density, reduced levels of D-serine, and disinhibition of excitatory synapses, increased binding of glutamate alone would likely activate non-ionotropic NMDAR signaling to promote shrinkage and loss of dendritic spines. Thus, investigation of the molecular pathway of non-ionotropic NMDAR signaling would not only help elucidate the mechanism that drives learning and memory formation, but could also further our understanding of how brain disorders develop.

Chapter 1 will be a review of our current understanding of the non-ionotropic NMDAR signaling pathway and its role in structural plasticity of dendritic spines, as well as other processes such as excitotoxicity and endocytosis of NMDARs. As non-ionotropic NMDAR

signaling is activated by glutamate binding, **Chapter 2** will detail published work in which we identify ion flux-independent signaling of NMDARs to be a crucial part for the induction of LTP associated spine growth. **Chapter 3** explores the potential role of non-ionotropic NMDAR signaling in reduced spine density associated with schizophrenia. Here I detail experiments using serine racemase knockout (SRKO) mice to observe changes in structural plasticity of spines and enhanced non-ionotropic NMDAR activation. **Chapter 4** will be a reflection on my scientific contribution to the field of structural plasticity, non-ionotropic NMDAR signaling, and schizophrenia. Lastly, the **Appendix** describes experiments in which a molecule required for non-ionotropic NMDAR signaling is identified, as well as a closer look to if and how dendritic spines or biochemical modifications and interactions are altered in SRKO mice.

Acknowledgements

The journey in completing a Ph.D. would not have been accomplished without the guidance and support of many individuals.

First and foremost, I am thankful for my graduate advisor, Dr. Karen Zito for taking me on as her student and providing valuable mentoring throughout the years. Dr. Zito has always been enthusiastic in her approach to scientific research and constantly encouraged critical thinking and thorough analysis and understanding of both my thesis experiments and the techniques utilized for my studies. I am grateful for her efforts in allowing me to have a productive PhD journey and helping me become an independent scientist.

I would also like to thank my thesis committee members. Drs. Johannes Hell, John Gray, and Jie Zheng, have all provided support, encouragement, and great advice on my thesis work that were critical in the development and troubleshooting various experiments.

I am also thankful of the other members of the Zito lab. I want to thank Julie Culp, Jennifer Jahncke, and Lorenzo Tom for their help with slice cultures. I am especially grateful of Dr. Ivar Stein for the immense amount of technical support and scientific discussions. Other members of the Zito lab have also provided constant moral support and humor that have brightened my days.

Finally, I want to thank my family for the overwhelming amount and much needed support, patience, and encouragement throughout the whole journey.

Table of Contents

Chapter 1: Diverse roles of non-ionotropic NMDAR signaling in the nervous system

Introduction:

The innate ability to form memories allows us to learn from past experiences and is invaluable for survival of many organisms. This crucial process involves dynamic rewiring of neural circuitry that is achieved through both short-term and long-lasting modifications of synaptic connections between neurons. As the majority of excitatory synaptic connections occurring on small protrusions of neuronal branches called dendritic spines, activity or experience-dependent modification integral for memory development can be readily studied by observing both functional and structural changes in spines.

Although a majority of dendritic spines are stable, both new spine outgrowth and elimination of spines in the mammalian cortex occur in response to new experience (Holtmaat et al 2005, Trachtenberg et al 2002), the dynamics of which are crucial for memory formation (Hayashi-Takagi et al 2015, Li et al 2017, Xu et al 2009, Yang et al 2009). Activity-dependent changes that result in new spine outgrowth, stabilization, and enlargement also lead to a functional increase in synaptic strength, or long-term potentiation (LTP) (Hill & Zito 2013, Kwon & Sabatini 2011, Matsuzaki et al 2004). In contrast, spine shrinkage and elimination are associated with decrease in synaptic strength, or long-term depression (LTD) (Oh et al 2013, Zhou et al 2004).

The ability of dendritic spines to change its structure and synaptic strength involves the modification of F-actin dynamics of the spine cytoskeleton that has the dual role of acting as a scaffold and providing structural support for the spine itself (Honkura et al 2008, Nakahata & Yasuda 2018). Actin modifying proteins such as Arp2/3 and cofilin that mediate F-actin assembly or breakdown are downstream of signaling pathways such as small GTPases and CaMKII that control its activity. These signaling cascades have been observed to be activated

by Ca^{2+} influx through a type of glutamate receptor called N-methyl-D-aspartate receptor (NMDAR) present on the surface of dendritic spines.

NMDARs are tetrameric channels that, upon the binding of glutamate and co-agonist, are permeable to Na^+, K^+, and Ca^{2+} ions when the magnesium block of the receptor pore is relieved with depolarization. Being one of the main sources of Ca^{2+} influx into dendritic spines, NMDARs are important for triggering calcium dependent signaling pathway critical for synaptic plasticity. Strong Ca^{2+} influx through the NMDAR activates kinases such as CaMKII that are required for the insertion of α-amino-3-hydroxy-5-methyl-4-isoxazolepropionic acid receptors (AMPARs) and spine growth associated with LTP (Nakahata & Yasuda 2018). Weak Ca^{2+} influx through the NMDAR is widely accepted to instead activate phosphatases such as PP1 that results in LTD through endocytosis of AMPARs and shrinkage of spines.

Within the hippocampus, NMDAR are composed of two obligatory GluN1 subunits and two subunits that are either GluN2A, GluN2B, or a combination of both, depending on the developmental period and location within a dendritic spine (Paoletti et al 2013). Each NMDAR subunit has a long intracellular C-terminal tail that can be modified and interact with various molecules that are essential for synaptic targeting and mediating NMDAR-dependent processes such as excitotoxicity. Ca^{2+} influx through the receptor pore, although crucial, is not the sole function of several NMDAR-mediated processes; a growing number of studies that suggest NMDARs have an ion flux-independent role, potentially through conformational changes and interactions at the C-terminal tail. Specifically, studies have shown that non-ionotropic NMDAR signaling is critical for the induction of LTD and spine shrinkage (Nabavi et al 2013, Stein et al 2015), which goes against the dogma that synaptic weakening and shrinkage is mediated by weak NMDAR-mediated Ca^{2+} influx (Volianskis et al 2015). Not much is known about this novel, ion flux-independent signaling of NMDARs that mediates LTD and associated spine shrinkage and, as discussed in the later sections, other processes such as excitotoxicity and Alzheimer's disease. Investigation delineating the key players of the non-ionotropic signaling pathway

required for spine shrinkage (Stein et al 2020) is partly discussed in the Appendix. A novel discovery that non-ionotropic NMDAR signaling is also crucial for LTP-associated spine growth is discussed in Chapter 2 and Appendix. Lastly, the possible contribution of non-ionotropic signaling in loss of dendritic spines associated with schizophrenia is addressed in Chapter 3.

Non-ionotropic NMDAR signaling mediates LTD:

In contradiction to the long-accepted model that NMDAR-mediated Ca^{2+} influx is an essential component of synaptic plasticity, LTD can occur independently of ion flux through the receptor pore (Carter & Jahr 2016, Nabavi et al 2013, Stein et al 2015, Wong & Gray 2018). NMDAR inhibitors such as co-agonist blocker 7CK or channel pore blocker MK-801 that allow for glutamate binding while obstructing ion flux through the pore fails to prevent LTD. The only pharmacological manipulation observed to block LTD is the glutamate antagonist APV, indicating that LTD is activated through glutamate binding and that Ca^{2+} influx through the receptor pore is not required. Further highlighting the requisite for only glutamate binding is that high frequency stimulations that normally induce LTP can instead be 'converted' into LTD by blocking ion flux during glutamate binding to the NMDAR (Nabavi et al 2013, Stein et al 2020).

Despite the differences between GluN2A and GluN2B in their expression time, synaptic location, protein modifications, and interactions at the C-tail (Paoletti et al 2013), there seems to be some common factor between the two GluN2 subunits that allows for LTD to occur upon agonist binding, as there is no subunit specificity for this ion flux-independent synaptic plasticity (Wong & Gray 2018). Downstream of glutamate binding, p38 MAPK has been shown to increase in activity and also be required for LTD (Nabavi et al 2013, Stein et al 2020), demonstrating that there is activation of an intracellular signaling pathway in an ion flux independent manner. Although Ca^{2+} influx may not be required, basal level of intracellular calcium is critical to maintain AMPAR-mediated neurotransmission via basal level of calcineurin activity restricting insertion of AMPARs to the synapse (Nabavi et al 2013).

Although other ion channels such as AMPARs (Bai et al 2002, Hayashi et al 1999, Wang et al 1997) and voltage-gated calcium channels (VGCCs) (Li et al 2016a) have also been observed to have non-ionotropic mechanisms, there is still scrutiny as to whether induction of NMDAR-LTD is truly independent of Ca^{2+} influx (Babiec et al 2014, Sanderson et al 2016, Volianskis et al 2015). Namely, there are concerns of calcium leak through the NMDAR being sufficient to mediate LTD. Indeed, intracellular application of MK801 does not completely block the receptor pore (Sun et al 2018), but co-agonist blockers such as 7CK or L689 that have been used in non-ionotropic studies do not allow for any detectable level of ion flux while still allowing for LTD (Nabavi et al 2013, Stein et al 2015, Wong & Gray 2018). Additionally, alternate sources of calcium such mGluR5s or VGCCs have also been demonstrated to not play a role in non-ionotropic NMDAR-LTD (Nabavi et al 2013, Stein et al 2020).

Non-ionotropic NMDAR signaling involves conformational change of the receptor:

If the binding of agonist to the NMDAR allows for activation p38 MAPK in an ion flux independent manner (Nabavi et al 2013), there must be some conformational change of the receptor, as seen in VGCCs (Li et al 2016a), that serves to activate the intracellular signaling pathway. Based on findings that suggest ligand binding to NMDAR induces a conformational state that precedes the opening of the receptor pore for ion flux (Durham et al 2020, Gibb et al 2018, Kazi et al 2013), this intermediate conformational state of the receptor may be essential for initiating non-ionotropic signaling. The use of FRET biosensors of NMDARs suggest that agonist binding to the GluN2 subunit causes GluN1 C-tails to move away from each other (Aow et al 2015, Dore et al 2015, Ferreira et al 2017), a particular conformational change that is independent of receptor pore opening (Dore et al 2015) and necessary for non-ionotropic LTD (Aow et al 2015). Agonist-binding driven conformational change also causes the GluN1 C-tail to move away from both PP1 and CaMKII, and, interestingly, the movement between the GluN1 C-tail and CaMKII is driven by PP1 activity and delayed by several minutes following ligand

binding (Aow et al 2015). It is unclear whether the relative movements between the GluN1 C-tails and PP1 and CaMKII are critical for non-ionotropic NMDAR signaling, but does provide insight as to what may be occurring near the NMDAR C-tail during non-ionotropic activation.

Non-ionotropic NMDAR activation also mediates spine shrinkage:

As decrease in synaptic strength occurs concurrently with structural decrease in spine volume (Oh et al 2013, Zhou et al 2004), non-ionotropic NMDAR signaling was also observed to induce shrinkage of stimulated dendritic spines (Stein et al 2015, Stein et al 2020, Thomazeau et al 2020). In addition to the increase in activity and requirement of p38 MAPK for non-ionotropic NMDAR-LTD and spine shrinkage, the signaling pathway for spine shrinkage has been further revealed to require the activity of neuronal nitric oxide synthase (nNOS) (Stein et al 2020), which sits close to NMDAR through its interaction to PSD-95 (Li et al 2013). NMDAR-nNOS signaling is mediated through the active recruitment of adaptor protein NOS1AP to nNOS (Li et al 2013, Zhu et al 2014), the interaction of which is also critical for non-ionotropic spine shrinkage (Stein et al 2020). Through its interaction to nNOS, NOS1AP can recruit certain substrates like p38 MAPK close to nNOS for modification (Li et al 2013) and potentially acts as a link between the two components of non-ionotropic signaling that was previously identified – NMDAR activation and p38 MAPK activity. Downstream target of p38 MAPK, MK2, and actin depolymerizing protein, cofilin, were also demonstrated to be essential players of non-ionotropic NMDAR-dependent spine shrinkage (Stein et al 2020). CaMKII, which has been well observed in LTP, spine growth, and LTD (Coultrap et al 2014, Halt et al 2012, Lee et al 2009) was also observed to be required for non-ionotropic NMDAR-dependent spine shrinkage. While the proposed model for spine shrinkage suggests a relatively linear signaling pathway starting from nNOS down to cofilin, it is unclear as to whether the role of CaMKII is upstream near the NMDAR (Aow et al 2015) or downstream at the actin cytoskeleton (Kim et al 2015). Additionally, mTORC1 activity, which is important for protein synthesis, is required for non-ionotropic spine

shrinkage, though it is not yet clear if it is directly downstream of any of the other identified signaling molecules of the non-ionotropic pathway for spine shrinkage (Thomazeau et al 2020). As functional and structural changes of synaptic plasticity generally occur together (Oh et al 2013, Zhou et al 2004), it poses a question as to whether LTD and spine shrinkage are, for the most part, mediated through the same non-ionotropic signaling pathway and if spine shrinkage can also occur independent of NMDAR subunit composition (Wong & Gray 2018).

Non-ionotropic NMDAR activation is required for spine growth:

Although non-ionotropic NMDAR activation leads to LTD and spine shrinkage, it shares a common factor with LTP and spine growth in that they also require glutamate binding to the receptor. This leads to a question as to what the role of non-ionotropic NMDAR signaling is during induction of LTP and associated spine growth **(Fig. 1A)**. The results of the investigation that probes the importance of non-ionotropic NMDAR signaling in spine growth will be discussed in Chapter 2.

Outside of glutamate binding induced conformational signaling, the binding of co-agonist to the NMDAR has also been observed to affect synaptic strength. Particularly, glycine binding to GluN2A containing NMDAR complexes increases AMPAR strength through ERK1/2 activation in an ion flux-independent manner (Li et al 2016b), although It is not yet determined if ERK1/2 fits within the identified non-ionotropic NMDAR signaling pathway for AMPAR potentiation after it branches out somewhere between nNOS and p38 MAPK **(Fig. 1B, C)**.

Non-ionotropic NMDAR signaling regulates spontaneous glutamate release:

The effects of non-ionotropic NMDAR signaling is not limited to just the postsynaptic terminal, as there are also reports of spontaneous release of glutamate being mediated in an ion flux-independent mechanism. One study demonstrated that ligand binding to NMDAR activates Src kinase and ion channel pannexin-1, which have previously been demonstrated to

form a complex with the NMDAR (Bialecki et al 2020, Weilinger et al 2016). The opening of pannexin-1 controls the extracellular levels of AEA, an endogenous ligand for presynaptically located TRPV1 channels that regulate the spontaneous release of glutamate (**Fig.1C**) (Bialecki et al 2020). This type of trans-synaptic signaling has been proposed to be a homeostatic mechanism in which decreased spontaneous release of glutamate is corrected when reduced non-ionotropic NMDAR signaling at the postsynaptic terminal ultimately increases the frequency of spontaneous release by indirectly increasing presynaptic TRPV1-mediated Ca^{2+} influx. In contrast to this finding, which is specific to synapses that express presynaptic TRPV1, another study demonstrated that glycine binding to GluN2A increases the frequency of mEPSCs in an ion flux-independent manner (**Fig. 1C**) (Li et al 2016b).

Presynaptic NMDARs have also been observed to mediate spontaneous release of glutamate in layer 5 pyramidal cells of the visual cortex in an ion flux-independent manner, although not much is known about how this particular signaling pathway (Abrahamsson et al 2017). These few studies on the presynaptic terminal bring attention to the fact that non-ionotropic NMDAR signaling is not limited to the postsynaptic sites, or dendritic spines, and the molecular mechanism may vary widely across different types of synapses.

Role of non-ionotropic NMDAR signaling in excitotoxicity and Alzheimer's disease:

In addition to its role in spontaneous neurotransmitter release and activity-dependent changes of the dendritic spine, non-ionotropic NMDAR signaling has also been observed to play role in excitotoxicity. In the context of sustained release of glutamate that occurs with transient cerebral ischemia, ligand binding to the NMDAR activates a non-ionotropic signaling pathway that involves opening of intracellular calcium stores that leads to phosphorylation of eEF-2 that then inhibits protein synthesis (**Fig. 2A**) (Gauchy et al 2002). Interestingly, calcium release from the endoplasmic reticulum plays a role in the inhibition of protein synthesis, whereas calcium

release from the mitochondria does not, which suggests a possible calcium nanodomain requirement for the non-ionotropic NMDAR-mediated inhibition of protein synthesis.

Another study demonstrated that both agonist and co-agonist binding to the NMDAR triggers a non-ionotropic signaling pathway in which Src kinase is activated and promotes pannexin1-mediated Ca^{2+} influx (**Fig. 2A**) (Weilinger et al 2016). Ca^{2+} influx through pannexin1, but not through NMDAR, is required for mitochondrial dysfunction and cell death, suggesting that this non-ionotropic NMDAR pathway for excitotoxicity also depends on the calcium nanodomain of pannexin1 despite the close association between NMDAR, Src, and pannexin1. As Src is specifically known to bind to NMDAR indirectly through NADH dehydrogenase 2, conformational change of the NMDAR may be sufficient to bring Src kinase in close proximity of Y308 on C-tail of pannexin1 for modification that is essential for cell death.

In addition to inhibition of protein synthesis and calcium dysregulation, non-ionotropic NMDAR signaling is also required for NOX2-mediated superoxide production (Minnella et al 2018). Triggered by glutamate binding alone, the regulatory subunit for PI3K, p85, interacts with the GluN2B C-tail (**Fig. 2A**). This change in interaction allows for activated PI3K to play a role in NOX2-mediated superoxide production that leads to cell death. Although Ca^{2+} influx, in conjunction with PI3K activity, is still required for NOX2-mediated superoxide production, there is no specific requirement for where the calcium comes from. Based on the different ligand binding and calcium nanodomain requirements, it is difficult to say if inhibition of protein synthesis, mitochondrial dysfunction, and superoxide production all occur simultaneously NMDAR activation.

Non-ionotropic NMDAR signaling is also implicated in Alzheimer's disease as it mediates amyloid beta-induced synaptic depression (Kessels et al 2013, Tamburri et al 2013) and spine loss (**Fig. 2B**) (Birnbaum et al 2015). As the effects of amyloid beta depend on the glutamate binding site of the NMDAR and is mediated by p38 MAPK, there is a possibility that there is at least some overlap in the signaling cascade that mediates non-ionotropic NMDAR synaptic

plasticity (**Fig. 1A, B**) and Alzheimer's disease (**Fig. 2B**) (Birnbaum et al 2015, Dore et al 2015, Kessels et al 2013, Stein et al 2015, Stein et al 2020, Tamburri et al 2013). One difference, however, between non-ionotropic mechanisms of LTD and amyloid beta induced synaptic depression is that the former does not have subunit specificity (Wong & Gray 2018) while the latter is specific to the GluN2B subunit containing complexes (Kessels et al 2013, Tamburri et al 2013). In addition to inducing synaptic dysfunction, amyloid beta has been observed to activate ion-flux independent metaplasticity of the NMDARs where GluN2Bs subunit containing complexes are switched out for those with GluN2A (Kessels et al 2013). As the subunit switch from GluN2B to GluN2A during development can be mediated by D-serine binding, which induces a different conformational change of the NMDAR than when glutamate binds (Ferreira et al 2017), it would be informative as to what type of conformational change amyloid binding induces to mediate both LTD, spine shrinkage, and NMDAR subunit switch.

Non-ionotropic NMDAR signaling from co-agonist binding:

As glutamate binding alone to the NMDAR has been shown to modulate synapses independently of ion flux through the receptor, it does not seem surprising that co-agonist binding also activates its own non-ionotropic signaling pathway. In one of the earliest studies demonstrating non-ionotropic NMDAR signaling, it was shown that NMDAR activation leads to dephosphorylation of Y842 on GluN2A subunits, independent of ion flux through the receptor (**Fig. 2C**) (Vissel et al 2001). This modification negatively affects Src interaction, but not AP2, and results in use-dependent downregulation of NMDARs via dynamin-mediated endocytosis. This signaling pathway for priming the NMDAR for internalization may be due to co-agonist binding to the receptor, as another study has shown that co-agonist binding alone primes the NMDAR for use-dependent endocytosis that involves clathrin and dynamin (Nong et al 2003). The binding of co-agonist to the A714 residue of the obligatory GluN1 subunit results in recruitment of adaptin β2 subunit of AP2 to the NMDAR (Han et al 2013). Additionally, as co-

agonist binding to GluN2A subunit has been demonstrated to activate Akt in an ion flux-independent manner to promote cell survival (**Fig. 1C**) (Chen et al 2017, Hu et al 2016), it is possible that these non-ionotropic effects of co-agonist binding to NMDAR all work together as a neuroprotective mechanism by simultaneous activating a signaling cascade for cell survival while promoting endocytosis of NMDARs to prevent over-activation of the receptor that could result in excitotoxicity (**Fig. 2A**).

Further demonstration of non-ionotropic NMDAR activation that depends on the co-agonist binding site of NMDARs is NYX-2925. A partial agonist to the glycine-binding site, NYX-2925 has a dose-dependent effect in non-ionotropic NMDAR activation (Bowers et al 2020). Picomolar concentration of NYX-2925 in the presence of glutamate increases synaptic enrichment of GluN2B via a non-ionotropic NMDAR signaling pathway that involves inhibition of endocytosis, EIF2, mTOR, and PKA. Interestingly, increasing the concentration of NYX-2925 to nanomolar range instead activates EIF2, mTOR, and PKA, resulting in enhancement of LTP and endocytosis (Bowers et al 2020, Khan et al 2018).

These non-ionotropic NMDAR signaling pathways specific to co-agonist binding is likely due to the different conformational states of the receptor that are unique from glutamate binding (Dore et al 2015, Ferreira et al 2017). While glutamate binding causes the GluN1 C-tails to move away from each other, D-serine causes an opposite effect in which the C-tails instead move closer (Ferreira et al 2017). Interestingly, glycine binding does not cause any noticeable movement of the GluN1 C-tails, although it may be that there is no net difference in the distance between the GluN1 C-tails or that the conformational state instead involves movement of the GluN2 C-tails. As glycine binding to GluN2A has been observed to increase AMPAR strength and frequency of glutamate release through non-ionotropic activation of ERK1/2 (Li et al 2016b), it warrants further investigation as to whether the different conformational changes of NMDARs between glycine and D-serine binding activate different non-ionotropic signaling pathways.

Non-ionotropic NMDAR activation in non-neuronal cells:

Non-ionotropic NMDAR signaling is not limited to neurons, as astrocytes have been observed to contain functional NMDARs that activates tyrosine kinases in an ion flux-independent manner for opening of intracellular calcium stores (Montes de Oca Balderas & Aguilera 2015, Montes de Oca Balderas et al 2020). This particular mechanism is activated by H^+, which implicates a potential role of acidic conditions in eliciting a similar non-ionotropic NMDAR signaling pathway in other cell types.

Outside of synapses, endothelial cells that make up the blood-brain barrier have also been reported to have non-ionotropic NMDAR signaling. Tissue plasminogen activator (tPA) interacts with GluN1 NTD to affect surface dynamics of neuronal extrasynaptic NMDARs (Lesept et al 2016). tPA with either agonist or co-agonist activates non-ionotropic NMDAR signaling of ROCK-mediated phosphorylation of MLC to increase permeability of the blood brain barrier (Mehra et al 2020).

Controversy of non-ionotropic NMDAR signaling:

Despite multiple independent observations of non-ionotropic NMDAR signaling in various types of cells and processes, the finding that an ionotropic glutamate receptor can signal in an ion flux-independent manner is still controversial. In particular, studies on non-ionotropic NMDAR signaling have contradicted the long-accepted dogma of Ca^{2+} influx mediating LTD and spine shrinkage, while other studies directly argue that LTD depends on calcium flux (Babiec et al 2014, Sanderson et al 2016, Volianskis et al 2015). Although the main reason for such discrepancy between various studies is still unclear, there are a couple potential variables that are worthwhile addressing. It has been proposed that higher expression of PSD95 observed in older animals blocks non-ionotropic NMDAR-LTD by obstructing the critical glutamate-binding induced conformational change of the GluN1 C-tails, but not ionotropic NMDAR-LTD (Dore & Malinow 2020), which could why explain non-ionotropic NMDAR-LTD

cannot be observed in older mice (Babiec et al 2014). However, if there needs to be a sufficient amount of PSD95 for specific substrates like nNOS to be in close proximity to the NMDAR, low PSD95 expression early in development (Dore & Malinow 2020) could explain the lack of non-ionotropic NMDAR-LTD in very young animals (Sanderson et al 2016). Additionally, other discrepancies that may contribute to the lack of non-ionotropic NMDAR-LTD in other studies is the use of a different chemical LTD treatment (Babiec et al 2014, Thomazeau et al 2020), lower concentrations of MK-801 and picrotoxin (Babiec et al 2014, Sanderson et al 2016, Thomazeau et al 2020), and washout of MK-801 after LFS (Babiec et al 2014). Further investigations are warranted to unravel this discrepancy between studies, and the findings could help better understand the physiological conditions in which non-ionotropic NMDAR signaling occurs.

Schizophrenia

In addition to its potential role in mediating synaptic changes associated with Alzheimer's disease, non-ionotropic NMDAR signaling could also be implicated in schizophrenia as well. Schizophrenia affects 1% of the world population and manifests a host of symptoms in early adulthood that include hallucinations and cognitive deficit (Penzes et al 2011). These debilitating symptoms are likely due to neuroanatomical changes that are observed with schizophrenia, as imaging studies reveal decreased spine density (Garey et al 1998, Glantz & Lewis 2000, Konopaske et al 2014, Rosoklija et al 2000, Sweet et al 2009) and brain volume (Cahn et al 2009, Haijma et al 2013, Takayanagi et al 2011, van Erp et al 2016, van Haren et al 2008, Zhang et al 2015) in various structures such as the hippocampus or the prefrontal cortex that relates to the specific neurological deficits of the disorder.

Based on clinical and preclinical studies on schizophrenia and mouse models of the disease that will be discussed below, the observed loss of synaptic connections associated with the disorder may be due to enhanced non-ionotropic NMDAR signaling.

Potential role of altered NMDAR signaling in the development schizophrenia:

Clinical studies have shown that NMDAR antagonists such as PCP and ketamine produce a variety of symptoms characteristic to schizophrenia in healthy patients while exacerbating symptoms specific to the individual for those with the disorder (Javitt & Zukin 1991, Krystal et al 1994, Lahti et al 2001, Newcomer et al 1999). Further highlighting the potential role of altered NMDAR function in schizophrenia are adjunctive therapies that increases NMDAR co-agonist binding improved various symptoms in patients better than dopamine-targeting anti-psychotics alone (Heresco-Levy et al 2005, Lane et al 2010, Singh & Singh 2011, Tsai et al 1998).

Dysfunctional NMDAR signaling may be due to decreased levels of D-serine as observed in CSF (Bendikov et al 2007, Hashimoto et al 2005) and serum (Calcia et al 2012, El-Tallawy et al 2017, Hashimoto et al 2003a) of patients with schizophrenia. This is potentially a consequence of both decreased expression of D-serine producing enzyme, serine racemase, and increased expression of catabolizing enzyme, D-amino acid oxidase (Bendikov et al 2007, Burnet et al 2008, El-Tallawy et al 2017, Madeira et al 2008, Verrall et al 2007). As schizophrenia is also associated with increased levels of kynurenic acid, an endogenous NMDAR co-agonist blocker (Plitman et al 2017), decreased bioavailability and increased antagonistic effect against co-agonist binding would work together towards altering NMDAR function.

Variety of studies that mimic NMDAR hypofunction in animals through either chronic drug treatment or genetic manipulation add further weight to the potential role of this glutamate receptor in the development of schizophrenia. For example, chronic treatment of uncompetitive NMDAR antagonist in rodents causes deficits in spatial learning, novel object recognition, visual attention, and decreased brain volume (Barnes et al 2014, Karasawa et al 2008, Latysheva & Raevskii 2003, Li et al 2011, Schobel et al 2013, Wu et al 2016). $Grin1^{D481N}$ KI mice in which mutation of the GluN1 subunit decreases co-agonist binding causes deficits in spatial learning (Ballard et al 2002). Decreasing NMDAR co-agonist levels by chronic treatment of serine

racemase inhibitor, phenazine methosulfate, leads to deficits in paired-pulse inhibition (PPI) (Hagiwara et al 2013). And, lastly, genetic deletion of serine racemase in mice results in severe reduction of D-serine, which then leads to increased ventricular size and glutamate levels, decreased spine density, and behavioral deficits such as impaired spatial learning and fear conditioning (Balu & Coyle 2014, Balu et al 2013, Basu et al 2009, DeVito et al 2011, Puhl et al 2015), as well as a deficit for LTP, a cellular mechanism integral for learning and memory (Hayashi-Takagi et al 2015, Hill & Zito 2013, Kwon & Sabatini 2011). All these aforementioned schizophrenia-like cognitive deficits and neuroanatomical changes can be rescued with D-serine treatment, suggesting that altered NMDAR signaling may be a major, underlying factor for the development of this debilitating psychiatric disease.

In addition to decreased co-agonist binding to the NMDARs, reduced D-serine levels may also affect inhibitory neurons. Due to its high sensitivity to NMDAR antagonists, GABAergic interneurons will have been greatly impacted in the aforementioned clinical and preclinical studies, resulting in disinhibition of excitatory neurons (Grunze et al 1996, Homayoun & Moghaddam 2007) and thus could explain the observed increase in glutamate levels in patients with schizophrenia (Gallinat et al 2016, Kraguljac et al 2013, Lorrain et al 2003, van Elst et al 2005). The combination of disinhibition of excitatory neurons and decreased NMDAR co-agonist binding creates a scenario in which glutamate is more likely to bind to the NMDAR by itself.

Enhanced non-ionotropic NMDAR signaling may contribute to spine loss associated with schizophrenia:

With all the studies demonstrating that there is increased release of glutamate and reduced levels of D-serine associated with schizophrenia, these two factors can be synergistic to create a condition in which there is a bias for non-ionotropic NMDAR signaling at glutamatergic synapses. As glutamate binding alone is sufficient to trigger non-ionotropic NMDAR signaling (Nabavi et al 2013, Stein et al 2015), excessive ion flux-independent signaling would result in

shrinkage of spines while also disrupting LTP necessary for spines growth and stabilization (Hill & Zito 2013). Over time, this bias towards spine shrinkage and destabilization due to non-ionotropic NMDAR signaling may contribute to the decrease in spine density, and subsequently cognitive deficit, observed in patients with schizophrenia.

As NMDAR activation is crucial for both growth and shrinkage of dendritic spines, there is a possibility that the decreased spine density associated with schizophrenia is either due to deficit in new spine outgrowth and stabilization or excessive shrinkage and elimination of spines; however, longitudinal studies suggest the latter. Imaging of high risk individuals who later develop psychosis shows normal development of gray matter that later declines prior to onset of symptoms, while white matter volume does not differ from healthy cohorts (Gogtay et al 2011). With little evidence of neurodegeneration in schizophrenia, the observed loss in gray matter may be due to a combination of decreased spine density, neuron size, neuropil, and number of inhibitory interneurons (Arnold 2000, Benes et al 1998, Benes et al 1991, Heckers et al 1991, Lieberman et al 2018, Moyer et al 2015, Roeske et al 2020, Zhang & Reynolds 2002). Thus, we hypothesize that enhanced non-ionotropic NMDAR signaling due to the combination of increased glutamate release and decreased D-serine levels creates a bias for spine shrinkage and elimination that then eventually culminates into spine loss that is observed with schizophrenia. This novel hypothesis of the potential role of non-ionotropic NMDAR signaling in schizophrenia will be further discussed in Chapter 3.

Figure legends and figures

Figure 1. Non-ionotropic NMDAR signaling mediates synaptic plasticity and glutamate release

(A) Glutamate binding to the NMDAR results in conformational change of the receptor in which the GluN1 C-tails move away from each other. This conformational change induces shrinkage of the dendritic spine through the interaction of nNOS-NOS1AP and activities of CaMKII, nNOS, p38 MAPK, MK2, and cofilin to modify the actin cytoskeleton. The shrinkage of dendritic spine also requires new protein synthesis through the activity of mTORC1. The actin-modifying signaling pathway is also a critical component of spine growth, but requires a simultaneous strong influx of calcium to activate calcium signaling that acts together with non-ionotropic signaling to mediate growth instead of shrinkage. **(B)** Long-term depression requires the activity of p38 MAPK. As CaMKII and nNOS have been shown to be required for both LTP and LTD, but p38 MAPK is not necessary for LTP, the signaling pathway for LTP may diverge from the non-ionotropic NMDAR signaling cascade at nNOS. **(C)** Ligand binding to postsynaptic NMDARs activates Pannexin1 channels through the activity of Src. Opening of Pannexin1 allows for clearance of AEA from the synaptic cleft that acts as a ligand for presynaptic TRPV1. With decreased binding of AEA, TRPV1 closes, reducing calcium signaling that is required for spontaneous release of glutamate. In contrast, co-agonist binding to GluN2A subunit containing postsynaptic NMDAR complexes results in activation of ERK1/2 that increases both the spontaneous release of glutamate and synaptic strength. Presynaptic NMDARs also play a role in spontaneous release of glutamate in an ion flux-independent manner, although it is not yet known how.

Figure 1

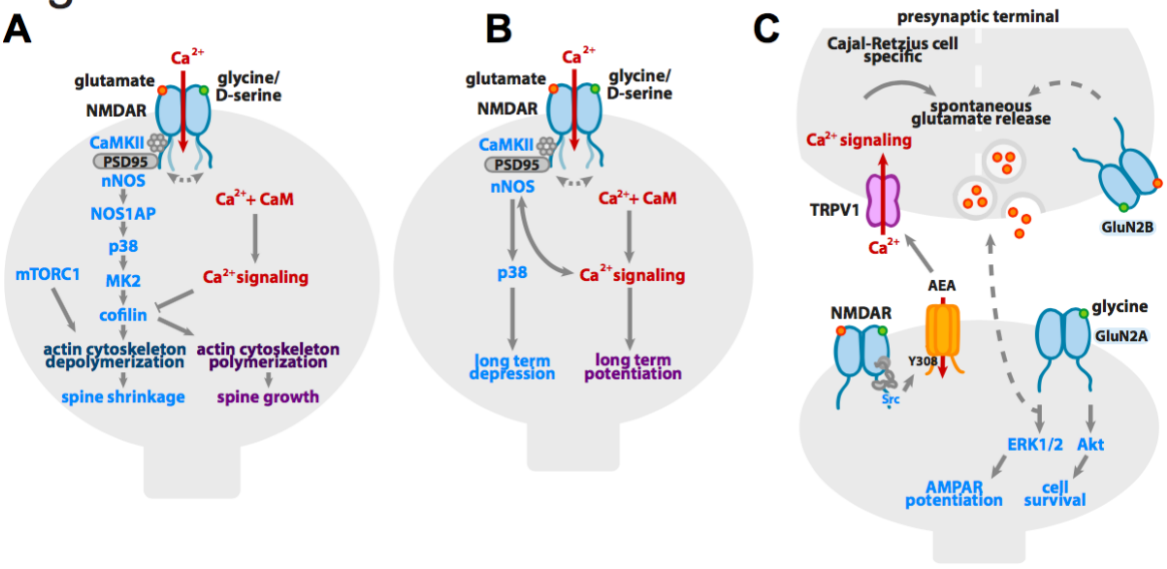
A
glutamate
glycine/
D-serine
NMDAR
Ca2+
CaMKII
PSD95
nNOS
NOS1AP
p38
MK2
mTORC1
cofilin
Ca2+ + CaM
Ca2+ signaling
actin cytoskeleton depolymerization
actin cytoskeleton polymerization
spine shrinkage
spine growth
B
glutamate
glycine/
D-serine
NMDAR
Ca2+
CaMKII
PSD95
nNOS
Ca2+ + CaM
p38
Ca2+ signaling
long term depression
long term potentiation
C
presynaptic terminal
Cajal-Retzius cell specific
spontaneous glutamate release
Ca2+ signaling
TRPV1
Ca2+
GluN2B
AEA
NMDAR
Y308
Src
glycine
GluN2A
ERK1/2
Akt
AMPAR potentiation
cell survival

Figure 2. Non-ionotropic NMDAR signaling mediates excitotoxicity and endocytosis of NMDARs

(A) Although calcium influx is a critical factor of excitotoxicity, it does not have to through NMDARs. In an ion flux-independent manner, ligand binding to the NMDAR mediates opening of intracellular calcium stores, that then results in obstruction of protein synthesis through inhibition of eEF-2. Additionally, glutamate and co-agonist binding to the NMDAR leads to activation of Src that then modifies Pannexin1 channels to open. The resulting Pannexin1-mediated Ca^{2+} influx, but not NMDAR-mediated Ca^{2+} influx, is a necessary component of mitochondrial dysfunction that then contributes to excitotoxicity. Ligand binding to GluN2B subunit containing NMDAR complexes increases binding of p85 to GluN2B C-tail, a movement that removes the PI3K regulatory domain so that PI3K can activate NOX2. PI3K activity and strong influx of calcium, which can come from any source, results in NOX2-mediated superoxide production that results in excitotoxicity. **(B)** Synaptic dysfunction that is associated with Alzheimer's disease can be mediated through non-ionotropic NMDAR signaling that is induced through amyloid binding to the receptor. Amyloid beta binding to GluN2B subunit containing NMDAR complexes results in activation of p38 MAPK and tyrosine phosphatases that results in elimination of dendritic spines and depotentiation, respectively. The peptide binding also leads to modification of the NMDARs that they bind to, as GluN2B subunit complexes are removed and replaced GluN2A subunit containing complexes. **(C)** Ligand binding to the NMDAR causes dephosphorylation of GluN2 Y842 and decreased interaction with Src that, in an ion flux-independent manner, primes the receptor for clathrin-adaptor protein AP2 mediated use-dependent endocytosis. This signaling pathway may overlap another observation of AP2, clathrin, and dynamin-dependent internalization of the NMDAR that is induced through co-agonist binding to the receptor, for which the co-agonist must bind to A714 residue of the obligatory GluN1 subunit to recruit adaptin β2 subunit of AP2 to the NMDAR.

Figure 2

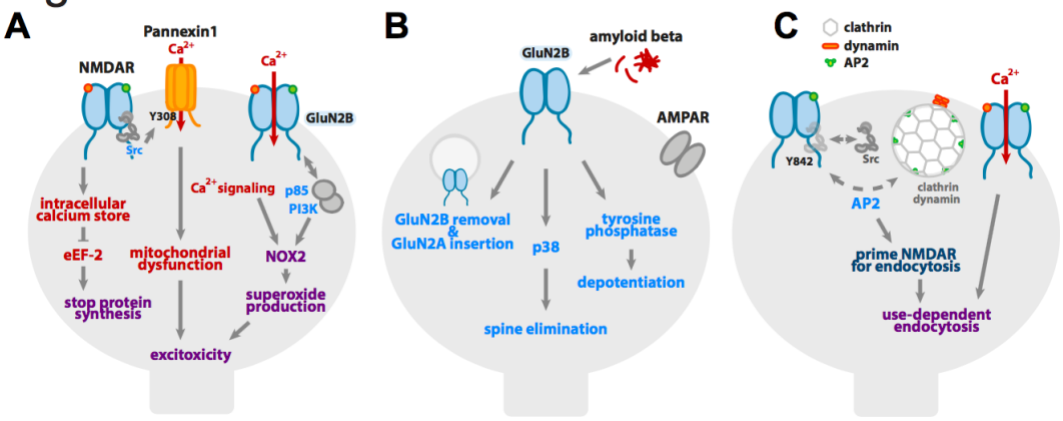
A
Pannexin1
Ca2+
NMDAR
Y308
Src
Ca2+
GluN2B
intracellular calcium store
Ca2+ signaling
p85
PI3K
eEF-2
mitochondrial dysfunction
NOX2
stop protein synthesis
superoxide production
excitoxicity
B
amyloid beta
GluN2B
AMPAR
GluN2B removal & GluN2A insertion
p38
tyrosine phosphatase
depotentiation
spine elimination
C
clathrin
dynamin
AP2
Ca2+
Y842
Src
AP2
clathrin
dynamin
prime NMDAR for endocytosis
use-dependent endocytosis

Chapter 2: Non-ionotropic NMDA receptor signaling gates bidirectional structural plasticity of dendritic spines

Preface

The following chapter was submitted as a manuscript titled “Non-ionotropic NMDA receptor signaling gates bidirectional structural plasticity of dendritic spines” to Cell Reports on August 24th, 2020 and was accepted for publication on January 26, 2021. Aside from layout changes to fit the guidelines of the thesis, the chapter is the accepted version of the manuscript. The authors of the manuscript are Ivar S. Stein, Deborah K. Park, Nicole Claiborne, and Karen Zito. Ivar S. Stein tested the role of p38 MAPK and MK2 for spine growth. Nicole Claiborne tested the role of nNOS activity in spine growth. Ivar S. Stein and I collaborated to test CaMKII inhibitor KN62, artificially drive spine growth by combining non-ionotropic NMDAR signaling with VGCC-mediated Ca^{2+} influx, test role of CaMKII in the artificial spine growth, and calcium imaging during artificial spine growth. Jennifer Jahncke and Lorenzo Tom prepared and maintained hippocampal slice cultures. Karen Zito, Ivar S. Stein, and I wrote the manuscript. All authors contributed comments on the manuscript.

Abstract

Experience-dependent refinement of neuronal connections is critically important for brain development and learning. Here, we show that ion-flow-independent NMDA receptor (NMDAR) signaling is required for the long-term dendritic spine growth that is a vital component of brain circuit plasticity. We find that inhibition of p38 mitogen-activated protein kinase (MAPK), which is downstream of non-ionotropic NMDAR signaling in long-term depression (LTD) and spine shrinkage, blocks long-term potentiation (LTP)-induced spine growth but not LTP. We hypothesize that non-ionotropic NMDAR signaling drives the cytoskeletal changes that support bidirectional spine structural plasticity. Indeed, we find that key signaling components down-stream of non-ionotropic NMDAR function in LTD-induced spine shrinkage are also necessary for LTP- induced spine growth. Furthermore, NMDAR conformational signaling with coincident Ca^{2+} influx is sufficient to drive calcium/calmodulin-dependent protein kinase II (CaMKII)-dependent long-term spine growth, even when Ca^{2+} is artificially driven through voltage-gated Ca^{2+} channels. Our results support a model in which non-ionotropic NMDAR signaling gates the bidirectional spine structural changes vital for brain plasticity.

Introduction

Dynamic alternations in neuronal connectivity are critical for the experience-dependent modification of brain circuits throughout development and during learning. In particular, the bidirectional structural plasticity of dendritic spines is a vital process in the refinement of synaptic circuits in the mammalian cortex (e.g. (Hayashi-Takagi et al 2015, Lai et al 2018). Increases in synaptic strength, as through the induction of long-term potentiation (LTP), are associated with spine enlargement and new spine formation (Matsuzaki et al 2004, Nishiyama & Yasuda 2015), while decreases in synaptic strength, as through the induction of long-term depression (LTD), are associated with spine shrinkage or loss (Stein & Zito 2019, Zhou et al 2004). Notably, activation of the NMDA-type glutamate receptor (NMDAR) is required for both the spine growth associated with LTP and the spine shrinkage associated with LTD.

Recent studies have demonstrated that LTD (Carter & Jahr 2016, Nabavi et al 2013, Wong & Gray 2018) and dendritic spine shrinkage (Birnbaum et al 2015, Stein et al 2015, Thomazeau et al 2020) can occur independent of ion flux through the NMDA receptor. These findings have supported a model in which glutamate binding leads to conformational changes in the NMDAR that drive spine shrinkage and synaptic weakening. Indeed, imaging studies using FRET reporters have shown that NMDA or glutamate binding triggers conformational changes in the NMDAR intracellular domains, and changes its interaction with calcium/calmodulin-dependent protein kinase II (CaMKII) and protein phosphatase 1 (PP1) (Aow et al 2015, Dore et al 2015, Ferreira et al 2017). p38 MAPK has been identified as a key component of the molecular pathway downstream of NMDAR conformational signaling (Birnbaum et al 2015, Nabavi et al 2013, Stein et al 2015), and a recent study further identified nNOS, nNOS-NOS1AP interactions, MAPK-activated protein kinase 2 (MK2) and cofilin as part of this signaling pathway (Stein et al 2020).

Here, we made the surprising discovery that ion flow-independent NMDAR signaling is required for the long-term spine growth associated with synaptic strengthening. We show that

p38 MAPK, an essential signaling component for LTD and spine shrinkage, is required for spine growth, but not LTP, suggesting that non-ionotropic NMDAR signaling is a vital component of bidirectional spine structural plasticity. Indeed, we further show that key components of ion flux-independent NMDAR signaling, including interaction between NOS1AP and nNOS, MK2, nNOS, and CaMKII activity are all required for LTP-induced spine growth. Importantly, we also demonstrate that, when combined with non-ionotropic NMDAR signaling, long-term spine growth can be driven by Ca^{2+} influx through voltage-gated Ca^{2+} channels. Our findings support a model whereby non-ionotropic NMDAR signaling leads to disruption of the spine F-actin network, which drives spine shrinkage unless coincident Ca^{2+}-influx converts F-actin remodeling to instead promote spine growth.

Materials and Methods

Animals. C57BL/6J or GFP-M (Feng et al 2000) mice and Sprague-Dawley rats of both sexes were used for the preparation of acute hippocampal slices at postnatal day 16-20 (P16-20) and organotypic hippocampal slice cultures at P6-8. All experimental protocols were approved by the University of California Davis Institutional Animal Care and Use Committee.

Preparation and transfection of organotypic hippocampal slice cultures. Organotypic hippocampal slices were prepared from P6-P8 Sprague-Dawley rats or C57BL/6J mice of both sexes, as described (Stoppini et al 1991). Cultures were transfected 1-2 d (EGFP) or 2 d (GCaMP6f) before imaging via biolistic gene transfer (180 psi), as previously described (Woods & Zito 2008). 10-15 µg of EGFP-n1 or 5 µg GCaMP6f (gift from Lin Tian and Karel Svoboda; (Chen et al 2013)) and 10 µg pCAG-CyRFP1 (Laviv et al 2016) were coated onto 6-8 mg of 1.6 µm gold beads.

Preparation of acute hippocampal slices. Acute hippocampal slices were prepared from P16-P20 GFP-M mice (Feng et al 2000) of both sexes in C57BL/6J background. Coronal 400 µm slices were cut (Leica VT100S vibratome) in cold choline chloride dissection solution containing (in mM): 110 choline chloride, 2.5 KCl, 25 $NaHCO_3$, 0.5 $CaCl_2$, 7 $MgCl_2$, 1.3 NaH_2PO_4, 11.6 sodium ascorbate, 3.1 sodium pyruvate, and 25 glucose, saturated with 95% O_2/5% CO_2. Slices were recovered first at 30˚C for 45 min and then at room temperature for an additional 45 min, in oxygenated artificial cerebrospinal fluid (ACSF) containing (in mM): 127 NaCl, 25 $NaHCO_3$, 1.25 NaH_2PO_4, 2.5 KCl, 25 glucose, 2 $CaCl_2$, and 1 $MgCl_2$, before imaging experiments were initiated.

Time-lapse two-photon imaging. Transfected CA1 pyramidal neurons [14-18 days in vitro (DIV)] at depths of 10-50 µm were imaged using a custom two-photon microscope (Woods et al 2011)

controlled with ScanImage (Pologruto et al 2003). Image stacks (512 × 512 pixels; 0.02 µm per pixel) with 1-µm z-steps were collected. For each neuron, one segment of secondary or tertiary basal dendrite was imaged at 5 min intervals at 29-30 °C in recirculating artificial cerebral spinal fluid (ACSF; in mM: 127 NaCl, 25 $NaHCO_3$, 1.2 NaH_2PO_4, 2.5 KCl, 25 D-glucose, aerated with 95%O_2/5%CO_2, ~310 mOsm, pH 7.2) with 1 µM TTX, 0 mM Mg^{2+}, and 2 mM Ca^{2+}, unless otherwise stated.

10 µM L-689,560 (L-689, 15 mM stock in DMSO), 100 µM 7CK (100 mM stock in H_2O), 2 µM SB203580 (4 mM stock in DMSO), 100 µM NG-Nitro-L-arginine (L-NNA, 200 mM stock in 0.25 N HCL), 10 µM Bay-K (10 mM stock in DMSO), 50 µM (RS)-CPP (50 mM stock in H_2O), 50 µM NBQX (10 mM stock in H_2O); 10 µM MK2 inhibitor III (20 mM stock in DMSO); and 5 µM TAT-CN21 (5 mM stock in H_2O; (Vest et al 2007)) and 5 µM TAT-SCR (5 mM stock in H_2O) were included, as indicated. Slices were pre-incubated for at least 30 min with the drug or vehicle control before glutamate uncaging. Peptides were obtained from GenicBio: L-TAT-GESV: NH2-GRKKRRQRRRYAGQWGESV-COOH, L-TAT-GASA: NH2-GRKKRRQRRRYAGQWGASA-COOH. Slices were pre-incubated with 1 µM (2 mM stock in H_2O) peptide for at least 60 min before stimulation.

Photolysis of MNI-caged glutamate with HFU and HFU+ stimulation. High-frequency uncaging (HFU) consisted of 60 pulses (720 nm; 2 ms duration, ~7-10 mW at the sample; adjusted to evoke an average response of ~10 pA at the soma) at 2 Hz, delivered in ACSF containing (in mM): 2 Ca^{2+}, 0 Mg^{2+}, 2.5 MNI-glutamate, and 0.001 TTX. The beam was parked at a point ~0.5-1 µm from the spine at the position farthest from the dendrite. HFU+ stimulation was designed to increase Ca^{2+}-influx through voltage-gated calcium channels. HFU+ consisted of 60 pulses (720 nm; 8 ms duration, ~7 mW at the sample) at 6 Hz, delivered in ACSF containing (in mM): 10 Ca^{2+}, 0 Mg^{2+}, 5 MNI-glutamate, and 0.001 TTX. Healthy and stimulus responsive cells were

selected based on a test HFU stimulus onto a test spine on a test dendrite before the application of pharmacological reagents. Only cells on which the test dendritic spine displayed transient growth in response to HFU were used for experiments. Spines targeted for HFU stimulation during experimental data collection were on a different dendrite than the test spine, and were well-isolated and of an average size and that did not fluctuate during baseline imaging. All remaining isolated spines within the region of interest were analyzed as unstimulated neighbors.

Electrophysiology. Whole-cell recordings (V_{hold} = −65 mV; series resistance 20-40 MΩ) were obtained from visually identified CA1 pyramidal neurons in slice culture (14-18 DIV, depths of 10-50 µm) at 25°C in ACSF containing in mM: 2 $CaCl_2$, 1 $MgCl_2$, 0.001 TTX, 2.5 MNI-glutamate. 2 µM SB203580 was included, as indicated. Recording pipettes (~5-7 MΩ) were filled with cesium-based internal solution (in mM: 135 Cs-methanesulfonate, 10 Hepes, 10 Na_2 phosphocreatine, 4 $MgCl_2$, 4 Na_2-ATP, 0.4 Na-GTP, 3 Na L-ascorbate, 0.2 Alexa 488, and ~300 mOsm, ~pH 7.25). For each cell, baseline uncaging-evoked excitatory postsynaptic currents (uEPSCs) were recorded from two spines (2-12 µm apart) on secondary or tertiary basal branches (50-120 µm from the soma). The high-frequency glutamate uncaging stimulus (720 nm, 1 ms duration, 8-10 mW at the sample) was then applied to one spine, during which the cell was depolarized to 0 mV. Following the HFU stimulus, uEPSCs were recorded from both the target and neighboring spine at 5 min intervals for 25 min.

Calcium imaging. CA1 pyramidal neurons (13-18 DIV) in slice culture co-expressing GCaMP6 and CyRFP1 were imaged in line-scan mode (500 Hz) to assess if they were healthy and responsive using a test stimulation of a single glutamate uncaging pulse at a dendritic spine. Using a different dendritic segment than the test spine, responsive CA1 neurons were then

imaged in frame-scan mode (64 pixels per line, 7.8 Hz) before and after glutamate uncaging (720 nm, 60 pulses, 8 ms duration at 6 Hz, ~7 mW at sample) adjacent to the spine head at 27 °C in ACSF containing the following (in mM): 10 Ca^{2+}, 0 Mg^{2+}, 5 MNI-glutamate, and 0.001 TTX. Neurons with high baseline GCaMP6f and neurons that exhibited large calcium transients extending across the dendritic shaft were excluded.

Quantification and statistical analysis. Data analysis was performed blind to the experimental condition. Cells for each condition were obtained from at least three independent preparations of either hippocampal acute slices or slice cultures, and only one cell per slice was imaged for any experimental condition.

Quantification of data from imaging experiments. For spine structural plasticity experiments, stimulated spine volume was estimated from background-subtracted green fluorescence using the integrated pixel intensity of a boxed region surrounding the spine head, as previously described (Woods et al 2011). Previous studies comparing the results from this method to those obtained from electron microscopy have shown that the use of integrated fluorescence intensity to be a valid method for estimating spine volume (Holtmaat et al 2005). For calcium imaging experiments, Ca^{2+} transient peak amplitude ($\Delta F/F_0$) was measured from background-subtracted green fluorescence in the spine as the ratio of fluorescence during HFU (of specified windows after HFU) to basal fluorescence (2.4 s window before uncaging). All images are maximum projections of three-dimensional (3D) image stacks after applying a median filter (3 × 3) to the raw image data.

Quantification of data from electrophysiology experiments. uEPSC amplitudes from individual spines were quantified as the average of 5-6 test pulses at 0.1 Hz) from a 2 ms window

centered on the maximum current amplitude within 50 ms following uncaging pulse delivery relative to the baseline.

Statistical analysis. All data are represented as mean ± standard error of the mean (SEM). All statistics were calculated across cells. Statistical significance was set at $p < 0.05$ (ANOVA). Data in the bar graphs of Fig 1-4 and Fig S3 were analyzed using two-way ANOVA with Tukey's multiple comparison test. Data in the line graphs of Fig 1-4 and Fig S3 were analyzed using two-way repeated measure ANOVA with Dunnett's post hoc test for comparison of HFU stimulation at each time point to baseline. Data in Fig S1 C, E were analyzed using two-way repeated measure ANOVA with Bonferroni's multiple comparison test and for Fig S1 F using one-way ANOVA with Tukey's multiple comparison test. Data were analyzed for Fig S2 A-F using unpaired t-test and for Fig S2 G using one-way ANOVA with Tukey's multiple comparison test. All p and n values are presented in the figure legends.

Results

p38 MAPK activity is required for LTP-induced spine growth, but not for LTP-induced synaptic strengthening

Glutamate binding to NMDARs initiates a signaling cascade that drives synaptic weakening (LTD) and the shrinkage of dendritic spines (sLTD), even when ion flow is blocked pharmacologically (Carter & Jahr 2016, Nabavi et al 2013, Stein et al 2015, Wong & Gray 2018). Furthermore, in the absence of ion flux, patterns of glutamatergic stimulation that would normally drive LTP and spine growth, instead drive LTD and spine shrinkage (Nabavi et al 2013, Stein et al 2020, Stein & Zito 2019). Because the non-ionotropic NMDAR signaling pathway should also be activated with glutamate binding when ion flow through the receptor is not blocked, we wondered whether it plays a role in bidirectional synaptic plasticity. We hypothesized non-ionotropic NMDAR signaling could function as part of a built in synaptic regulatory mechanism to fine tune structural rearrangement and prevent spine overgrowth during LTP induction.

Intriguingly, inhibition of p38 MAPK activity by SB203580 (Cuenda et al 1995, Davies et al 2000) did not lead to excessive high frequency uncaging (HFU)-induced spine growth, but instead blocked persistent spine enlargement following HFU stimulation (**Fig. 1A-C**; veh: 220 ± 18%; SB: 117 ± 11%). As p38 MAPK activation previously only had been implicated in LTD and not LTP (Zhu et al 2002), we examined next whether expression of HFU-induced single spine LTP was normal during inhibition of p38 MAPK activity. HFU stimulation under vehicle conditions successfully induced LTP of the target spine that lasted for at least 25 min following stimulation but did not increase the uncaging-evoked excitatory postsynaptic current (uEPSC) amplitude of the unstimulated neighboring spine (**Fig. 1D, F**; target: 153 ± 11%; neighbor: 93 ± 7%). Unlike spine enlargement, functional LTP induction was not blocked by SB203580 and was indistinguishable from LTP during vehicle conditions (**Fig. 1E, F**; target: 157 ± 6%;

neighbor: 98 ± 9%). SB203580 did not alter baseline spine volume (**Fig. S1A**). These results support a specific role for p38 MAPK signaling in structural, but not functional LTP.

Non-ionotropic NMDAR signaling pathway is required for LTP-induced spine growth

The requirement of p38 MAPK for spine growth, but not for LTP, and the previously implicated role of p38 MAPK in non-ionotropic signaling during LTD and spine shrinkage led us to the unexpected hypothesis that non-ionotropic NMDAR signaling might be required for bidirectional spine structural plasticity. We have previously shown that non-ionotropic NMDAR-dependent spine shrinkage is dependent on the interaction between NOS1AP and nNOS, which during NMDAR-mediated excitoxicity is required for p38 MAPK activation (Li et al 2013), and the p38 MAPK substrate MK2, NOS activation, and cofilin (Stein et al 2020). We therefore set out to test whether these molecules are also required for LTP-induced spine growth.

We tested whether NOS1AP binding to nNOS, MK2 activity, and nNOS activity, like p38 MAPK activation, are also required for persistent structural LTP. Indeed, we found that inhibition of NOS1AP binding to nNOS using L-TAT-GESV (Li et al 2013) impaired persistent HFU-induced structural LTP (**Fig. 2A-C**; 110 ± 13%) compared to the inactive L-TAT-GASA control peptide (**Fig. 2A-C**; 173 ± 17%). Spine size of the unstimulated neighboring spines was not changed (**Fig. 2A-C**; L-TAT-GASA: 101 ± 4%; L-TAT-GESV: 107 ± 6%). In addition, HFU-induced spine enlargement was significantly reduced in the presence of MK2 inhibitor III (Anderson et al 2007, Fiore et al 2016) compared to vehicle conditions (**Fig. 2D-F**; veh: 241 ± 34%; MK2 inhibitor III: 152 ± 24%), and no change in the size of the unstimulated neighboring spines was observed (**Fig. 2D-F**; veh: 109 ± 6%; MK2 inhibitor III: 109 ± 7%). Furthermore, in the presence of the NOS inhibitor, L-NNA (Pigott et al 2013, Reif & McCreedy 1995), HFU-induced spine enlargement was significantly reduced compared to vehicle conditions (**Fig. 2G-I**; veh: 201 ± 28%; L-NNA: 136 ± 14%), and no change in the size of the unstimulated neighboring spines was observed (**Fig. 2G-I**; veh: 105 ± 5%; L-NNA: 110 ± 6%). L-TAT-GESV, MK2 inhibitor

III, and L-NNA did not alter baseline spine volume (**Fig. S1B-D**). Our findings strongly support a role for the non-ionotropic NMDAR signaling pathway in LTP-induced spine growth.

Non-ionotropic NMDAR signaling in combination with VGCC-mediated Ca^{2+}-influx is sufficient to drive LTP-induced spine growth

Our results support a model in which non-ionotropic NMDAR signaling leads to the p38 MAPK- and cofilin-dependent disruption of the F-actin network, which, in the absence of strong Ca^{2+}-influx, drives spine shrinkage, but during LTP provides new actin filament nucleation and branching points for subsequent spine enlargement by Ca^{2+}-dependent actin modifying and stabilizing proteins. Based on this model, we hypothesized that it should be possible to drive spine growth through a combination of non-ionotropic NMDAR signaling with NMDAR-independent Ca^{2+}-influx (**Fig. 3A**).

In order to drive non-ionotropic NMDAR signaling together with voltage-gated calcium channel (VGCC)-mediated Ca^{2+}-influx, we used the co-agonist binding site NMDAR antagonist, L-689,560 (Leeson et al 1992), which blocks all current through the NMDAR (Stein et al 2020, Wong & Gray 2018), along with the L-type Ca^{2+} channel agonist Bay K 8644 (Hess et al 1984). Furthermore, to ensure sufficient L-type VGCC-mediated Ca^{2+}-influx into the stimulated spine during glutamate uncaging, we increased extracelluar Ca^{2+} and we increased the intensity and frequency of our high-frequency uncaging protocol (HFU+; see STAR Methods) to facilitate stronger AMPAR-dependent depolarization of the target spine. Remarkably, HFU+-stimulation in the presence of L-689 and Bay K induced long-term spine growth (**Fig. 3B-D**; L-689 + Bay K: 147 ± 12%). Importantly, adding the glutamate binding site NMDAR antagonist, CPP (Davies et al 1986, Lehmann et al 1987) to inhibit non-ionotropic NMDAR signaling, blocked HFU+-induced long-term spine growth (**Fig. 3B-D**; L-689 + Bay K + CPP: 102 ± 7%) without affecting the magnitude of VGCC-mediated Ca^{2+}-influx (**Fig. S2**). Size of unstimulated neighboring spines (**Fig. 3B-D**; L-689 + Bay K: 104 ± 6%; L-689 + CPP + Bay K: 89 ± 3%) and baseline spine

volume (**Fig S1E)** were unaffected by Bay K, excluding acute and activity-independent effects of Bay K alone on spine morphology.

In order to confirm that our modified HFU+ stimulation paradigm still drives non-ionotropic NMDAR signaling induced spine shrinkage in acute hippocampal slices from mice, we replaced Bay K with NBQX (Sheardown et al 1990) to block uncaging-induced AMPAR-driven spine depolarization and VGCC activation, and tested whether the same stimulation now in the absence of Ca^{2+}-influx drives dendritic spine shrinkage. Indeed, HFU+ stimulation in the presence of L-689 and NBQX resulted in non-ionotropic NMDAR-dependent spine shrinkage (**Fig. 3E-G**; L-689 + NBQX: 55 ± 9%), which was inhibited if glutamate binding and thus conformational non-ionotropic NMDAR signaling was blocked with CPP (**Fig. 3E-G**; L-689 + CPP + NBQX: 94 ± 8%). Spine size of unstimulated neighbors (**Fig. 3E-G**; L-689 + NBQX: 92 ± 3%; L-689 + CPP + NBQX: 89 ± 10%) and baseline spine volume (**Fig. S1F)** were unaffected. Our results confirm the generalizability of ion flux-independent NMDAR signaling in driving dendritic spine shrinkage across slice preparations and species, which is further confirmed in studies of ion flux-independent LTD, which showed consistent results across species, slice preparations, and dissociated rat cultures (Aow et al 2015, Nabavi et al 2013, Wong & Gray 2018). These results strongly support our model that non-ionotropic NMDAR signaling primes the actin cytoskeleton for bidirectional structural plasticity.

CaMKII activity is required for long-term spine growth, independent of calcium source

CaMKII is a Ca^{2+}-dependent kinase that has been extensively studied in LTP induction (Bayer & Schulman 2019) and is required for the long-term spine growth associated with LTP (Matsuzaki et al 2004, Murakoshi et al 2011) (**Fig. S3**). Notably, disruption of interaction of CaMKII with the C terminus of the NMDAR interferes with LTP (Barria & Malinow 2005, Halt et al 2012, Sanhueza et al 2011) and long-term spine stabilization (Hill & Zito 2013), suggesting that the

local calcium microdomains produced by calcium flow through the NMDAR may be critical in activating CaMKII during LTP-induced structural and functional plasticity.

We tested whether Ca^{2+}/CaMKII-dependent signaling is also required for long-term spine growth driven by NMDAR-independent Ca^{2+} influx through VGCCs using acute hippocampal slices from mice. We found that when Ca^{2+} is supplied through VGCCs and not through the NMDAR under our HFU+ stimulation conditions, long-term spine growth (**Fig. 4A-C**; L-689 + Bay K + TAT-SCR: 173 ± 17%) was also blocked in the presence of KN-62 (Hidaka & Yokokura 1996, Tokumitsu et al 1990) (**Fig. 4A-C**; L-689 + Bay K + KN-62: 106 ± 11%) or TAT-CN21 (**Fig. 4A-C**; L689 + Bay K + TAT-CN21: 102 ± 15%), a CaMKII specific peptide inhibitor (Vest et al 2007). Size of unstimulated neighboring spines (**Fig. 4A-C**; L-689 + Bay K + TAT-SCR: 87 ± 3%; L-689 + Bay K + KN-62: 97 ± 10%; L-689 + Bay K + TAT-CN21: 100 ± 7%) and baseline spine volume (**Fig.S1G**) were not affected. Our results demonstrate the requirement of CaMKII for LTP-induced long-term spine growth, regardless of calcium source.

Discussion

Non-ionotropic NMDAR signaling drives bidirectional spine structural plasticity

Ion flow-independent NMDAR signaling has been implicated by many independent studies in spine shrinkage and synaptic weakening (Aow et al 2015, Birnbaum et al 2015, Carter & Jahr 2016, Nabavi et al 2013, Stein et al 2015, Stein et al 2020, Thomazeau et al 2020, Wong & Gray 2018). Here, we made the unexpected discovery that this non-ionotropic NMDAR signaling pathway is also required for spine growth during synaptic strengthening. It may appear contradictory that the same signaling pathway could support both spine shrinkage and spine growth; however, it is notable that cofilin activation, which has been implicated in spine shrinkage during LTD (Hayama et al 2013, Stein et al 2020, Zhou et al 2004) is also important for long-term spine growth during LTP (Bosch et al 2014). We propose a model for spine structural plasticity (**Fig. 4D**), whereby non-ionotropic NMDAR signaling leads to the p38 MAPK- and cofilin-dependent destabilization of the F-actin network, which in the absence of Ca^{2+} influx drives spine shrinkage, but with Ca^{2+}-influx instead provides new actin filament nucleation and branching points for subsequent spine enlargement by Ca^{2+}-dependent actin modifying and stabilizing proteins. Indeed, the Ca^{2+}- and CaMKII-dependent activation of small Rho GTPases has been shown to drive LIMK-dependent phosphorylation and inactivation of cofilin and to promote Arp2/3-mediated actin branching activity (Bosch et al 2014, Murakoshi et al 2011, Nakahata & Yasuda 2018). Our model highlights ion flux-independent NMDAR signaling as a vital component for the bidirectional structural plasticity of dendritic spines.

Role of p38 MAPK in LTP-induced spine growth, but not synaptic strengthening

Our studies support an unexpected role for p38 MAPK, a classical LTD molecule implicated in non-ionotropic NMDAR signaling during both LTD and spine shrinkage (Nabavi et al 2013, Stein et al 2015), in spine growth during LTP. Notably, we found that inhibition of p38 MAPK blocked spine growth but not synaptic strengthening during LTP, at least not in the short-term. Our

results are in line with previous studies reporting no role for p38 MAPK in tetanus- or pairing-induced NMDAR-dependent LTP (Zhu et al 2002). In addition, MK2, a p38 MAPK substrate identified as part of the non-ionotropic NMDAR signaling pathway in spine shrinkage (Stein et al 2020), is required for spine growth but not for LTP (Privitera et al 2019) and NOS signaling, presumably upstream of p38 MAPK in non-ionotropic NMDAR signaling (Stein et al 2020), is required for both spine growth and LTP (Lu et al 1999, O'Dell et al 1994). Because inhibition of p38 MAPK and MK2 lead to a pharmacological dissociation of spine growth and LTP, which are normally tightly linked (Matsuzaki et al 2004), our results suggest that these molecules are downstream of a branch point in signaling that drives synaptic strengthening and spine growth during LTP.

Role of CaMKII in bidirectional spine structural plasticity

During LTP-induced spine growth, Ca^{2+}-influx through the NMDAR leads to activation of CaMKII, which then activates small Rho GTPases, whose concerted activity drives spine enlargement via the actin regulatory proteins LIMK and Arp2/3, promoting actin polymerization and branching and spine growth (Bosch et al 2014, Hedrick et al 2016, Kim et al 2013, Lee et al 2009, Murakoshi et al 2011, Nakahata & Yasuda 2018, Okamoto et al 2004, Saneyoshi et al 2019). Our results surprisingly show that the Ca^{2+} influx that drives LTP-induced spine growth does not need to enter the spine through the NMDAR, instead it can be supplied by VGCCs, as long as non-ionotropic NMDAR signaling is intact. Although it has been shown that specific local signaling microdomains are important for independently driving LTP and LTD (Zhang et al 2018), our results suggest that local calcium microdomains produced by ion flow through the NMDAR are not critical for driving LTP-induced spine growth.

CaMKII has been extensively studied in LTP induction (Bayer & Schulman 2019) and LTP-induced spine growth (Nishiyama & Yasuda 2015); however, lately CaMKII also has been implicated in LTD (Coultrap et al 2014, Woolfrey et al 2018) and spine shrinkage driven by non-

ionotropic NMDAR signaling (Stein et al 2020). A key question is whether and how CaMKII carries out multiple roles in bidirectional spine structural plasticity. It is possible that the kinase mediates ion-flux dependent and independent signaling pathways sequentially during spine structural plasticity. Such a situation has been shown for VGCCs, in which ion flux prior to conformational signaling drives nuclear transcription (Li et al 2016a). Another possibility is that CaMKII acts simultaneously in the two pathways through different populations, perhaps one Ca^{2+}/CaM bound and the other not. Indeed, synaptic activity has been proposed to activate different populations of CaMKII (Pi et al 2010, Yasuda et al 2003), which could then have different substrate specificities, as shown for Ca^{2+}-bound versus autonomous CaMKII activity during LTP and LTD (Coultrap et al 2014, Woolfrey et al 2018).

Figure legends and figures

Figure 1. p38 MAPK activity is required for LTP-induced spine growth, but not for synaptic strengthening

(A) Images of dendrites from DIV14-18 EGFP-expressing CA1 neurons from rat organotypic slices before and after HFU stimulation (yellow cross) at individual dendritic spines (yellow arrowhead) with and without p38 MAPK inhibitor SB203580 (SB, 2 µM). **(B, C)** Inhibition of p38 MAPK with SB (black filled circles/bar; 11 spines/11 cells) reduced HFU-induced spine growth compared to vehicle (red filled circles/bar; 11 spines/11 cells). Volume of unstimulated neighbors (open circles/bars) was unaffected. **(D, E)** Top, average traces of uEPSCs from a target spine and an unstimulated neighbor on CA1 neurons from mouse organotypic slices before (gray) and 25 min after HFU stimulation during vehicle conditions (target, red; neighbor, dark gray) or in the presence of SB (target, black; neighbor, dark gray). Bottom, HFU-induced increases in uEPSC amplitude in vehicle (red; 8 spines/8 cells) were unaffected by p38 MAPK inhibition with SB (black; 9 spines/9 cells). uEPSC amplitudes of unstimulated neighboring spines (gray) were unaffected. **(F)** HFU induced a long-lasting uEPSC amplitude increase (red filled bar) compared to baseline, which is unaffected by p38 MAPK inhibition (black filled bar). Two-way ANOVA with Tukey's test used in (C, F) and two-way RM ANOVA with Dunnett's test to baseline used in (B, D, E). Data are represented as mean ± SEM. *$p < 0.05$; **$p < 0.01$, ***$p < 0.001$.

Figure 1

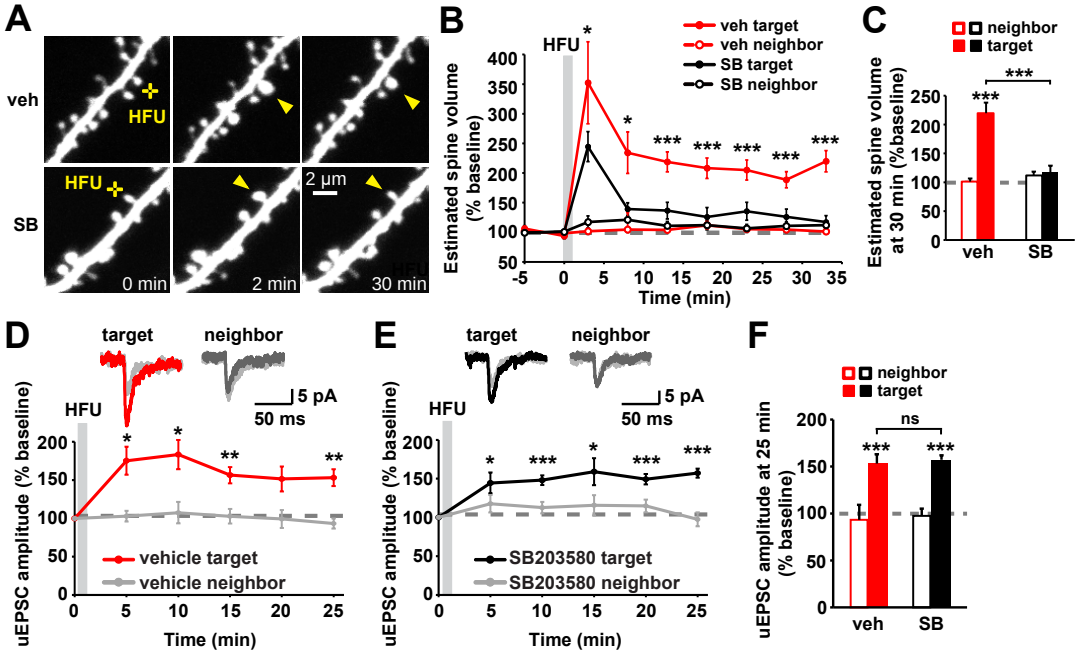
A
veh
SB
HFU
HFU
2 µm
0 min
2 min
30 min
B
HFU
veh target
veh neighbor
SB target
SB neighbor
Estimated spine volume (% baseline)
Time (min)
C
neighbor
target
Estimated spine volume at 30 min (%baseline)
veh
SB
D
target
neighbor
HFU
5 pA
50 ms
vehicle target
vehicle neighbor
uEPSC amplitude (% baseline)
Time (min)
E
target
neighbor
HFU
5 pA
50 ms
SB203580 target
SB203580 neighbor
uEPSC amplitude (% baseline)
Time (min)
F
neighbor
target
ns
uEPSC amplitude at 25 min (% baseline)
veh
SB

Figure 2. Non-ionotropic NMDAR signaling pathway is required for LTP-induced spine growth

(A, D, G) Images of dendrites from EGFP-expressing CA1 neurons from rats (A, D) and mice (G) organotypic slices at DIV14-18 before and after HFU stimulation (yellow cross) of individual spines (yellow arrowhead) in the presence of L-TAT-GESV (1 µM) and the L-TAT-GASA control peptide (1 µM), during vehicle conditions and in the presence of MK2 inhibitor III (10 µM) or the NOS inhibitor, L-NNA (100 µM). **(B, C)** Disruption of the NOS1AP/nNOS interaction with L-TAT-GESV (black filled circles/bar; 9 spines/9 cells), but not application of the inactive L-TAT-GASA control peptide (red filled circles/bar; 9 spines/9 cells) inhibited persistent spine growth following LTP induction. Volume of the unstimulated neighbors (open circles/bars) was unchanged. **(E, F)** Inhibition of MK2 activity (black filled circles/bar; 11 spines/11 cells) prevented HFU-induced persistent spine enlargement (red filled circles/bar; 12 spines/12 cells). Volume of the unstimulated neighbors did not change (open circles/bars). **(H, I)** Inhibition of NOS activity (black filled circles/bar; 11 spines/11 cells) prevented HFU-induced persistent spine enlargement (red filled circles/bar; 12 spines/12 cells). Volume of the unstimulated neighbors did not change (open circles/bars). Two-way ANOVA with Tukey's test used in (C, F, I) and two-way RM ANOVA with Dunnett's test to baseline. Data are represented as mean ± SEM. *$p < 0.05$; **$p < 0.01$, ***$p < 0.001$.

Figure 2

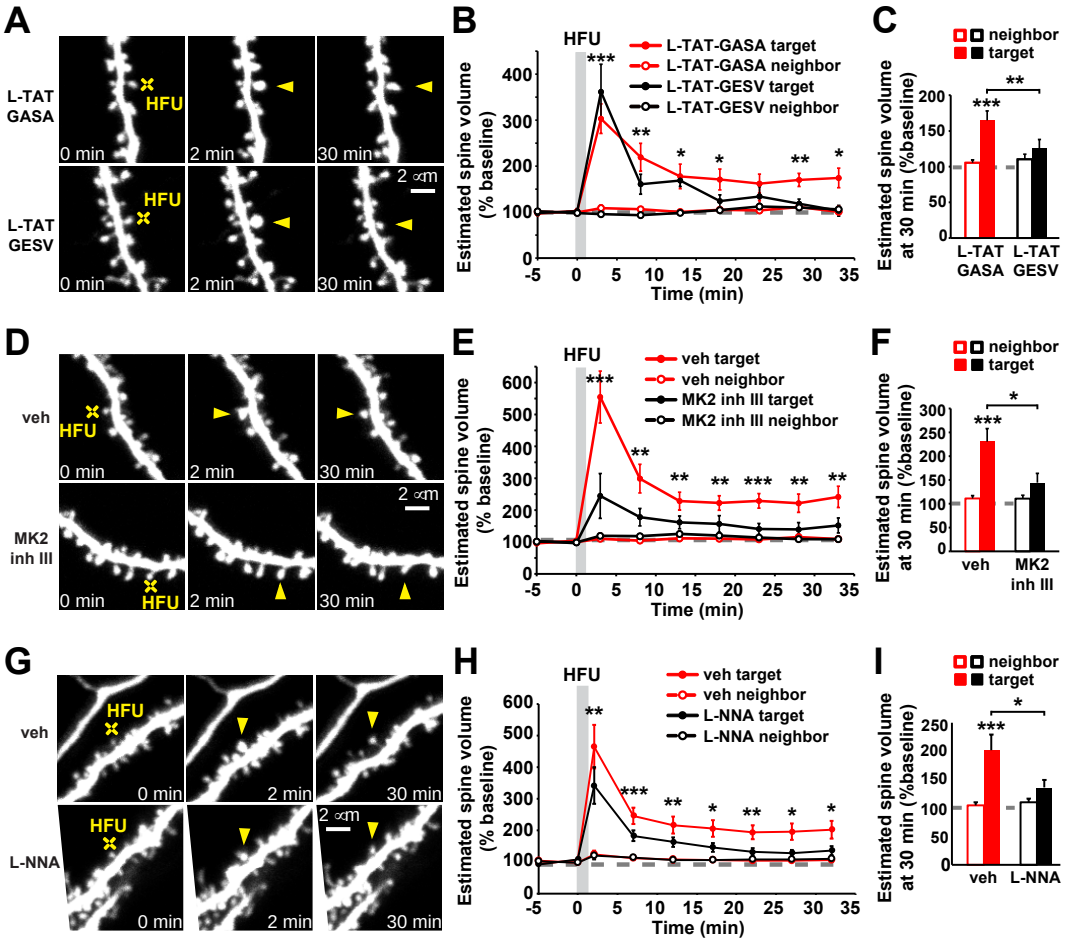
A
L-TAT GASA
L-TAT GESV
HFU
0 min
2 min
30 min
2 µm
B
HFU
L-TAT-GASA target
L-TAT-GASA neighbor
L-TAT-GESV target
L-TAT-GESV neighbor
Estimated spine volume (% baseline)
Time (min)
C
neighbor
target
Estimated spine volume at 30 min (%baseline)
L-TAT GASA
L-TAT GESV
D
veh
MK2 inh III
E
veh target
veh neighbor
MK2 inh III target
MK2 inh III neighbor
F
G
L-NNA
H
L-NNA target
L-NNA neighbor
I

Figure 3. Non-ionotropic NMDAR signaling with Ca^{2+}-influx through voltage-gated calcium channels is sufficient to drive LTP-induced spine growth

(A) Left: Proposed model whereby activity-induced spine growth requires both non-ionotropic and ionotropic NMDAR signaling. Middle: Schematic of experiment to test proposed model. Non-ionotropic NMDAR signaling is activated with glutamate while calcium influx through the NMDAR is blocked with L-689. Instead, calcium influx is driven through VGCCs with the stronger HFU+ conditions in the presence of Bay K to favor opening of VGCCs. Right: Control experiments block non-ionotropic NMDAR signaling by blocking glutamate binding to the NMDAR with CPP. **(B)** Images of dendrites from CA1 neurons of acute slices from P16-20 GFP-M mice before and after HFU+ stimulation (yellow cross) of individual spines (yellow arrowhead) in the presence of L-689 (10 µM) and Bay K (10 µM) or in combination with CPP (50 µM). **(C, D)** HFU+ stimulation drives spine growth in the presence of Bay K, even when ion flow through the NMDAR is blocked with L-689 (red filled circles/bar; 9 spines/9 cells), but not when non-ionotropic NMDAR signaling is blocked with CPP (black filled circles/bar; 10 spines/10 cells). Volume of the unstimulated neighbors (open circles/bars) was unchanged. **(E)** Images of dendrites under experimental conditions in B-D, except blocking the influx of calcium through VGCCs by removing Bay K and adding NBQX (50 µM). **(F, G)** HFU+ stimulation in the presence of L-689 and NBQX (blue filled circles/bar; 7 spines/7 cells) led to spine shrinkage, which was blocked when non-ionotropic NMDAR signaling was inhibited with the presence of CPP (black filled circles/bar; 6 spines/6 cells). Volume of the unstimulated neighbors (open circles/bars) did not change. Two-way ANOVA with Tukey's test used in (D, G) and two-way RM ANOVA with Dunnett's test to baseline. Data are represented as mean ± SEM. *$p < 0.05$; **$p < 0.01$, ***$p < 0.001$. See also Figure S2.

Figure 3

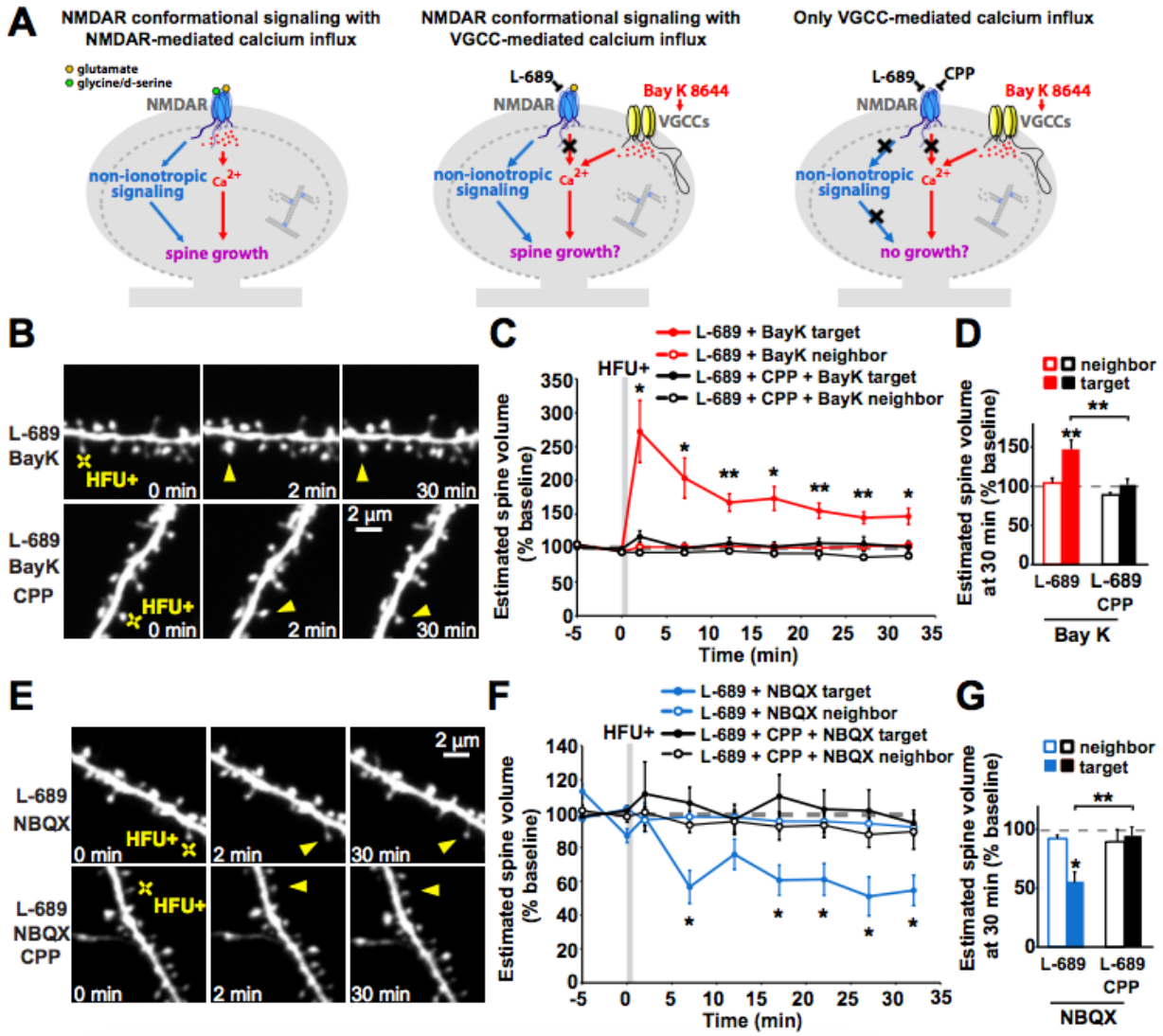
A
NMDAR conformational signaling with NMDAR-mediated calcium influx
NMDAR conformational signaling with VGCC-mediated calcium influx
Only VGCC-mediated calcium influx
glutamate
glycine/d-serine
NMDAR
non-ionotropic signaling
Ca2+
spine growth
spine growth?
no growth?
L-689
CPP
Bay K 8644
VGCCs
B
L-689 BayK
L-689 BayK CPP
HFU+
0 min
2 min
30 min
2 µm
C
L-689 + BayK target
L-689 + BayK neighbor
L-689 + CPP + BayK target
L-689 + CPP + BayK neighbor
Estimated spine volume (% baseline)
Time (min)
D
neighbor
target
Estimated spine volume at 30 min (% baseline)
L-689
L-689 CPP
Bay K
E
L-689 NBQX
L-689 NBQX CPP
F
L-689 + NBQX target
L-689 + NBQX neighbor
L-689 + CPP + NBQX target
L-689 + CPP + NBQX neighbor
G
NBQX

Figure 4. CaMKII activity is required for LTP-induced spine growth, independent of calcium source

(A) Images of dendrites from CA1 neurons of acute slices from P16-20 GFP-M mice before and after HFU+ stimulation (yellow cross) of individual spines (yellow arrowhead) in the presence of L-689 (10 µM) and Bay K (10 µM) or in combination with TAT-SCR (5 µM), TAT-CN21 (5 µM), or KN-62 (10 µM). **(B, C)** HFU+-induced spine growth in the presence of Bay K and L-689 is blocked by TAT-CN21 peptide (black filled circles/bar; 6 spines/ 6 cells) or KN-62 (gray filled circles/bars; 6 spines/6 cells), but not in the presence of control TAT-SCR peptide (red filled circles/bar; 6 spines/ 6 cells). Volume of the unstimulated neighbors (open circles/bars) was unchanged. Two-way ANOVA with Tukey's test used in (C) and two-way RM ANOVA with Dunnett's test to baseline. Data are represented as mean ± SEM. *$p < 0.05$; **$p < 0.01$, ***$p < 0.001$. **(D)** Proposed model. Plasticity-inducing glutamatergic stimulation activates non-ionotropic NMDAR signaling, driving cofilin-dependent severing of the actin cytoskeleton, which in the absence of strong Ca^{2+}-influx leads to spine shrinkage. On the other hand, during the strong Ca^{2+}-influx associated with LTP induction, severed actin filaments serve as new starting points for actin filament nucleation and branching by the Ca^{2+}- and CaMKII-dependent actin modifying proteins to expand the F-actin cytoskeleton and drive spine growth.

Figure 4

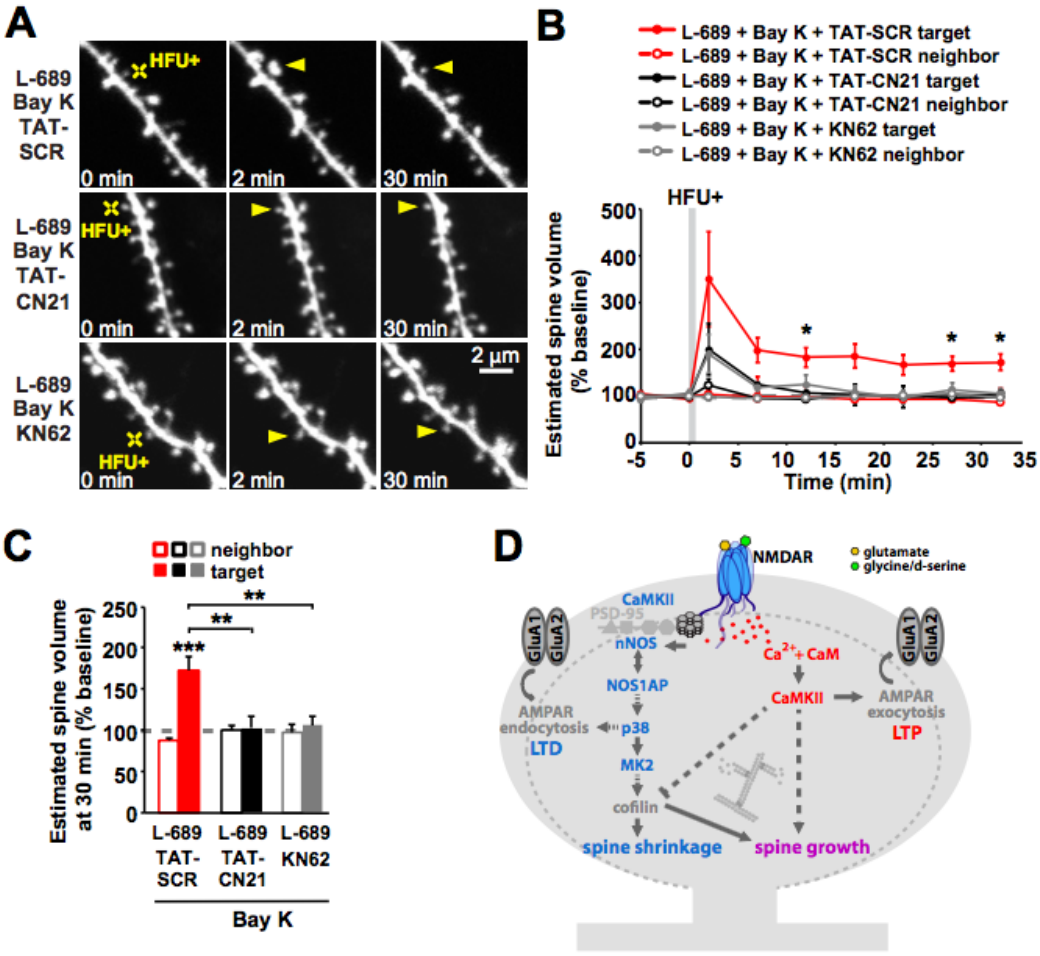
A
L-689 Bay K TAT-SCR
L-689 Bay K TAT-CN21
L-689 Bay K KN62
HFU+
0 min
2 min
30 min
2 µm
B
L-689 + Bay K + TAT-SCR target
L-689 + Bay K + TAT-SCR neighbor
L-689 + Bay K + TAT-CN21 target
L-689 + Bay K + TAT-CN21 neighbor
L-689 + Bay K + KN62 target
L-689 + Bay K + KN62 neighbor
HFU+
Estimated spine volume (% baseline)
Time (min)
C
neighbor
target
Estimated spine volume at 30 min (% baseline)
L-689 TAT-SCR
L-689 TAT-CN21
L-689 KN62
Bay K
D
NMDAR
glutamate
glycine/d-serine
CaMKII
PSD-95
nNOS
Ca2+ + CaM
NOS1AP
p38
MK2
cofilin
GluA1
GluA2
AMPAR endocytosis
LTD
AMPAR exocytosis
LTP
spine shrinkage
spine growth

Figure S1, related to Figures 1-4: Drug incubation does not alter baseline spine volumes. **(A)** No difference in baseline volume of spines between vehicle (red bar; 11 spines/11 cells) and SB203580 (2 μM) (black bar;11 spines/11 cells) after incubation for 30 min**. (B)** No difference in baseline volume of spines between 1 μM L-TAT-GASA (red bar; 9 spines/9 cells) and 1 μM L-TAT-GESV (black bar; 9 spines/9 cells). **(C)** No difference in baseline volume of spines between vehicle (red bar; 12 spines/ 12 cells) and 10 μM MK2 inhib III (black bar;11 spines/11 cells). **(D)** No difference in baseline volume of spines between vehicle (red bar; 11 spines/11 cells) and 100 μM L-NNA (black bar;12 spines/12 cells). (**E)** No difference in baseline volume of spines between 10 μM Bay-K + 10 μM L-689 (black bar; 9 spines/9 cells) and those also with 50 μM CPP (black bar; 10 spines/10 cells). **(F)** No difference in baseline volume of spines between L-689 and 50 μM NBQX (blue bar; 7 spines/7 cells) and those also with 50 μM CPP (black bar; 6 spines/6 cells). **(G)** No difference in baseline volume of spines between 10 μM Bay-K + 10 μM L-689 + 5 μM TAT-SCR (red bar; 6 spines/6 cells), Bay-K + L-689 + 5 μM TAT-CN21 (black bar; 6 spines/6 cells), and Bay-K + L-689 + KN62 (10 μM) (grey bar; 6 spines/6 cells). Two-tailed t-test in (A-F), and one-way ANOVA with Tukey's test in (G). Data are represented as mean +/- SEM. *$p < 0.05$; **$p < 0.01$, ***$p < 0.001$.

Figure S1

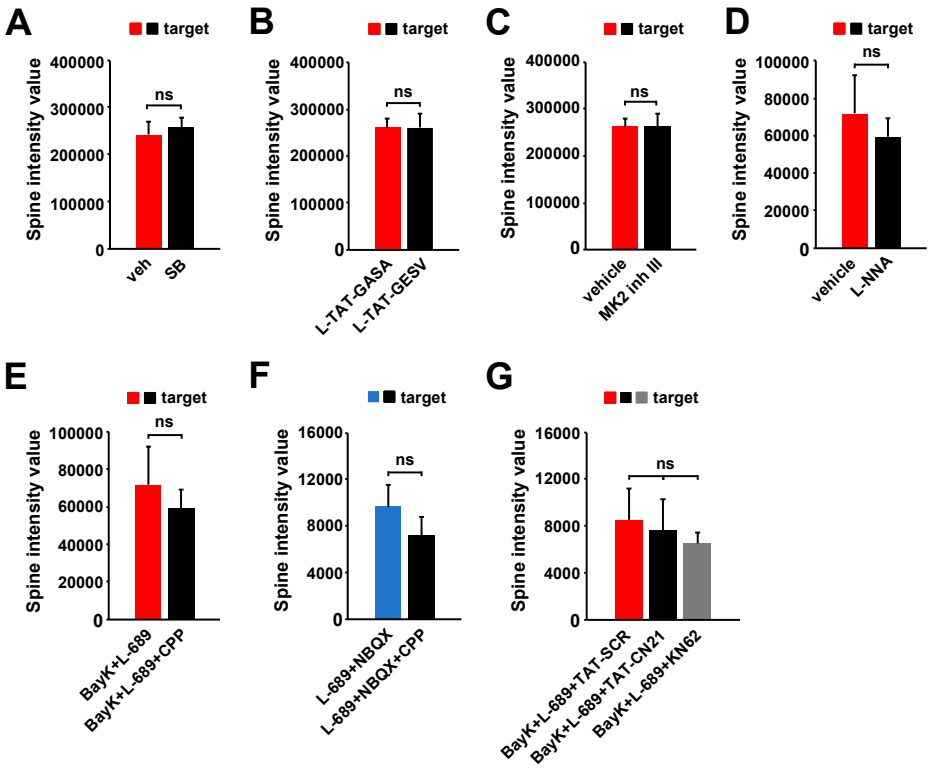
A
target
Spine intensity value
400000
300000
200000
100000
0
ns
veh
SB
B
target
Spine intensity value
400000
300000
200000
100000
0
ns
L-TAT-GASA
L-TAT-GESV
C
target
Spine intensity value
400000
300000
200000
100000
0
ns
vehicle
MK2 inh III
D
target
Spine intensity value
100000
80000
60000
40000
20000
0
ns
vehicle
L-NNA
E
target
Spine intensity value
100000
80000
60000
40000
20000
0
ns
BayK+L-689
BayK+L-689+CPP
F
target
Spine intensity value
16000
12000
8000
4000
0
ns
L-689+NBQX
L-689+NBQX+CPP
G
target
Spine intensity value
16000
12000
8000
4000
0
ns
BayK+L-689+TAT-SCR
BayK+L-689+TAT-CN21
BayK+L-689+KN62

Figure S2, related to Figure 3: Blocking non-ionotropic NMDAR signaling with CPP does not affect the magnitude of Ca^{2+} influx during HFU+ stimulation.

(A) Images of dendrites from CA1 neurons of organotypic slices expressing both CyRFP and GCaMP6f at DIV13-18 before, during, and after HFU+ at individual spines in the presence of L-689 (10 μM) and Bay K (10 μM), in combination with CPP (50 μM) alone or with CPP (50 μM) and NBQX (50 μM). Middle images in each row show bleed through of uncaging laser stimulation. **(B, C)** HFU+ led to comparable levels of calcium influx into spines in the presence of L-689 and Bay K (red filled circles/bar; 11 spines/11 cells) and in combination with CPP (black filled circles/bar; 12 spines/11 cells). Calcium influx through VGCCs is blocked by inhibition of AMPARs with NBQX (gray filled circles/bar; 10 spines/9 cells). **(D, E)** Small, delayed calcium influx is observed in dendrite during HFU+ in the presence of L689 and Bay K (red filled circles/bar; 11 spines/11 cells) or in combination with CPP (black filled circles/bar; 12 spines/11 cells) or NBQX (gray filled circles/bar;10 spines/9 cells). **(F)** Left: No difference in baseline volume of spines in Bay K, L-689, and CPP (red; 8 spines/8 cells); and Bay K, L-689, CPP, and NBQX (gray; 5 spines/5 cells) relative to those exposed to Bay K and L-689 alone (black; 8 spines/8 cells). Right: No difference in baseline GCaMP6 fluorescence of spines in Bay K, L-689, and CPP (red; 8 spines/8 cells); and Bay K, L-689, CPP, and NBQX (gray; 5 spines/ 5 cells) relative to that for Bay K and L-689 alone (black; 8 spines/8 cells). Two-way RM ANOVA with Bonferroni test was used in (C) and (E), and one-way ANOVA with Dunnett's test was used in (F). Data are represented as mean +/- SEM. *$p < 0.05$; **$p < 0.01$, ***$p < 0.001$.

Figure S2

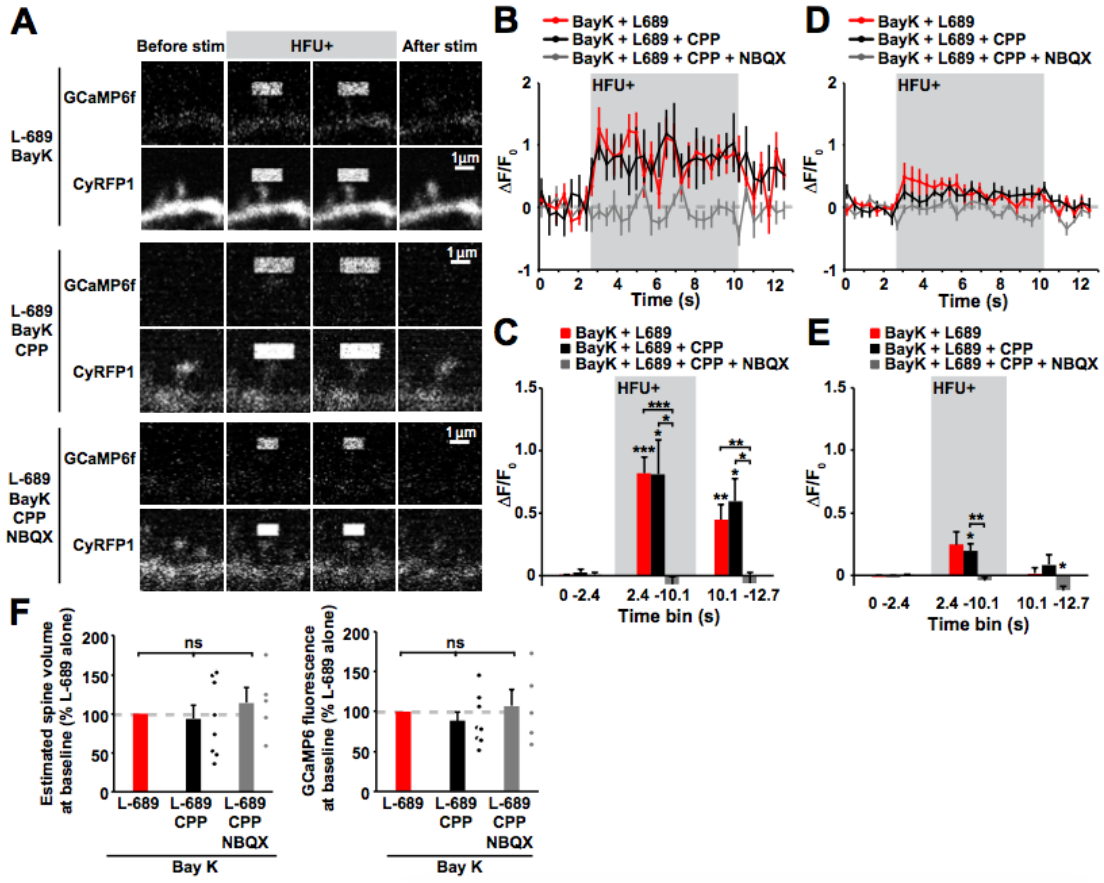
A
Before stim
HFU+
After stim
L-689 BayK
GCaMP6f
CyRFP1
1μm
L-689 BayK CPP
L-689 BayK CPP NBQX
B
BayK + L689
BayK + L689 + CPP
BayK + L689 + CPP + NBQX
HFU+
ΔF/F0
Time (s)
D
C
Time bin (s)
0 -2.4
2.4 -10.1
10.1 -12.7
E
F
Estimated spine volume at baseline (% L-689 alone)
GCaMP6 fluorescence at baseline (% L-689 alone)
ns
L-689
L-689 CPP
L-689 CPP NBQX
Bay K

Figure S3, related to Figure 4: Inhibition of CaMKII blocks LTP-induced long-term spine growth (A) Images of dendrites from CA1 neurons of acute slices from P16-20 GFP-M mice before and after HFU stimulation (yellow cross) of individual spines during vehicle conditions and in the presence of the CaMKII inhibitor KN-62 (10 μM). **(B, C)** HFU-induced dendritic spine growth (vehicle, red filled circles/bar; 8 spines/8 cells) was prevented by KN-62 (black filled circles/bar; 6 spines/6 cells). Volume of the unstimulated neighbors did not change (open bars). Two-way repeated measure ANOVA with Dunnett's test used in (B) and two-way ANOVA with Tukey's test used in (C). Data are represented as mean +/- SEM. *$p < 0.05$; **$p < 0.01$.

Figure S3

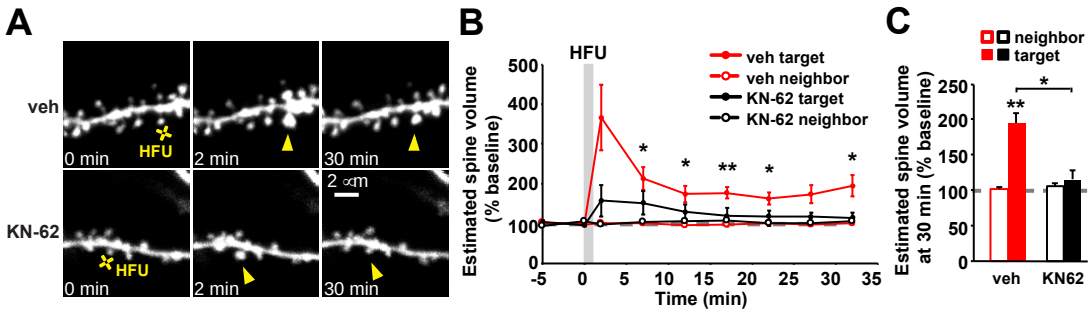
A
veh
KN-62
0 min
HFU
2 min
30 min
2 μm
B
HFU
veh target
veh neighbor
KN-62 target
KN-62 neighbor
Estimated spine volume (% baseline)
Time (min)
C
neighbor
target
Estimated spine volume at 30 min (% baseline)
veh
KN62

Chapter 3: Non-ionotropic NMDA receptor signaling alters structural plasticity of dendritic spines in a mouse model of schizophrenia

Preface

The following chapter was submitted as a manuscript titled “Non-ionotropic NMDA receptor signaling alters structural plasticity of dendritic spines in a mouse model of schizophrenia” to bioRxiv on March 5th, 2021 (https://doi.org/10.1101/2021.03.04.434016) and is pending submission for peer review. Aside from layout changes to fit the guidelines of the thesis, the chapter is the submitted version of the manuscript. The authors of the manuscript are Deborah K. Park, Ivar S. Stein, Eden V. Barragan, John A. Gray, and Karen Zito. Ivar S. Stein developed the initial hypothesis and experimental design of the research. Eden V. Barragan contributed electrophysiological data. Karen Zito and I wrote the manuscript. All authors contributed comments on the manuscript.

Abstract

Schizophrenia is a psychiatric disorder that affects over 20 million people globally. Notably, schizophrenia is associated with decreased density of dendritic spines and decreased levels of -serine, a co-agonist required for opening of the *N*-methyl-D-aspartate receptor (NMDAR). Hypofunction of NMDARs is thought to play a role in the pathophysiology of schizophrenia. We hypothesized that the lowered D-serine levels associated with schizophrenia would enhance ion flux-independent signaling by the NMDAR, which drives spine destabilization and loss, and eventually lead to the spine loss associated with schizophrenia. We tested our model using a schizophrenia mouse model lacking the enzyme for D -serine production (serine racemase knock out; SRKO). We show that activity-dependent spine growth is inhibited in SRKO mice of both sexes but can be acutely rescued by exogenous D -serine. When examining a wider range of stimulus strengths, we observed activity-dependent spine growth at higher stimulus strengths, but overall found a strong bias toward spine shrinkage in the SRKO mice as compared to wild-type littermates. We demonstrate that enhanced ion flux-independent signaling through the NMDAR contributes to this bias toward spine shrinkage, which is exacerbated by an increase in synaptic NMDARs in hippocampal synapses of SRKO mice. Our results support a model in which the lowered D-serine levels associated with schizophrenia lead to increased ion flux-independent NMDAR signaling and a bias toward spine shrinkage and destabilization.

Introduction

Experience-dependent growth and long-term stabilization of dendritic spines are critical for learning and memory formation (Hayashi-Takagi et al 2015, Xu et al 2009, Yang et al 2009). These spine structural changes are tightly associated with long-term potentiation (LTP) (Matsuzaki et al 2004) and long-term depression (LTD) (Oh et al 2013, Zhou et al 2004) of synaptic strength and are mediated through *N*-methyl-d-aspartate receptors (NMDARs). NMDARs open to allow influx of calcium upon the binding of glutamate and co-agonist, glycine or D-serine, and they also signal in an ion flux-independent manner upon the binding of glutamate alone (Dore et al 2015, Nabavi et al 2013, Stein et al 2015, Wong & Gray 2018). Notably, ion-flux independent (non-ionotropic) NMDAR signaling mediates LTD and spine shrinkage, and is also critical for LTP-induced spine growth (Stein et al 2021).

Dysfunctional NMDAR signaling is thought to contribute to the etiology of schizophrenia, a psychiatric disorder that affects up to 1% of the global population and is characterized by a variety of symptoms such as hallucinations and cognitive deficits (Coyle 2017). These debilitating symptoms may be linked to synaptic and neuroanatomical changes in the brain, such as decreased spine densities (Rosoklija et al 2000, Sweet et al 2009). As NMDARs mediate bidirectional structural plasticity and stabilization of spines (Hill & Zito 2013, Stein et al 2021), alterations in NMDAR function influence spine densities and impact the ability to learn and form memories (Alvarez et al 2007, Brigman et al 2010, Kannangara et al 2015, Ultanir et al 2007). Notably, patients have decreased levels of D-serine (Bendikov et al 2007, Hashimoto et al 2003a) and elevated levels of the endogenous NMDAR co-agonist blocker, kynurenic acid (Plitman et al 2017), and the enzyme for D-serine production is a risk gene for schizophrenia (Coyle 2017). Importantly, animal studies that mimic NMDAR hypofunction by reducing co-agonist binding or ion flux produce both cognitive deficits and decreased spine density similar to those associated with schizophrenia (Barnes et al 2014, Basu et al 2009, Latysheva & Raevskii 2003, Schobel et al 2013, Wu et al 2016).

We hypothesized that the decreased D-serine level associated with schizophrenia promotes ion flux-independent NMDAR signaling (Nabavi et al 2013, Stein et al 2015), creating a bias for spine shrinkage and ultimately leading to decreased spine density. To test our hypothesis, we used a schizophrenia mouse model, serine racemase knockout (SRKO) (Basu et al 2009), which lacks the enzyme required for D-serine production. Similar to patients with schizophrenia, these mutant mice have decreased levels of D-serine, decreased spine densities and cognitive deficits (Balu et al 2013, Basu et al 2009). We found that SRKO mice have impaired activity-dependent spine growth, and that activity-dependent spine structural plasticity is biased toward spine shrinkage. Furthermore, we observed increased numbers of synaptic NMDARs, reduced CaMKII activation, and increased non-ionotropic NMDAR signaling at hippocampal synapses of SRKO animals. Our study supports a model in which decreased D-serine levels lead to increased ion flux-independent NMDAR signaling that promotes spine shrinkage and drives decreased spine densities associated with schizophrenia.

Materials and methods

Animals. SRKO (Basu et al 2009) and GFP-M (Feng et al 2000) mice in a C57BL/6J background were crossed to generate serine racemase knockout and wild-type mice with a GFP cell fill in a subset of CA1 hippocampal pyramidal neurons. All experimental protocols were approved by the University of California Davis Institutional Animal Care and Use Committee.

Two-photon imaging and image analysis. Acute hippocampal slices were prepared from P14-21 WT and SRKO littermates of both sexes as described (Stein et al 2021). GFP-expressing CA1 pyramidal neurons at depths of 10-50 µm were imaged using a custom two-photon microscope (Woods et al 2011). For each neuron, image stacks (512 × 512 pixels; 0.02 µm per pixel; 1-µm z-steps) were collected from one segment of secondary or tertiary basal dendrite at 5 min intervals at 27-30 °C in recirculating artificial cerebral spinal fluid (ACSF; in mM: 127 NaCl, 25 $NaHCO_3$, 1.2 NaH_2PO_4, 2.5 KCl, 25 D-glucose, aerated with 95%O_2/5%CO_2, ~310 mOsm, pH 7.2) with 1 µM TTX, 0.1 mM Mg^{2+}, and 2 mM Ca^{2+}, unless otherwise stated. Cells were pre-incubated for at least 10 min with 10 µM D-serine or for at least 30 min with 10 µM L-689,560 (L-689) and 10 µM Bay-K (all from Tocris), which were included as indicated. Images are maximum projections of three-dimensional image stacks after applying a median filter (3 × 3) to raw image data. Estimated spine volume was measured from background-subtracted green fluorescence using the integrated pixel intensity of a boxed region surrounding the spine head, as described (Woods et al 2011).

Glutamate uncaging. High-frequency uncaging (HFU) consisted of 60 pulses (720 nm; 2 ms duration, 7-11 mW at the sample) at 2 Hz delivered in ACSF containing (in mM): 2 Ca^{2+}, 0.1 Mg^{2+}, 2.5 MNI-glutamate, and 0.001 TTX. The beam was parked at a point 0.5-1 µm from the spine at the position farthest from the dendrite. HFU+ stimulation consisted of 60 pulses (720

nm; 8 ms duration, 6-10 mW at the sample) at 6 Hz, delivered in ACSF containing (in mM): 10 Ca^{2+}, 0.1 Mg^{2+}, 5 MNI-glutamate, and 0.001 TTX. For experiments using HFU+ stimulation, healthy and stimulus responsive cells were selected as described (Stein et al 2021).

Electrophysiology. Modified transverse 300 µm slices of dorsal hippocampus were prepared from P15–P19 mice anesthetized with isoflurane (Bischofberger et al 2006), and mounted cut side down on a Leica VT1200 vibratome in ice-cold sucrose cutting buffer containing (in mM): 210 sucrose, 25 $NaHCO_3$, 2.5 KCl, 1.25 NaH_2PO_4, 7 glucose, 7 $MgCl_2$, and 0.5 $CaCl_2$. Slices were recovered for 1 h in 32°C ACSF solution containing (in mM): 119 NaCl, 26.2 $NaHCO_3$, 11 glucose, 2.5 KCl, 1 NaH2PO4, 2.5 $CaCl_2$, and 1.3 $MgSO_4$. Slices were perfused in ACSF at RT containing picrotoxin (0.1 mM) and TTX (0.5 µM) and saturated with 95%O_2/5%CO_2. mEPSCs were recorded from CA1 pyramidal neurons patched with 3–5 MΩ borosilicate pipettes filled with intracellular solution containing (in mM): 135 cesium methanesulfonate, 8 NaCl, 10 HEPES, 0.3 Na-GTP, 4 Mg-ATP, 0.3 EGTA, and 5 QX-314 (290 mOsm, pH 7.3). Series resistance was monitored and not compensated. Cells were discarded if series resistance varied by more than 25%. Recordings were obtained with a MultiClamp 700B amplifier (Molecular Devices), filtered at 2 kHz, digitized at 10 Hz. Miniature synaptic events were analyzed using Mini Analysis software (Synaptosoft) using a threshold amplitude of 5 pA for peak detection. To generate cumulative probability plots for amplitude and inter-event time interval, events from each CA1 pyramidal neuron (>100 per cell) were pooled for each group. The Kolmogorov-Smirnov two-sample test (KS test) was used to compare the distribution of events between WT and SRKO. Statistical comparisons were made using Graphpad Prism 8.0.

Biochemistry. Hippocampi of P20 mice of either sex were homogenized with 1% deoxycholate. For immunoprecipitation, 50 µL of Protein G Dynabeads (Invitrogen) were pre-incubated with 2.4 µg of either CaMKIIα (Leonard et al 1998, Leonard et al 1999, Lu et al 2007) or mouse IgG

antibody (sc-2025, Santa Cruz Biotechnology) at RT for 10 min, washed with 0.05% TBS-tween, incubated with 1000-1500 µg of protein lysate for 30 min at RT, washed four times with 0.01% TBS-triton, and then eluted. For PSD isolation, lysates were fractionated by centrifugation and sucrose gradient, and extracted with Triton X-100, as described (Dosemeci et al 2006). Protein samples were run on a SDS-PAGE gel at 30 mA and transferred to 0.45 um PVDF membrane for 210 min at 50 V. Blots were stained for total protein with Revert 700 Total Protein Stain Kit (LICOR). Membranes were blocked with TBS Odyssey Blocking Buffer (LICOR) and incubated overnight at 4°C with primary antibodies for GluN2B, GluN2A, GluN1, CaMKIIα (Leonard et al 1998, Leonard et al 1999, Lu et al 2007), pT286 CaMKIIα (sc-12886R, Santa Cruz), synaptophysin (Sigma S5768), or serine racemase (sc-365217, Santa Cruz). Secondary antibody (IRDye; LICOR) incubation was for 1 h at RT and the blots scanned and analyzed using Odyssey CLx and Image Studio.

Experimental Design and Statistical analysis. Cells for each condition were obtained from at least 3 independent hippocampal acute slices preparations of both sexes. Data analysis was done blind to the experimental condition. All statistics were calculated across cells and performed in GraphPad Prism 8.0. Student's unpaired t-test was used for all experiments. Details on 'n' are included in the figure legends. All data are represented as mean ± standard error of the mean (SEM). Statistical significance was set at $p < 0.05$ (two-tailed t test).

Results

LTP-associated growth of dendritic spines is impaired in SRKO mice

NMDAR-dependent LTP and associated spine growth, mediated by simultaneous binding of glutamate and synaptic co-agonist, D-serine, is an important cellular process for memory formation and maintenance of spine density. Based on the requirement for robust calcium influx during NMDAR-dependent spine growth and stabilization, we hypothesized that reduced bioavailability of D-serine observed in patients with schizophrenia (Bendikov et al 2007, Hashimoto et al 2003a) would obstruct LTP-associated spine growth and instead result in spine destabilization and the reduced spine density associated with the disorder (Rosoklija et al 2000, Sweet et al 2009).

To test our hypothesis, we crossed the SRKO mouse model of schizophrenia (Basu et al 2009) with the GFP-M (Feng et al 2000) mouse line to obtain D-serine deficient mice that have sparse neuronal GFP expression in the hippocampus allowing visualization of dendrites and spines. High-frequency uncaging (HFU) of glutamate at single dendritic spines on basal dendrites of CA1 neurons resulted in long-term growth of WT, but not SRKO spines (**Fig. 1A-C;** WT: 168 ± 17%; KO: 103 ± 7%). Notably, the lack of long-term spine growth in SRKO was rescued with acute treatment of 10 µM D-serine (**Fig. 1D-F;** WT: 201 ± 23%; KO: 169 ± 16%), demonstrating that the deficit in long-term spine growth is not due to chronic alterations in the SRKO animals or a role for serine racemase other than its role in synthesis of D-serine. Thus, LTP-associated spine growth is impaired in SRKO mice, as expected, and in line with the previously reported observation of LTP deficit in these mice (Basu et al 2009).

Structural plasticity curve is shifted to favor spine shrinkage in SRKO mice

Upon observing a complete block of activity-dependent spine growth in the SRKO mice, we wondered whether this result was indicative of a complete inability to support spine structural plasticity in the SRKO, or whether a stronger stimulus might be sufficient to overcome the

impairment of LTP-associated spine growth in the SRKO. To test this, we increased the extracellular Ca^{2+} concentration to 5 mM in order to strengthen the influx of Ca^{2+} in response to HFU stimulation. We found that HFU in 5 mM $CaCl_2$ led to long-term spine growth for both WT and SRKO (**Fig. 2A, B;** WT: 192 ± 30%; KO: 178 ± 20%), demonstrating that the signaling mechanisms downstream of Ca^{2+} influx that support long-term spine growth are intact in SRKO. We next wondered whether SRKO mice exhibit an overall bias for spine shrinkage across a broad range of stimulus strengths. Notably, although HFU normally leads to spine growth, this LTP-inducing stimulation can instead lead to spine shrinkage in the absence of co-agonist binding and strong influx of Ca^{2+}, due to glutamate-induced, ion flux-independent signaling of the NMDAR (Stein et al 2015). By delivering HFU across a broad range of $CaCl_2$ concentrations, we probed for bias in the direction of spine structural plasticity in SRKO mice relative to WT. Plotting the spine volume change at various $CaCl_2$ concentrations should produce an S-shaped plasticity curve that depicts spine shrinkage turning into growth as the $CaCl_2$ concentration increases. A bias for growth should result in the structural plasticity curve of SRKO shifting leftward relative to the WT, whereas a bias for shrinkage would result in a shift to the right.

We found that HFU in 3 mM $CaCl_2$ also causes spines of both WT and SRKO to undergo growth as non-ionotropic NMDAR signaling is still paired with sufficient amount of Ca^{2+} influx for growth to occur (**Fig. 2C, D;** WT: 187 ± 25%; KO: 193 ± 35%). In contrast, HFU in 1.5 mM $CaCl_2$ leads to spine shrinkage in SRKO while WT does not undergo any structural change (**Fig. 2E, F;** WT: 109 ± 5%; KO: 76 ± 5%). Finally, HFU in 0.3 mM $CaCl_2$ causes both WT and SRKO spines to undergo shrinkage as non-ionotropic NMDAR signaling occurs with minimal amounts of calcium influx (**Fig. 2G, H;** WT: 69 ± 7%; KO: 82 ± 3%). Plotting this data together with our results from Figure 1, we observe that both genotypes have similar S-shaped plasticity curves, but the SRKO structural plasticity curve is shifted to the right (**Fig. 2I**). The rightward shift in the

plasticity curve of SRKO mice supports that there is a bias for spine shrinkage in the SRKO as compared to WT.

Increased synaptic NMDARs and decreased CaMKII activation in SRKO

Because elevated NMDAR expression has been observed in SRKO (Balu & Coyle 2011, Mustafa et al 2010), we wondered if this was also the case in the hippocampus in young mice and thus, in combination with the reduction in D-serine levels, would allow for even more non-ionotropic NMDAR signaling during glutamatergic signaling. We hypothesized that the bias for spine shrinkage in SRKO may be due to the combination of reduced D-serine levels and increased expression of NMDARs available for non-ionotropic NMDAR signaling.

To investigate whether SRKO mice have more NMDARs at dendritic spines within the hippocampus, we isolated PSD fractions of P20 SRKO mice. We found an increased band intensity in SRKO for obligatory subunit GluN1, suggesting greater number of synaptic NMDARs in SRKO animals (**Fig. 3A, B;** KO: 141 ± 11%). Interestingly, we also observed increased synaptic enrichment (**Fig. 3A, B;** KO: 237 ± 15%) and total expression (**Fig. 3C, D;** KO: 122 ± 3%) of GluN2B in SRKO relative to WT. Despite the greater number of NMDARs, we expected disrupted calcium-dependent downstream signaling due to reduced co-agonist binding and thus reduction of calcium influx through the NMDAR. Indeed, when we probed CaMKII-GluN2B interaction by immunoprecipitation and for phosphorylation of CaMKII at the T286 autophosphorylation site, which are both integral for LTP and indicative of strong calcium influx (Halt et al 2012, Lee et al 2009), we found that basal levels of CaMKII-GluN2B interaction and pT286 are both decreased in SRKO (**Fig. 3E, F;** KO CaMKII-GluN2B: 68 ± 6%; KO pT286: 89 ± 1%), despite no change in CaMKII expression or enrichment levels in SRKO (**Fig. 3A, B;** KO CaMKII expression: 112 ± 4%; KO synaptic enrichment: 114 ± 15%), supporting decreased NMDAR calcium-dependent downstream signaling in these mutant mice.

Enhanced non-ionotropic NMDAR signaling in SRKO mice

Our observations of increased number of synaptic NMDARs in mice with reduced D-serine levels support that altered structural plasticity in SRKO could be due to increased non-ionotropic NMDAR signaling driven by glutamate binding to the increased number of NMDARs, in the absence of co-agonist binding (Stein et al 2020). Notably, non-ionotropic NMDAR signaling is required not only for spine shrinkage, but also for spine growth, which occurs in the presence of strong Ca^{2+} influx (Stein et al 2021). Because there is no direct means of measuring the relative amount of non-ionotropic signaling, we set out to probe the relative contribution of non-ionotropic NMDAR signaling to spine structural plasticity between the SRKO and WT in an assay that combines non-ionotropic signaling through the NMDAR with independently increased calcium influx through voltage-gated calcium channels (VGCCs) to drive spine growth (**Fig. 4A**). We speculated that we would see enhanced spine growth in the SRKO due to the enhanced numbers of NMDARs driving more glutamate-induced non-ionotropic NMDAR signaling.

To isolate non-ionotropic NMDAR signaling in SRKO mice, we used the NMDAR co-agonist site inhibitor L-689,560 (L-689) to mimic the absence of co-agonist and thus block NMDAR-mediated Ca^{2+} influx following glutamate binding. We combined this with the L-type Ca^{2+} channel agonist Bay K 8644 (Bay K) to promote Ca^{2+} influx through voltage-gated calcium channels (VGCCs). A modified HFU paradigm (HFU+) of higher frequency and longer duration stimuli was used to ensure strong AMPAR-dependent depolarization of the spine for VGCC opening, adjusted to induce a smaller, non-saturated increase in long-term spine size in WT (**Fig. 4B-D**). Remarkably, this same HFU+ stimulation drove a robust increase in spine growth in SRKO mice (**Fig. 4B-D;** WT: 122 ± 4%; KO: 171 ± 11%). This enhancement in spine growth was not due to increased AMPAR function in SRKO mice, as the amplitude of miniature excitatory postsynaptic currents (mEPSCs) was not different between WT and SRKO (**Fig. 4E;** WT: 10 ± 0.6 pA; KO: 9.3 ± 0.3 pA). As the amount of AMPAR-mediated depolarization and thus VGCC opening between the two genotypes should be of comparable level, we interpret the

greater amount of spine growth in SRKO to be indicative of a higher level of non-ionotropic NMDAR signaling. These results support our model (**Fig. 4F**) in which increased synaptic NMDARs in conditions of reduced D-serine levels in SRKO lead to more non-ionotropic NMDAR signaling that creates a bias toward spine shrinkage and loss.

Discussion

Lowered D-serine levels create a bias towards spine shrinkage

It has been widely reported that schizophrenia is associated with a reduction in dendritic spine density that is thought to contribute to cognitive deficits. As changes in spine density and gray matter volume mirror each other (Bennett 2011), and longitudinal MRI studies of high risk individuals report normal increase in gray matter during childhood that then declines in adolescence (Job et al 2005, Pantelis et al 2003, Thompson et al 2001), a time when spine pruning increases (Penzes et al 2011), it has been suggested that excessive spine elimination, rather than a deficit in new spine outgrowth, is the potential cause of decreased spine density in schizophrenia (Glausier & Lewis 2013).

Here, we show a disruption of long-term spine growth and a bias toward activity-induced spine shrinkage in the SRKO mouse model of schizophrenia, which is reported to have decreased spine density at older ages (Balu et al 2013). Although we observed a shift in the plasticity curve for the SRKO, we were able to induce both spine shrinkage and growth, and it has been demonstrated that spine density can be rescued in these mice with D-serine treatment (Balu & Coyle 2014). Thus, our studies support that serine racemase, the enzyme that produces d-serine and observed to interact with various synaptic structural proteins such as PSD95 (Lin et al 2016, Ma et al 2014), is itself not required for structural plasticity of spines. Notably, D-serine has been shown to promote spine stability (Lin et al 2016), likely through increased incidence of simultaneous glutamate and co-agonist binding to the NMDAR for Ca^{2+} influx required for stabilization (Hill & Zito 2013). As glutamate binding alone to the NMDAR drives spine shrinkage in an ion-flux independent manner (Stein et al 2015), we propose that the enhancement of non-ionotropic NMDAR signaling due to the decreased levels of D-serine biases toward spine shrinkage in the SRKO mice and may subsequently drive the spine loss associated with schizophrenia.

Enhanced levels and altered composition of synaptic NMDARs in SRKO mice

Our observation of increased synaptic enrichment of NMDARs relative to WT within the hippocampus is expected based on previous studies on SRKO mice showing increased expression of GluN1 (Balu & Coyle 2011, Mustafa et al 2010) and GluN2B (Basu et al 2009, Wong et al 2020). These changes in the overall number and composition of NMDARs are likely to be the consequence of lack of D-serine, as prior studies have demonstrated the role of co-agonist binding in priming of the NMDAR for endocytosis, with D-serine specifically acting on GluN2B subunits (Ferreira et al 2017, Nong et al 2003). In addition, we found that this increase in the number of NMDARs led to an increase in the magnitude of non-ionotropic signaling in SRKO, which would be expected to drive enhanced spine loss (Stein et al 2021).

Notably, despite the enhancement of NMDAR levels at the synapse, we observed decreased CaMKII-GluN2B interaction and decreased autophosphorylation of CaMKII in SRKO mice, which we attribute to the lack of strong Ca^{2+} influx required for increasing both CaMKII activity and interaction to GluN2B (Goodell et al 2017). This altered downstream CaMKII signaling likely contributes to NMDAR hypofunction in schizophrenia (Banerjee et al 2015).

Enhanced non-ionotropic NMDAR signaling in SRKO mice

We made several observations that support our hypothesis that there is increased ion flux-independent NMDAR signaling driving spine destabilization in the SRKO mice. First, we observed that stimulation protocols which normally induce spine growth in WT mice can instead drives spine shrinkage in SRKO. Second, we found increased NMDARs at hippocampal synapses in the SRKO mice, which, in combination with the reduced D-serine levels, would further bias NMDARs toward ion flux-independent signaling. Finally, we showed that supplementing non-ionotropic NMDAR activation with Ca^{2+} influx from voltage-gated Ca^{2+} channel leads to more spine growth in SRKO than in WT, supporting increased ion flux-

independent NMDAR signaling in these animals. This enhanced non-ionotropic NMDAR signaling would be expected to drive enhanced spine shrinkage and eventual spine elimination.

Notably, studies in which uncompetitive antagonists of NMDARs produce schizophrenia like symptoms in healthy individuals and exacerbate them in patients with the disorder helped give rise to the NMDAR hypofunction hypothesis (Javitt & Zukin 1991, Krystal et al 1994, Lahti et al 2001, Newcomer et al 1999). Due to high sensitivity of inhibitory GABAergic neurons to NMDAR blockers (Grunze et al 1996, Homayoun & Moghaddam 2007), decreased expression of interneurons (Hashimoto et al 2008, Hashimoto et al 2003b, Mellios et al 2009), and GABAergic markers (Glausier & Lewis 2017, Gonzalez-Burgos et al 2011, Lewis et al 2008, Lewis et al 1999), NMDAR hypofunction caused by reduced D-serine levels in schizophrenia may lead to disinhibition of excitatory neurons and result in glutamate spillover (Gallinat et al 2016, Kraguljac et al 2013, Lorrain et al 2003, van Elst et al 2005). Indeed, SRKO mice have been observed to have decreased PV expression and altered excitatory/inhibitory balance from GABAergic dysfunction (Jami et al 2020, Ploux et al 2020, Steullet et al 2017). This disinhibition should result in greater release of glutamate at dendritic spines that, when paired with reduced D-serine levels, would increase the amount of non-ionotropic NMDAR activation even further to promote spine shrinkage (Stein et al 2020) and decrease in spine density in the SRKO and schizophrenia (Balu et al 2013, Rosoklija et al 2000, Sweet et al 2009).

Here we show that the SRKO mouse model of schizophrenia displays altered dendritic structural plasticity that biases toward spine shrinkage. We further report an increased number of synaptic NMDARs in the hippocampus of the SRKO mice and increased ion flux-independent NMDAR signaling at hippocampal spines. Taken together, our findings support a model in which NMDAR hypofunction brought on by lack of D-serine, promotes increased NMDAR expression and excessive non-ionotropic NMDAR signaling that drives a bias towards spine shrinkage and likely contributes to decreased spine density associated with schizophrenia.

Figure Legends and Figures

Figure 1. LTP-associated growth of dendritic spines is impaired in SRKO mice.

(A, D) Representative images of basal dendrites of CA1 pyramidal neurons in acute hippocampal slices from of P14-21 WT and SRKO mice. Individual spines (yellow arrow) are stimulated with HFU of MNI-glutamate (yellow crosshair) during vehicle condition and in the presence of D-serine (10 µM). (**B, C)** HFU leads to growth in WT (black filled circles/bar; n=7 cells/7 mice; p=0.004) but not in SRKO (red filled circles/bar; n=9 cells/8 mice; p=0.63). Volume of unstimulated neighboring spines were not affected (open circles/bars). **(E, F)** Supplementing D-serine in SRKO (black filled circles/bar; n=6 cells/5 mice; p=0.007) rescues HFU-induced growth (red filled circles/bar; n=8 cells/7 mice; p=0.005). Data are represented as mean +/- SEM. *p<0.05; **p<0.01; ***p<0.001.

Figure 1

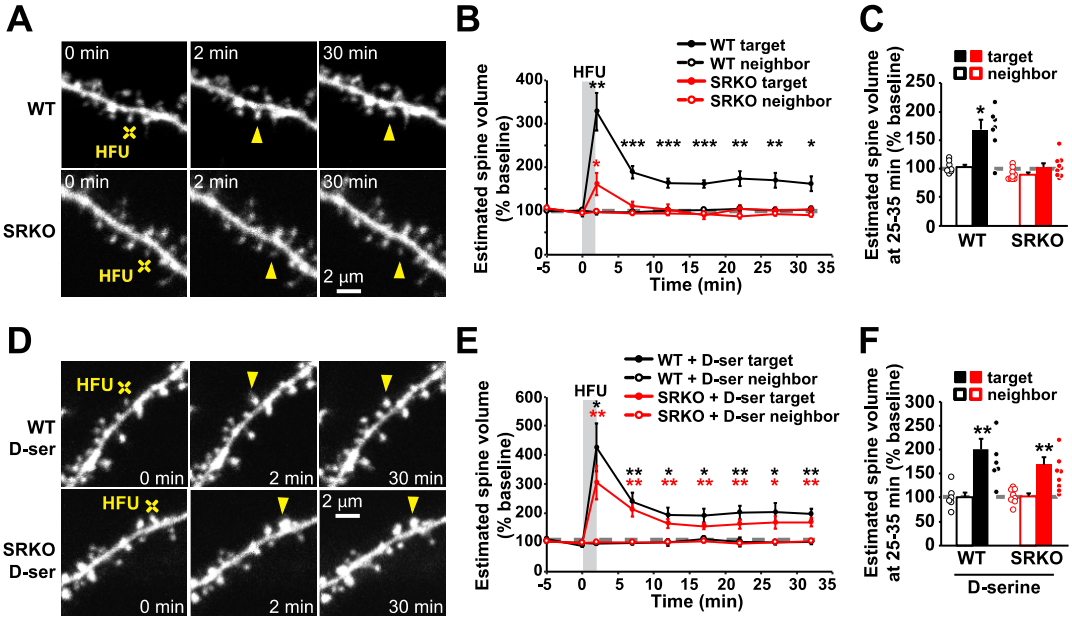
A
0 min
2 min
30 min
WT
HFU
SRKO
2 µm
B
WT target
WT neighbor
SRKO target
SRKO neighbor
HFU
Estimated spine volume (% baseline)
Time (min)
C
target
neighbor
Estimated spine volume at 25-35 min (% baseline)
WT
SRKO
D
WT D-ser
SRKO D-ser
E
WT + D-ser target
WT + D-ser neighbor
SRKO + D-ser target
SRKO + D-ser neighbor
F
D-serine

Figure 2. Structural plasticity is shifted to favor spine shrinkage in SRKO mice.

(A, B) HFU in 5 mM $CaCl_2$ shows spine growth is saturated to comparable levels between WT (black filled circles/bar; n=7 cells/3 mice; p=0.022) and SRKO (red filled circles/bar; n=6 cells/2 mice; p=0.010). **(C, D)** HFU in 3 mM $CaCl_2$ allows for spine growth in both WT (black filled circles/bar; n=7 cells/5 mice; p=0.013) and SRKO (red filled circles/bar; n=9 cells/3 mice; p=0.020). **(E, F)** HFU in 1.5 mM $CaCl_2$ does not lead to any spine volume change in WT (black filled circles/bar; n=6 cells/6 mice; p=0.13) while shrinkage already occurs in SRKO (red filled circles/bar; n=8 cells/5 mice; p=0.001). **(G, H)** HFU in ACSF of 0.3 mM $CaCl_2$ leads to spine shrinkage in both WT (black filled circles/bar; n=7 cells/4 mice; p=0.0061) and SRKO (red filled circles/bar; n=8 cells/5 mice; p=0.0002). **(I)** Structural plasticity curve of SRKO mice is shifted to the right, demonstrating a bias for spine shrinkage over growth. Data are represented as mean +/- SEM. *p<0.05; **p<0.01; ***p<0.001.

Figure 2

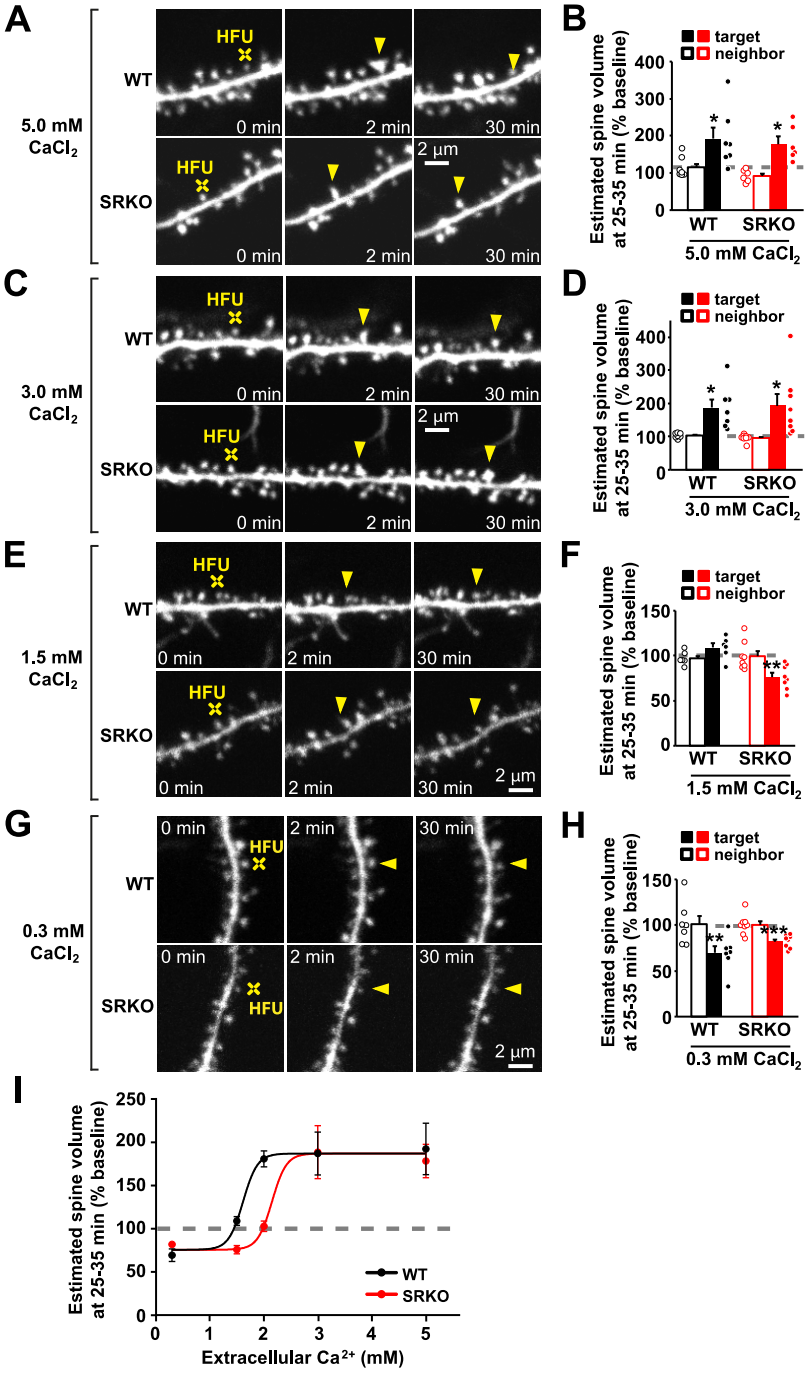
A
5.0 mM CaCl2
WT
SRKO
HFU
0 min
2 min
30 min
2 µm
B
target
neighbor
Estimated spine volume at 25-35 min (% baseline)
WT
SRKO
5.0 mM CaCl2
C
3.0 mM CaCl2
D
3.0 mM CaCl2
E
1.5 mM CaCl2
F
1.5 mM CaCl2
G
0.3 mM CaCl2
H
0.3 mM CaCl2
I
Extracellular Ca2+ (mM)

Figure 3. Increased synaptic NMDARs and decreased CaMKII activation in SRKO.

(A, B) PSD signals from P20 SRKO hippocampi (n=4 preps/12 mice) shows increased levels of GluN2B (p=0.003) and GluN1 (p=0.033) relative to WT. There is no change in GluN2A (p=0.49) and CaMKII (p=0.41). **(C, D)** Total homogenate (n=4 preps/4 mice) signal shows increased levels of GluN2B (p=0.004) relative to WT. There is no change in GluN2A (p=0.41), GluN1 (p=0.50), and CaMKII (p=0.074). **(E, F)** Immunoprecipitation of CaMKII from P20 SRKO hippocampi (n=3 preps/ 3 mice) shows decreased CaMKII-GluN2B interaction (p=0.034) and pT286 levels of CaMKII (p=0.010) relative to WT. Data are represented as mean +/- SEM. *p<0.05; **p<0.01; ***p<0.001.

Figure 3

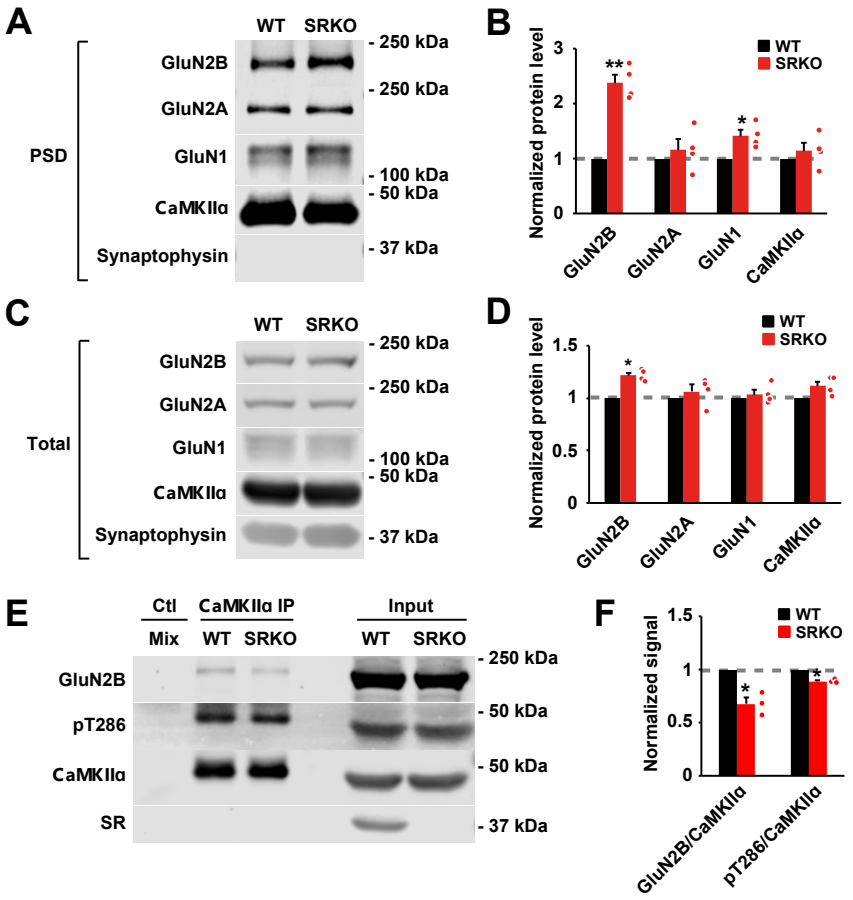
A
WT
SRKO
PSD
GluN2B
GluN2A
GluN1
CaMKIIα
Synaptophysin
250 kDa
250 kDa
100 kDa
50 kDa
37 kDa
B
Normalized protein level
WT
SRKO
GluN2B
GluN2A
GluN1
CaMKIIα
C
Total
D
E
Ctl
CaMKIIα IP
Input
Mix
pT286
SR
F
GluN2B/CaMKIIα
pT286/CaMKIIα
Normalized signal

Figure 4. Enhanced non-ionotropic NMDAR signaling in SRKO mice.

(A) Left: model of the components required for spine growth. Right: schematic of experiment in which the critical components of spine growth that originate from NMDARs are split and Ca^{2+} influx instead comes from VGCCs to observe relative amount of non-ionotropic NMDAR signaling between WT and SRKO. **(B)** Images of spines (yellow arrowhead) before and after HFU+ stimulation (yellow crosshair) in the presence of L689 (10 µM) and Bay K (10 µM) for non-ionotropic NMDAR activation and VGCC-mediated Ca^{2+} influx, respectively. **(C, D)** HFU+ stimulation drives spine growth in WT (black filled circles/bar; n=5 cells/5 mice; p=0.005) and SRKO (red filled circles/bar; n=6 cells/4 mice; p=0.001), but the amount of growth is larger in SRKO than WT (p=0.006). **(E)** Amplitude of mEPSCs of P15-19 CA1 pyramidal neurons are not changed in SRKO (WT: black line/bar; n=20 cells/3 mice; SRKO red line/bar: n=17 cells/3 mice; p=0.26). **(F)** Proposed model. Coincident binding of glutamate and D-serine allows for both non-ionotropic NMDAR signaling and calcium influx required for spine growth. In contrast, reduced levels of D-serine in schizophrenia mouse model SRKO results in glutamate binding alone to more NMDARs in the absence of D-serine that allows for strong non-ionotropic NMDAR activation with small calcium influx that promotes spine shrinkage. Data are represented as mean +/- SEM. *p<0.05; **p<0.01; ***p<0.001.

Figure 4

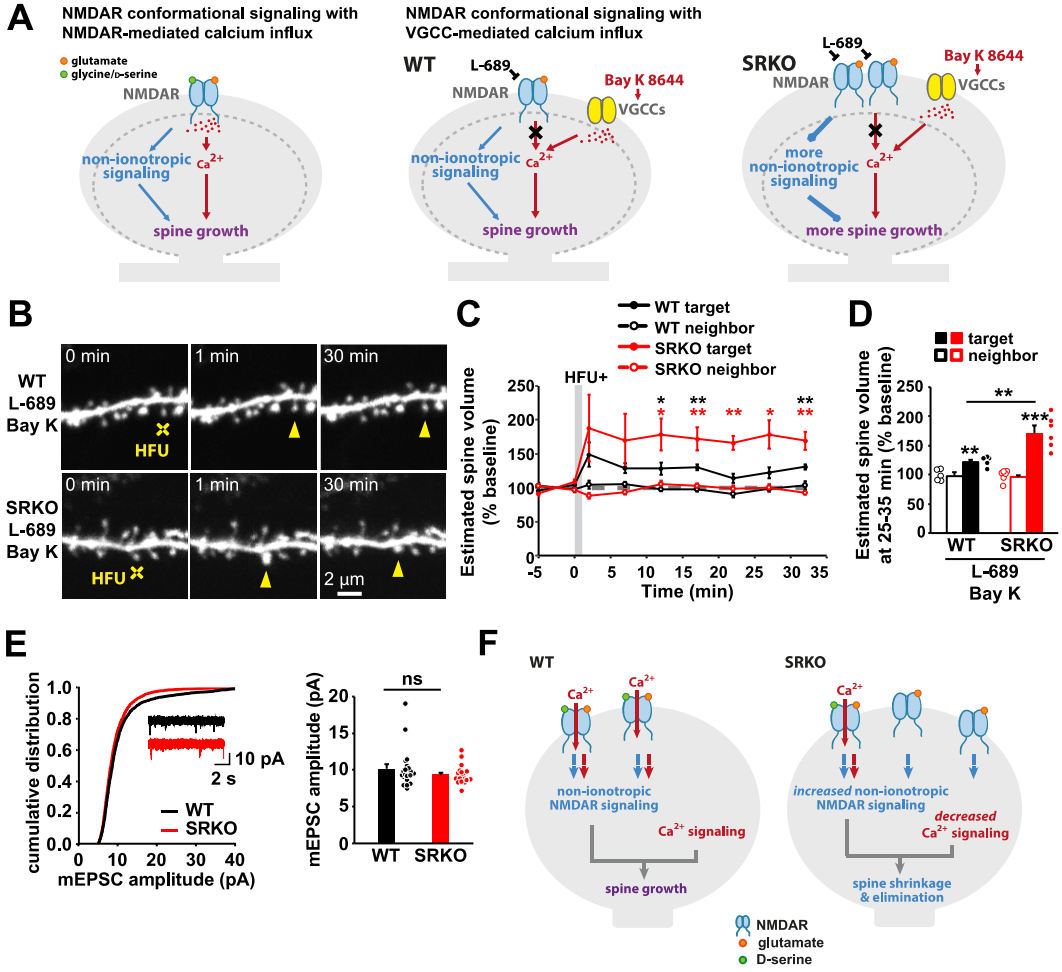
A
NMDAR conformational signaling with NMDAR-mediated calcium influx
glutamate
glycine/D-serine
NMDAR
non-ionotropic signaling
Ca2+
spine growth
NMDAR conformational signaling with VGCC-mediated calcium influx
WT
L-689
Bay K 8644
NMDAR
VGCCs
non-ionotropic signaling
Ca2+
spine growth
SRKO
L-689
Bay K 8644
NMDAR
VGCCs
more non-ionotropic signaling
Ca2+
more spine growth
B
WT
L-689
Bay K
0 min
1 min
30 min
HFU
SRKO
L-689
Bay K
0 min
1 min
30 min
HFU
2 µm
C
WT target
WT neighbor
SRKO target
SRKO neighbor
HFU+
Estimated spine volume (% baseline)
Time (min)
D
target
neighbor
Estimated spine volume at 25-35 min (% baseline)
WT
SRKO
L-689
Bay K
E
cumulative distribution
mEPSC amplitude (pA)
10 pA
2 s
WT
SRKO
ns
mEPSC amplitude (pA)
WT
SRKO
F
WT
SRKO
Ca2+
non-ionotropic NMDAR signaling
Ca2+ signaling
spine growth
increased non-ionotropic NMDAR signaling
decreased Ca2+ signaling
spine shrinkage & elimination
NMDAR
glutamate
D-serine

Chapter 4: Concluding Remarks

Contributions to the field

In a field where NMDARs were long thought to mediate synaptic plasticity by controlling calcium influx into the dendritic spine, the emergence of studies that demonstrated a novel, ion-flux independent mechanism of NMDARs emphasized that the molecular mechanism important for learning and memory is still largely unknown. Even more so is the fact that, for several years, our understanding of non-ionotropic NMDAR-dependent synaptic plasticity was limited to the requirement of glutamate-binding induced conformational change of the NMDAR and activity of p38 MAPK (Dore et al 2015, Nabavi et al 2013). In an effort to shed light on the molecular mechanism of non-ionotropic NMDAR signaling pathway responsible for shrinkage of dendritic spines, I first established that this ion-flux independent shrinkage of dendritic spines can be observed in acute slices and later identified CaMKII as a key molecule of the signaling pathway, which greatly expands the signaling cascade required for non-ionotropic NMDAR spine shrinkage (**Appendix**).

As glutamate binding to the NMDAR is sufficient to induce ion-flux independent signaling of the receptor, we next investigated the possible role of this signaling pathway during the induction of spine growth, which requires the binding of both glutamate and co-agonist to the receptor (**Chapter 2**). As inhibition of the key molecules of non-ionotropic NMDAR signaling cascade obstructed activity-dependent growth of spines, and spine growth could be artificially driven through the combination of non-ionotropic NMDAR activation with VGCC-mediated calcium influx, we demonstrated that non-ionotropic NMDAR signaling cascade is required for spine growth. With these surprising findings, we were able to further define the molecular mechanism of spine growth to involve both non-ionotropic and calcium-dependent signaling pathways, instead of only the latter. Our experimental design of driving spine growth by combining non-ionotropic NMDAR activation with VGCC-mediated calcium influx also suggests

that calcium nanodomains are not crucial for structural plasticity of spines. Another key finding in these experiments was that while p38 MAPK is required for spine growth, it is not necessary for LTP. Although both functional and structural changes of spines occur concurrently but are not completely mediated by the same signaling pathway, as previously observed that PP1 is required for LTD but not spine shrinkage (Zhou et al 2004), our study helps identify a similar divergence in the mechanism for LTP and spine growth.

We also explored the possibility that this ion-flux independent NMDAR signaling is implicated in schizophrenia (**Chapter 3**). A psychiatric disorder characterized by decreased spine density and reduced levels of NMDAR co-agonist, D-serine, we tested a novel hypothesis that decreased D-serine binding to NMDAR would create conditions in which non-ionotropic activation would be favored and thus block spine growth and stabilization that would eventually lead to decreased spine density associated with schizophrenia (Bendikov et al 2007, Hashimoto et al 2003a, Rosoklija et al 2000, Sweet et al 2009). To address this question, we used serine racemase knockout mice (SRKO) that lacks the enzyme required for D-serine production, resulting in reduced D-serine levels, decreased spine density, attenuated LTP, and cognitive deficits (Balu et al 2013, Basu et al 2009). By demonstrating that these SRKO mice have a bias for spine shrinkage over growth, our study provided a first look at the effects reduced D-serine levels has on the structural plasticity of dendritic spines. Our further experiments that demonstrate greater enrichment of synaptic NMDARs and greater structural plasticity of spines of SRKO mice when non-ionotropic NMDAR activation is combined with VGCC-mediated calcium influx suggest this change in structural plasticity of SRKO mice is due to enhanced non-ionotropic NMDAR signaling. Altogether, our research demonstrates a novel, potential role of non-ionotropic NMDAR signaling in the development of connectivity issues associated with schizophrenia.

In conclusion, I believe my thesis work has helped contribute to elucidating the molecular pathway that drives both shrinkage and growth of dendritic spines, as well as probing

the potential cause of dendritic spine loss observed with schizophrenia. Although the work discussed in the thesis advances our understanding of the molecular mechanisms of memory formation and development of schizophrenia, there is still a variety of unanswered questions that, if addressed, could further benefit the field of synaptic plasticity and development.

Future directions

Although our work has identified various key molecules to be critical components of the non-ionotropic NMDAR signaling pathway, it is not yet clear whether basal activity or change in activity level of these molecules is sufficient for mediating non-ionotropic NMDAR spine shrinkage. Due to the well-observed calcium-dependent activities of CaMKII and nNOS, it would be highly informative to observe if activation of non-ionotropic NMDAR signaling leads to increased activity of these enzymes, as observed with p38 MAPK during non-ionotropic cLTD (Nabavi et al 2013). The use of photoactivatable CaMKII inhibitor would also provide a look as to exactly when CaMKII activity is required for non-ionotropic NMDAR signaling (Murakoshi et al 2017). Additional investigation includes if nNOS-NOS1AP interactions that is crucial for non-ionotropic NMDAR signaling undergoes any active changes in an environment that does not involve strong influx of calcium (Li et al 2013, Stein et al 2020).

The involvement of CaMKII in both non-ionotropic and calcium-dependent signaling pathways is quite fascinating based on its already identified roles in synaptic plasticity. As studies have shown that LTP requires CaMKII-GluN2B interaction and release of CaMKII-actin interaction (Halt et al 2012, Kim et al 2015), but LTD requires the kinase to have a different substrate specificity and its interaction to GluN2B to be blocked (Coultrap et al 2014, Goodell et al 2017), investigating the possible mechanism of how CaMKII can mediate both spine shrinkage and growth can shed light on the fine mechanistic details of non-ionotropic NMDAR signaling. Based on observations that there is no change in CaMKII-GluN2B interaction during non-ionotropic cLTD (Aow et al 2015), lack of necessity for CaMKII-GluN2B during LTD

(Goodell et al 2017), and our result that calcium nanodomain is not required for spine growth, it is possible that non-ionotropic NMDAR signaling does not require any kinase or structural role of CaMKII near the NMDAR. As our model proposes that non-ionotropic NMDAR signaling culminates to cofilin acting on the actin skeleton, and it has been observed that CaMKII must dissociate from f-actin to make room for cofilin and other actin binding proteins for LTP and spine growth (Kim et al 2015), I hypothesize that non-ionotropic NMDAR signaling involves the release of CaMKII-actin interaction, which can be probed through the use of CaMKII-actin FRET sensor or mutant constructs of CaMKII that cannot dissociate from actin.

Although we demonstrated that spine growth requires both non-ionotropic NMDAR activation and strong calcium influx, we do not yet know the temporal requirements of these two factors relative to each other. As studies suggest that the agonist binding to the NMDAR leads to a conformational state that precedes opening of the pore (Durham et al 2020, Gibb et al 2018, Kazi et al 2013), non-ionotropic signaling and ion flux-dependent signaling may occur one after the other. The importance of the order at which ion flux-dependent and independent signaling occur has been observed in VGCC. VGCC-mediated gene transcription was demonstrated to be optimal when conformational change of the channel follows calcium influx, and reversing this order blocks gene transcription (Kobrinsky et al 2003, Li et al 2016a, Servili et al 2018). If the strong increase of intracellular calcium is not simultaneous to non-ionotropic NMDAR activation, would spine growth still occur? Would a sufficient delay of calcium influx lead to spine shrinkage? These questions could be addressed by timing non-ionotropic NMDAR signaling with calcium influx, whether through VGCC or uncaging of calcium. Delineating the temporal requirements of calcium signaling and non-ionotropic NMDAR activation required for LTP and spine growth would help provide further insight into how NMDARs mediate bidirectional structural plasticity of spines.

As evidenced by the different conformational changes of the NMDAR induced whether glutamate, glycine, or D-serine binds to the receptor (Dore et al 2015, Ferreira et al 2017), the

binding of co-agonists is capable of activating unique signaling pathways (Hu et al 2016, Li et al 2016b, Nong et al 2003) that can potentially be implicated in LTP and spine growth. For example, are LTP-associated surface diffusion and endocytosis of NMDARs (Dupuis et al 2014, Ferreira et al 2017) mediated by the non-ionotropic effects of co-agonist binding to the receptor, given that co-agonist binding primes the NMDAR for endocytosis (Nong et al 2003)? This could be investigated through the comparison of NMDAR surface diffusion between spine growth and 'artificial' growth in which NMDAR co-agonist binding is blocked and calcium influx is supplemented through an alternative source. And given that non-ionotropic NMDAR signaling is required for LTP-associated growth (Dupuis et al 2014), does this signaling pathway also depend on surface diffusion of NMDARs that is integral for LTP? Would crosslinking NMDARs with the use of antibodies obstruct non-ionotropic NMDAR signaling?

In contrast to the potential role enhanced non-ionotropic NMDAR signaling induced by glutamate binding in schizophrenia that was discussed in Chapter 3, ion flux-independent NMDAR signaling induced by the binding of both glutamate and co-agonist may be reduced and subsequently contribute to the bias toward shrinkage of dendritic spines. Non-ionotropic NMDAR signaling induced by both agonist and co-agonist binding has been shown to activate Src kinase (Weilinger et al 2016), which may have reduced activity in people with schizophrenia (Banerjee et al 2015). Because Src kinase alters NMDAR function, reduced kinase activity could contribute to decreased ion flux through the NMDAR in people with schizophrenia (Salter & Pitcher 2012). Thus, decreased levels of D-serine associated with the disorder (Bendikov et al 2007, Hashimoto et al 2003a) not only decreases the chance of pore opening that occurs when there is simultaneous binding of glutamate and co-agonist, but Src kinase would also not be activated through co-agonist binding induced non-ionotropic signaling (Weilinger et al 2016) and subsequently reduce ion flux through the NMDAR for when the pore does open. The combination of decreased D-serine levels (Bendikov et al 2007, Hashimoto et al 2003a), increased levels of endogenous co-agonist blocker kynurenic acid (Plitman et al 2017), and

decreased ion flux-independent activation of Src kinase can all work in a synergistic way of promoting shrinkage of elimination of spines through enhanced non-ionotropic NMDAR signaling in the absence of NMDAR-mediated calcium influx. This could be investigated with the use of SRKO mice and probing for possible changes in NMDAR-Src interaction and phosphorylation level of Src Y419 and Y530 associated with kinase activity (Banerjee et al 2015, Weilinger et al 2016).

Our understanding of ion-flux independent processes and signaling of NMDAR have rapidly expanded over the last several years. My thesis research has contributed to this recent advancement and can hopefully act as a stepping stone for others in further elucidating the complicated pathways of the various non-ionotropic NMDAR signaling cascades that dictate various processes ranging from synaptic plasticity to excitotoxicity.

Appendix: Identification of CaMKII in non-ionotropic NMDAR signaling and further look at the changes in molecular signaling and dendritic spines of SRKO mice

Preface

The following chapter contains a figure from published data titled “Molecular Mechanisms of Non-ionotropic NMDA Receptor Signaling in Dendritic Spine Shrinkage” that was accepted in JNeurosci on April 5th, 2020. It also contains unpublished data on SRKO that are related to the contents of Chapter 3 in investigating how non-ionotropic NMDAR-dependent structural plasticity is altered in these mutant mice and contributes to spine loss associated with schizophrenia. Ivar S. Stein and I collaborated with testing the role of CaMKII activity during non-ionotropic NMDAR-dependent spine shrinkage. Samuel Petshow assisted with the analysis of spine density of SRKO mice.

Abstract

Activity-dependent modification of dendritic spines is a crucial process for both proper development of the brain and formation of memories. In particular, the shrinkage of dendritic spines depends on ion flux-independent signaling of *N*-methyl-d-aspartate receptors (NMDARs) that is activated by glutamate binding to the receptor. Not only are the downstream signaling molecules that mediate this novel signaling pathway largely unknown, but this non-ionotropic signaling of NMDARs may also contribute to the loss of dendritic spines that is associated with schizophrenia. Here, we identify the activity of CaMKII to be a key player in mediating non-ionotropic NMDAR-dependent spine shrinkage. With the use of schizophrenia mouse model that lacks the enzyme for D-serine production (SRKO), we show that spine shrinkage occurs normally in physiological levels of Mg^{2+}. Spine dynamics and density of young mice are not significantly changed compared to wild-type littermates. While phosphorylation level of GluA1 S845 is not altered, we demonstrate that nNOS-NOS1AP interaction that is crucial for non-ionotropic NMDAR signaling to be elevated in male SRKO mice, but not females.

Introduction

Activity-dependent remodeling of neural circuitry is a critical cellular process thought to underlie learning and memory (Hayashi-Takagi et al 2015, Xu et al 2009, Yang et al 2009). Dynamic modifications of dendritic spines, which includes long-term potentiation (LTP) and long-term depression (LTD) and associated growth and shrinkage of spines, respectively (Matsuzaki et al 2004, Oh et al 2013), that are required for memory formation is mediated through the activation of *N*-methyl-d-aspartate receptors (NMDARs). Although LTP and associated growth of dendritic spines depend on ion flux through the receptor pore, NMDARs can also signal in an ion flux-independent manner to induce LTD and associated shrinkage of dendritic spines (Nabavi et al 2013, Stein et al 2015). Glutamate binding alone is sufficient to cause a conformational change that activates non-ionotropic signaling of the NMDAR (Dore et al 2015), but not much else is known about the molecular signaling pathway that occurs downstream of the receptor conformational change. As CaMKII has been implicated in LTD despite its calcium-dependent activity (Coultrap et al 2014), we investigated if this kinase would be a key player in non-ionotropic NMDAR-dependent spine shrinkage.

Additionally, this novel non-ionotropic NMDAR signaling is also potentially implicated in the development of schizophrenia. A psychiatric disorder with debilitating symptoms, patients have been observed to have decreased spine density (Rosoklija et al 2000, Sweet et al 2009) and decreased levels of D-serine (Bendikov et al 2007, Hashimoto et al 2003a), a co-agonist of NMDARs. As ion flux through the NMDAR requires simultaneous binding of glutamate and co-agonist to the receptor, we hypothesize that decreased levels of D-serine observed with schizophrenia promotes non-ionotropic NMDAR signaling that then creates a bias for shrinkage of dendritic spines that eventually culminates into decreased spine density associated with the disorder. To test this hypothesis, we used a schizophrenia mouse model, serine racemase knockout (SRKO), that lacks the enzyme required for D-serine production and thus has reduced

D-serine levels in addition to decreased spine density and cognitive deficits (Balu et al 2013, Basu et al 2009).

We demonstrate that CaMKII is a key molecule of the non-ionotropic NMDAR signaling cascade. We also show that non-ionotropic NMDAR-dependent spine shrinkage occurs normally in SRKO at physiological levels of Mg^{2+}. Biochemical characterization of SRKO mice reveal that while there is no change in the phosphorylation level of GluA1 S845, there is increased nNOS-NOS1AP interaction that is observed only in male mutant mice. Although previously observed to have reduced spine density at older ages, we demonstrate that SRKO mice have unaltered spine dynamics and densities at younger ages.

Materials and methods

Animals. SRKO (Basu et al 2009) and GFP-M (Feng et al 2000) mice in a C57BL/6J background were crossed to generate serine racemase knockout and wild-type mice with a GFP cell fill in a subset of CA1 hippocampal pyramidal neurons. All experimental protocols were approved by the University of California Davis Institutional Animal Care and Use Committee.

Two-photon imaging and image analysis. Acute hippocampal slices were prepared from P14-21 WT and SRKO littermates of both sexes as described (Stein et al 2021). GFP-expressing CA1 pyramidal neurons at depths of 10-50 µm were imaged using a custom two-photon microscope (Woods et al 2011). For each neuron, image stacks (512 × 512 pixels; 0.02 µm per pixel; 1-µm z-steps) were collected from one segment of secondary or tertiary basal dendrite at 5 min intervals at 27-30 °C in recirculating artificial cerebral spinal fluid (ACSF; in mM: 127 NaCl, 25 $NaHCO_3$, 1.2 NaH_2PO_4, 2.5 KCl, 25 D-glucose, aerated with 95%O_2/5%CO_2, ~310 mOsm, pH 7.2) with 1 µM TTX, 0.1 mM Mg^{2+}, and 2 mM Ca^{2+}, unless otherwise stated. Cells were pre-incubated for at least 30 min with 10 µM L-689,560 (Tocris), 10 µM KN-62 (Tocris) or 5 µM TAT-CN21 (purchased from Ulli Bayer). Images are maximum projections of three-dimensional image stacks after applying a median filter (3 × 3) to raw image data. Estimated spine volume was measured from background-subtracted green fluorescence using the integrated pixel intensity of a boxed region surrounding the spine head, as described (Woods et al 2011).

Glutamate uncaging. High-frequency uncaging (HFU) consisted of 60 pulses (720 nm; 2 ms duration, 7-11 mW at the sample) at 2 Hz delivered in ACSF containing (in mM): 2 Ca^{2+}, 0.1 Mg^{2+}, 2.5 MNI-glutamate, and 0.001 TTX. The beam was parked at a point 0.5-1 µm from the spine at the position farthest from the dendrite. HFU+ stimulation consisted of 60 pulses (720

nm; 8 ms duration, 6-10 mW at the sample) at 6 Hz, delivered in ACSF containing (in mM): 10 Ca^{2+}, 0.1 Mg^{2+}, 5 MNI-glutamate, and 0.001 TTX.

Biochemistry. Hippocampi of P20-26 mice of either sex were homogenized with 1% deoxycholate. For immunoprecipitation, 50 µL of Protein G Dynabeads (Invitrogen) were pre-incubated with 4 µg of either nNOS (sc-5302, Santa Cruz Biotechnology) or mouse IgG antibody (sc-2025, Santa Cruz Biotechnology) at RT for 10 min, washed with 0.05% TBS-tween, incubated with 1000-1500 µg of protein lysate for 30 min at RT, washed four times with 0.01% TBS-triton, and then eluted. Protein samples were run on a SDS-PAGE gel at 30 mA and transferred to 0.45 um PVDF membrane for 210 min at 50 V. Membranes were blocked with TBS Odyssey Blocking Buffer (LICOR) and incubated overnight at 4°C with primary antibodies for GluA1 (Leonard et al 1998, Leonard et al 1999, Lu et al 2007), pS845 GluA1 (ab76321, Abcam), nNOS (sc-5302), NOS1AP (sc-374504), or serine racemase (sc-365217). Secondary antibody (IRDye; LICOR) incubation was for 1 h at RT and the blots scanned and analyzed using Odyssey CLx and Image Studio.

Experimental Design and Statistical analysis. Cells for each condition were obtained from at least 3 independent hippocampal acute slices preparations of both sexes. Data analysis was done blind to the experimental condition. All statistics were calculated across cells and performed in GraphPad Prism 8.0. Student's unpaired t-test was used for all experiments. Details on 'n' are included in the figure legends. All data are represented as mean ± standard error of the mean (SEM). Statistical significance was set at $p < 0.05$ (two-tailed t test).

Results

We first tested if non-ionotropic NMDAR-dependent spine shrinkage can also be observed in acute slices, in addition to what has been previously observed in organotypic slices (Stein et al 2015). High-frequency uncaging (HFU) of glutamate at single dendritic spines in the presence of NMDAR co-agonist blocker, L689, led to spine shrinkage, as expected (**Fig. 1A-C**). After confirming that non-ionotropic NMDAR spine shrinkage can be induced in acute slices, we then questioned what molecule could be mediating this ion flux-independent signaling of NMDARs. Based on studies that demonstrated CaMKII to be critical for LTD and also associated with conformational change of the NMDARs required for non-ionotropic NMDAR LTD (Aow et al 2015, Coultrap et al 2014, Dore et al 2015), we next investigated if CaMKII activity was required for non-ionotropic NMDAR spine shrinkage. The presence of either CaMKII inhibitors, KN-62 or TAT-CN21, blocked spine shrinkage (**Fig. 1A-C**). This suggests that CaMKII activity is a key component of non-ionotropic NMDAR signaling which mediates shrinkage of dendritic spines.

Because structural plasticity of serine racemase knockout mice (SRKO) is altered to bias spine shrinkage over growth, as shown and discussed in **Chapter 3**, we next questioned if this resulted in altered formation and elimination of dendritic spines. Time-lapse imaging of acute slices show that the rate of both spine formation and elimination are not different between WT and SRKO (**Fig. 2A-C**). In line with the lack of change in spine dynamics, we observed that spine density and spine length were also not significantly altered in SRKO (**Fig. 3A-C**).

As the imaging experiments are done in 0.1 mM Mg^{2+}, we investigated if non-ionotropic NMDAR spine shrinkage could occur at a more physiological level of Mg^{2+} in SRKO without the presence of any co-agonist blockers. HFU in 1 mM Mg^{2+} leads to spine shrinkage in both SRKO and WT (**Fig. 4A-C**).

With our hypothesis that there is more non-ionotropic NMDAR signaling in SRKO and the nNOS-NOS1AP interaction being an important component of this ion-flux independent signaling cascade (Stein et al 2020), we then investigated if the basal level of nNOS-NOS1AP

interaction in SRKO was different from WT littermates. Based on observation that nNOS-NOS1AP interaction increases with strong influx of calcium (Li et al 2013), which may be reduced significantly in SRKO (Balu et al 2013, Basu et al 2009), it was expected that the nNOS-NOS1AP interaction would be reduced in SRKO. When nNOS was immunoprecipitated from hippocampi of P20 animals, we observed that the nNOS-NOS1AP interaction to be increased in SRKO males but not in SRKO females (**Fig. 5A-C**).

As non-ionotropic NMDAR activation leads to LTD (Nabavi et al 2013), we then questioned if SRKO would have decreased synaptic strength. To address this question, we took both the cortex and hippocampus of P22-26 and P60 mice and probed for pS845, a site on GluA1 subunit of AMPARs that is associated with LTD (Lee et al 1998). For both the cortex and hippocampus of younger and older animals, we observed no difference in the phosphorylation level of S845 (**Fig. 6A, B**). This lack of change in pS845 matches our observation of no difference in amplitude of mEPSC between WT and SRKO as shown in **Chapter 3**.

Discussion

Lack of changes in spine density and dynamics in SRKO mice

Although we demonstrate that HFU at 1 mM Mg^{2+} in SRKO and WT both lead to comparable levels of non-ionotropic NMDAR-dependent spine shrinkage, and, as discussed in Chapter 3, that the non-ionotropic signaling pathway may be enhanced in SRKO mice, we surprisingly did not observe any changes to dynamics or density of dendritic spines at P14-21. As SRKO mice are reported to have decreased spine density at older ages (Balu et al 2013), the lack of change in younger mice potentially mirrors the human longitudinal imaging studies of high risk individuals that show normal development of gray matter during childhood that declines later on (Job et al 2005, Pantelis et al 2003, Thompson et al 2001), suggesting excessive spine elimination as the cause of loss in synaptic connectivity observed with schizophrenia (Glausier & Lewis 2013). Thus, enhanced non-ionotropic NMDAR signaling in SRKO may promote excessive pruning of spines later on in the developmental period of the animal.

nNOS-NOS1AP expression is altered only in male SRKO mice

The unexpected increase in interaction between nNOS and NOS1AP may be due to increased expression of the latter; as D-serine decreases NOS1AP expression in male rodents, but not in females (Svane et al 2018), lack of D-serine in SRKO could instead lead to an increase in NOS1AP expression and subsequently drive basal level of interaction with nNOS only in male SRKO mice. Although there are mixed reports as to whether there is an association between NOS1AP and schizophrenia, NOS1AP may at least be linked to depression phenotypes in male patients of schizophrenia (Cheah et al 2015). Although the onset of the disorder occurs slightly earlier in males, it is also not quite clear if there is a sex difference with regards to the extent of neuroanatomical changes associated with schizophrenia (Adriano et al 2012, Gogtay et al 2011, Haijma et al 2013). However, the role of NOS1AP in structural plasticity of dendritic spines (Stein et al 2020) and the influence of D-serine on NOS1AP expression both suggest that

NOS1AP may play a role in the loss of dendritic spines associated with schizophrenia in a sex-dependent manner.

Figure legends and figures

Figure 1. CaMKII activity is required for spine shrinkage driven by non-ionotropic NMDAR signaling

(A) Images of dendrites from CA1 neurons of acute slices from P16-20 GFP-M mice before and after HFU (yellow cross) at single spines (yellow arrowhead) in the presence of L-689, L-689 with 10 μM KN-62 or L-689 with 5 μM TAT-CN21. **(B, C)** Inhibition of CaMKII activity with KN-62 (red filled circles/bar; 9 spines/9 cells) or TAT-CN21 (gray filled circles/bar; 9 spines/9 cells) blocked spine shrinkage induced by HFU in the presence of L-689 (black filled circles/bar; 8 spines/8 cells). Volume of unstimulated neighboring spines (open bars) was not changed. *$p < 0.05$, ***$p < 0.001$, paired two-tailed T-Test compared to baseline and calculated across cells. **(D)** Proposed model for the non-ionotropic NMDAR signaling pathway that drives spine shrinkage. Glutamate binding to the NMDAR induces conformational changes that drive dendritic spine shrinkage through NOS1AP-nNOS interactions, and the activities of nNOS, p38, MAPK, MK2, CaMKII, and cofilin-dependent severing of the actin cytoskeleton.

Figure 1

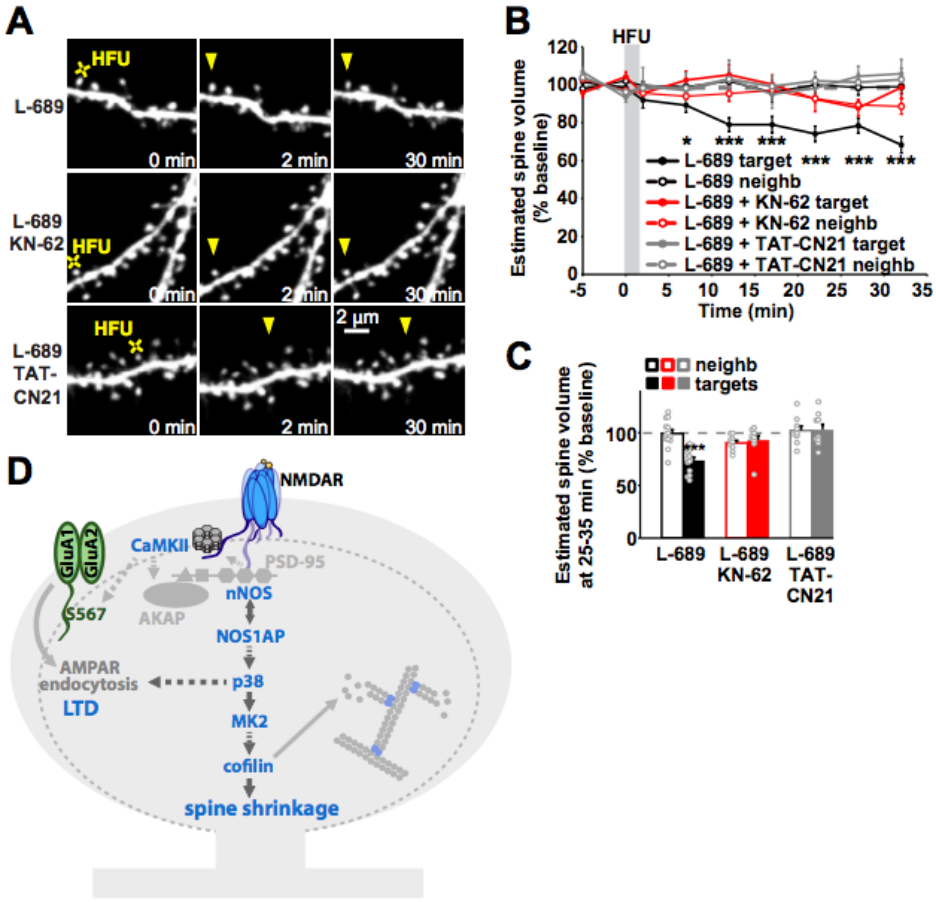
A
L-689
L-689 KN-62
L-689 TAT-CN21
HFU
0 min
2 min
30 min
2 µm
B
HFU
Estimated spine volume (% baseline)
Time (min)
L-689 target
L-689 neighb
L-689 + KN-62 target
L-689 + KN-62 neighb
L-689 + TAT-CN21 target
L-689 + TAT-CN21 neighb
C
neighb
targets
Estimated spine volume at 25-35 min (% baseline)
L-689
L-689 KN-62
L-689 TAT-CN21
D
NMDAR
CaMKII
PSD-95
GluA1
GluA2
S567
AKAP
nNOS
NOS1AP
AMPAR endocytosis
LTD
p38
MK2
cofilin
spine shrinkage

Figure 2. Spine dynamics and density are not altered in young SRKO mice. (A) Representative images of dendritic spine elimination in CA1 pyramidal neurons of P14-21 WT and SRKO acute hippocampal slices. **(B)** Representative images of new spine outgrowth in WT and SRKO. **(C)** Rate of spine formation and elimination are not different between WT (n=11) and SRKO (n=11). **(D)** Representative images of dendritic spines of CA1 pyramidal neurons of P14-21 WT (n=21) and SRKO (n=19) acute hippocampal slices. **(E, F)** Spine volume and length of WT and SRKO are not significantly different from each other. Data are represented as mean +/- SEM. *p<0.05; **p<0.01; ***p<0.001.

Figure 2

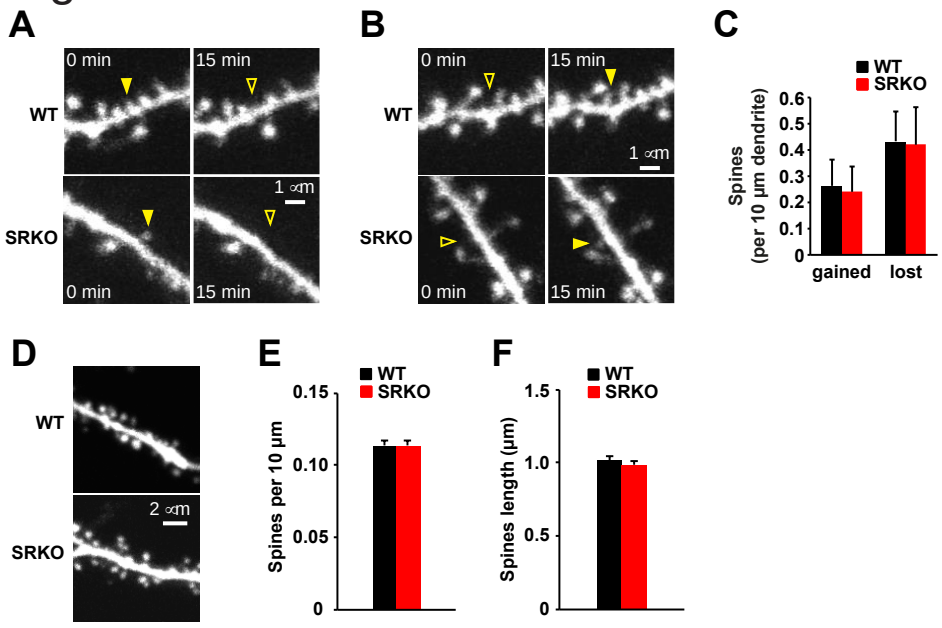
A
0 min
15 min
WT
SRKO
1 ∝m
0 min
15 min
B
0 min
15 min
WT
1 ∝m
SRKO
0 min
15 min
C
WT
SRKO
Spines
(per 10 µm dendrite)
0.6
0.5
0.4
0.3
0.2
0.1
0
gained
lost
D
WT
2 ∝m
SRKO
E
WT
SRKO
Spines per 10 µm
0.15
0.10
0.05
0
F
WT
SRKO
Spines length (µm)
1.5
1.0
0.5
0

Figure 3. HFU in 1 mM magnesium leads to shrinkage of spines in SRKO mice. (A) Representative images of dendritic spines of CA1 pyramidal neurons of P14-21 WT and SRKO acute hippocampal slices. **(B, C)** Spine volume of WT and SRKO decrease at different rates upon HFU in 1 mM magnesium. Data are represented as mean +/- SEM. *p<0.05; **p<0.01; ***p<0.001.

Figure 3

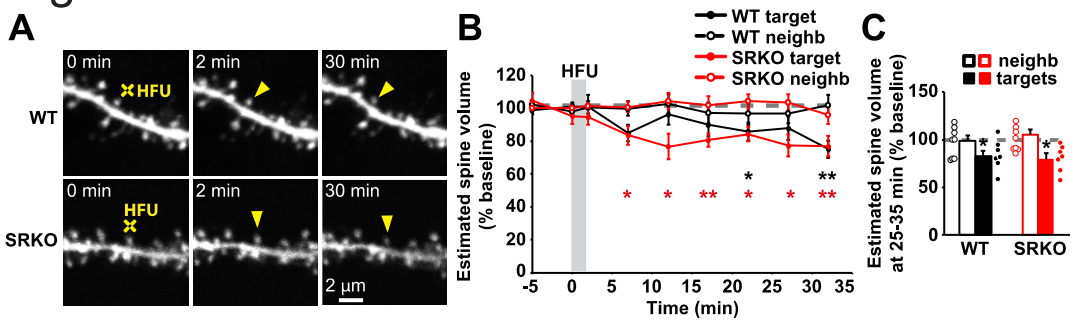
A
0 min
HFU
2 min
30 min
WT
0 min
HFU
2 min
30 min
SRKO
2 µm
B
WT target
WT neighb
SRKO target
SRKO neighb
HFU
Estimated spine volume (% baseline)
Time (min)
C
neighb
targets
Estimated spine volume at 25-35 min (% baseline)
WT
SRKO

Figure 4. nNOS-NOS1AP interaction is increased in male SRKO mice. (A, B) Representative blot images of nNOS immunoprecipitation prepared from male and female hippocampal tissue of P20 WT and SRKO mice. **(C)** nNOS-NOS1AP interaction is increased in male SRKO (n=5) relative to WT, while there is no difference in female SRKO (n=4). Data are represented as mean +/- SEM. *p<0.05; **p<0.01; ***p<0.001.

Figure 4

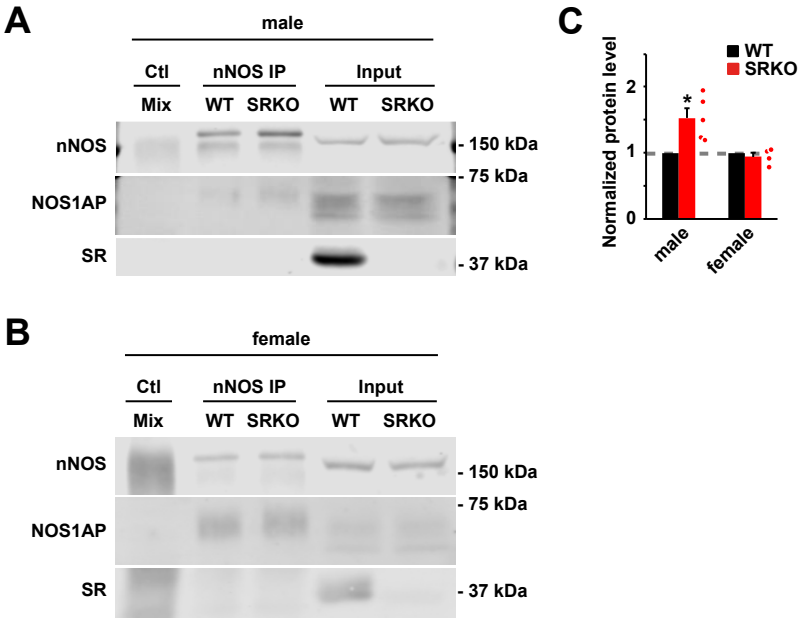
A
male
Ctl
nNOS IP
Input
Mix
WT
SRKO
WT
SRKO
nNOS
NOS1AP
SR
- 150 kDa
- 75 kDa
- 37 kDa
B
female
Ctl
nNOS IP
Input
Mix
WT
SRKO
WT
SRKO
nNOS
NOS1AP
SR
- 150 kDa
- 75 kDa
- 37 kDa
C
WT
SRKO
Normalized protein level
2
1
0
*
male
female

Figure 5. pS845 level is not different in SRKO mice. (A) Representative blot image of pS845 and GluA1 signals in P22-26 and P60 WT and SRKO mice. **(B)** pS845 is not changed in SRKO (n=3) relative to WT regardless of age and brain structure. Data are represented as mean +/- SEM. *p<0.05; **p<0.01; ***p<0.001.

Figure 5

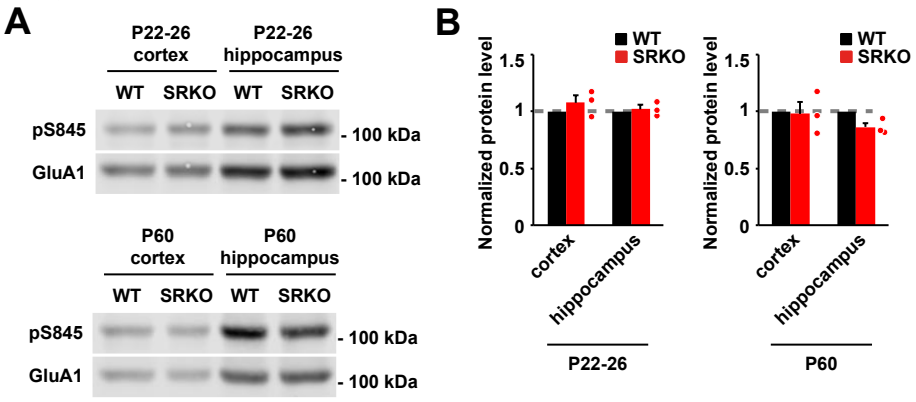
A
P22-26 cortex
P22-26 hippocampus
WT SRKO WT SRKO
pS845
GluA1
- 100 kDa
- 100 kDa
P60 cortex
P60 hippocampus
WT SRKO WT SRKO
pS845
GluA1
- 100 kDa
- 100 kDa
B
WT
SRKO
Normalized protein level
1.5
1
0.5
0
cortex
hippocampus
P22-26
P60

References

Abrahamsson T, Chou CYC, Li SY, Mancino A, Costa RP, et al. 2017. Differential Regulation of Evoked and Spontaneous Release by Presynaptic NMDA Receptors. *Neuron* 96: 839-55 e5

Adriano F, Caltagirone C, Spalletta G. 2012. Hippocampal volume reduction in first-episode and chronic schizophrenia: a review and meta-analysis. *Neuroscientist* 18: 180-200

Alvarez VA, Ridenour DA, Sabatini BL. 2007. Distinct structural and ionotropic roles of NMDA receptors in controlling spine and synapse stability. *J Neurosci* 27: 7365-76

Anderson DR, Meyers MJ, Vernier WF, Mahoney MW, Kurumbail RG, et al. 2007. Pyrrolopyridine inhibitors of mitogen-activated protein kinase-activated protein kinase 2 (MK-2). *J Med Chem* 50: 2647-54

Aow J, Dore K, Malinow R. 2015. Conformational signaling required for synaptic plasticity by the NMDA receptor complex. *Proc Natl Acad Sci U S A* 112: 14711-6

Arnold SE. 2000. Cellular and molecular neuropathology of the parahippocampal region in schizophrenia. *Ann N Y Acad Sci* 911: 275-92

Babiec WE, Guglietta R, Jami SA, Morishita W, Malenka RC, O'Dell TJ. 2014. Ionotropic NMDA receptor signaling is required for the induction of long-term depression in the mouse hippocampal CA1 region. *J Neurosci* 34: 5285-90

Bai D, Muller RU, Roder JC. 2002. Non-ionotropic cross-talk between AMPA and NMDA receptors in rodent hippocampal neurones. *J Physiol* 543: 23-33

Ballard TM, Pauly-Evers M, Higgins GA, Ouagazzal AM, Mutel V, et al. 2002. Severe impairment of NMDA receptor function in mice carrying targeted point mutations in the glycine binding site results in drug-resistant nonhabituating hyperactivity. *J Neurosci* 22: 6713-23

Balu DT, Coyle JT. 2011. Glutamate receptor composition of the post-synaptic density is altered in genetic mouse models of NMDA receptor hypo- and hyperfunction. *Brain Res* 1392: 1-7

Balu DT, Coyle JT. 2014. Chronic D-serine reverses arc expression and partially rescues dendritic abnormalities in a mouse model of NMDA receptor hypofunction. *Neurochem Int* 75: 76-8

Balu DT, Li Y, Puhl MD, Benneyworth MA, Basu AC, et al. 2013. Multiple risk pathways for schizophrenia converge in serine racemase knockout mice, a mouse model of NMDA receptor hypofunction. *Proc Natl Acad Sci U S A* 110: E2400-9

Banerjee A, Wang HY, Borgmann-Winter KE, MacDonald ML, Kaprielian H, et al. 2015. Src kinase as a mediator of convergent molecular abnormalities leading to NMDAR hypoactivity in schizophrenia. *Mol Psychiatry* 20: 1091-100

Barnes SA, Sawiak SJ, Caprioli D, Jupp B, Buonincontri G, et al. 2014. Impaired limbic cortico-striatal structure and sustained visual attention in a rodent model of schizophrenia. *Int J Neuropsychopharmacol* 18

Barria A, Malinow R. 2005. NMDA receptor subunit composition controls synaptic plasticity by regulating binding to CaMKII. *Neuron* 48: 289-301

Basu AC, Tsai GE, Ma CL, Ehmsen JT, Mustafa AK, et al. 2009. Targeted disruption of serine racemase affects glutamatergic neurotransmission and behavior. *Mol Psychiatry* 14: 719-27

Bayer KU, Schulman H. 2019. CaM Kinase: Still Inspiring at 40. *Neuron* 103: 380-94

Bendikov I, Nadri C, Amar S, Panizzutti R, De Miranda J, et al. 2007. A CSF and postmortem brain study of D-serine metabolic parameters in schizophrenia. *Schizophr Res* 90: 41-51

Benes FM, Kwok EW, Vincent SL, Todtenkopf MS. 1998. A reduction of nonpyramidal cells in sector CA2 of schizophrenics and manic depressives. *Biol Psychiatry* 44: 88-97

Benes FM, Sorensen I, Bird ED. 1991. Reduced neuronal size in posterior hippocampus of schizophrenic patients. *Schizophr Bull* 17: 597-608

Bennett MR. 2011. Schizophrenia: susceptibility genes, dendritic-spine pathology and gray matter loss. *Prog Neurobiol* 95: 275-300

Bialecki J, Werner A, Weilinger NL, Tucker CM, Vecchiarelli HA, et al. 2020. Suppression of Presynaptic Glutamate Release by Postsynaptic Metabotropic NMDA Receptor Signalling to Pannexin-1. *J Neurosci* 40: 729-42

Birnbaum JH, Bali J, Rajendran L, Nitsch RM, Tackenberg C. 2015. Calcium flux-independent NMDA receptor activity is required for Abeta oligomer-induced synaptic loss. *Cell Death Dis* 6: e1791

Bischofberger J, Engel D, Li L, Geiger JR, Jonas P. 2006. Patch-clamp recording from mossy fiber terminals in hippocampal slices. *Nat Protoc* 1: 2075-81

Bosch M, Castro J, Saneyoshi T, Matsuno H, Sur M, Hayashi Y. 2014. Structural and molecular remodeling of dendritic spine substructures during long-term potentiation. *Neuron* 82: 444-59

Bowers MS, Cacheaux LP, Sahu SU, Schmidt ME, Sennello JA, et al. 2020. NYX-2925 induces metabotropic N-methyl-d-aspartate receptor (NMDAR) signaling that enhances synaptic NMDAR and alpha-amino-3-hydroxy-5-methyl-4-isoxazolepropionic acid receptor. *J Neurochem* 152: 523-41

Brigman JL, Wright T, Talani G, Prasad-Mulcare S, Jinde S, et al. 2010. Loss of GluN2B-containing NMDA receptors in CA1 hippocampus and cortex impairs long-term depression, reduces dendritic spine density, and disrupts learning. *J Neurosci* 30: 4590-600

Burnet PW, Eastwood SL, Bristow GC, Godlewska BR, Sikka P, et al. 2008. D-amino acid oxidase activity and expression are increased in schizophrenia. *Mol Psychiatry* 13: 658-60

Cahn W, Rais M, Stigter FP, van Haren NE, Caspers E, et al. 2009. Psychosis and brain volume changes during the first five years of schizophrenia. *Eur Neuropsychopharmacol* 19: 147-51

Calcia MA, Madeira C, Alheira FV, Silva TC, Tannos FM, et al. 2012. Plasma levels of D-serine in Brazilian individuals with schizophrenia. *Schizophr Res* 142: 83-7

Carter BC, Jahr CE. 2016. Postsynaptic, not presynaptic NMDA receptors are required for spike-timing-dependent LTD induction. *Nat Neurosci* 19: 1218-24

Cheah SY, Lawford BR, Young RM, Morris CP, Voisey J. 2015. Association of NOS1AP variants and depression phenotypes in schizophrenia. *J Affect Disord* 188: 263-9

Chen J, Hu R, Liao H, Zhang Y, Lei R, et al. 2017. A non-ionotropic activity of NMDA receptors contributes to glycine-induced neuroprotection in cerebral ischemia-reperfusion injury. *Sci Rep* 7: 3575

Chen TW, Wardill TJ, Sun Y, Pulver SR, Renninger SL, et al. 2013. Ultrasensitive fluorescent proteins for imaging neuronal activity. *Nature* 499: 295-300

Coultrap SJ, Freund RK, O'Leary H, Sanderson JL, Roche KW, et al. 2014. Autonomous CaMKII mediates both LTP and LTD using a mechanism for differential substrate site selection. *Cell Rep* 6: 431-7

Coyle JT. 2017. Schizophrenia: Basic and Clinical. *Adv Neurobiol* 15: 255-80

Cuenda A, Rouse J, Doza YN, Meier R, Cohen P, et al. 1995. SB 203580 is a specific inhibitor of a MAP kinase homologue which is stimulated by cellular stresses and interleukin-1. *FEBS Lett* 364: 229-33

Davies J, Evans RH, Herrling PL, Jones AW, Olverman HJ, et al. 1986. CPP, a new potent and selective NMDA antagonist. Depression of central neuron responses, affinity for [3H]D-AP5 binding sites on brain membranes and anticonvulsant activity. *Brain Res* 382: 169-73

Davies SP, Reddy H, Caivano M, Cohen P. 2000. Specificity and mechanism of action of some commonly used protein kinase inhibitors. *Biochem J* 351: 95-105

DeVito LM, Balu DT, Kanter BR, Lykken C, Basu AC, et al. 2011. Serine racemase deletion disrupts memory for order and alters cortical dendritic morphology. *Genes Brain Behav* 10: 210-22

Dore K, Aow J, Malinow R. 2015. Agonist binding to the NMDA receptor drives movement of its cytoplasmic domain without ion flow. *Proc Natl Acad Sci U S A* 112: 14705-10

Dore K, Malinow R. 2020. Elevated PSD-95 Blocks Ion-flux Independent LTD: A Potential New Role for PSD-95 in Synaptic Plasticity. *Neuroscience*

Dosemeci A, Tao-Cheng JH, Vinade L, Jaffe H. 2006. Preparation of postsynaptic density fraction from hippocampal slices and proteomic analysis. *Biochem Biophys Res Commun* 339: 687-94

Dupuis JP, Ladepeche L, Seth H, Bard L, Varela J, et al. 2014. Surface dynamics of GluN2B-NMDA receptors controls plasticity of maturing glutamate synapses. *EMBO J* 33: 842-61

Durham RJ, Paudyal N, Carrillo E, Bhatia NK, Maclean DM, et al. 2020. Conformational spread and dynamics in allostery of NMDA receptors. *Proc Natl Acad Sci U S A* 117: 3839-47

El-Tallawy HN, Saleem TH, El-Ebidi AM, Hassan MH, Gabra RH, et al. 2017. Clinical and biochemical study of d-serine metabolism among schizophrenia patients. *Neuropsychiatr Dis Treat* 13: 1057-63

Feng G, Mellor RH, Bernstein M, Keller-Peck C, Nguyen QT, et al. 2000. Imaging neuronal subsets in transgenic mice expressing multiple spectral variants of GFP. *Neuron* 28: 41-51

Ferreira JS, Papouin T, Ladepeche L, Yao A, Langlais VC, et al. 2017. Co-agonists differentially tune GluN2B-NMDA receptor trafficking at hippocampal synapses. *Elife* 6

Fiore M, Forli S, Manetti F. 2016. Targeting Mitogen-Activated Protein Kinase-Activated Protein Kinase 2 (MAPKAPK2, MK2): Medicinal Chemistry Efforts To Lead Small Molecule Inhibitors to Clinical Trials. *J Med Chem* 59: 3609-34

Gallinat J, McMahon K, Kuhn S, Schubert F, Schaefer M. 2016. Cross-sectional Study of Glutamate in the Anterior Cingulate and Hippocampus in Schizophrenia. *Schizophr Bull* 42: 425-33

Garey LJ, Ong WY, Patel TS, Kanani M, Davis A, et al. 1998. Reduced dendritic spine density on cerebral cortical pyramidal neurons in schizophrenia. *J Neurol Neurosurg Psychiatry* 65: 446-53

Gauchy C, Nairn AC, Glowinski J, Premont J. 2002. N-Methyl-D-aspartate receptor activation inhibits protein synthesis in cortical neurons independently of its ionic permeability properties. *Neuroscience* 114: 859-67

Gibb AJ, Ogden KK, McDaniel MJ, Vance KM, Kell SA, et al. 2018. A structurally derived model of subunit-dependent NMDA receptor function. *J Physiol* 596: 4057-89

Glantz LA, Lewis DA. 2000. Decreased dendritic spine density on prefrontal cortical pyramidal neurons in schizophrenia. *Arch Gen Psychiatry* 57: 65-73

Glausier JR, Lewis DA. 2013. Dendritic spine pathology in schizophrenia. *Neuroscience* 251: 90-107

Glausier JR, Lewis DA. 2017. GABA and schizophrenia: Where we stand and where we need to go. *Schizophr Res* 181: 2-3

Gogtay N, Vyas NS, Testa R, Wood SJ, Pantelis C. 2011. Age of onset of schizophrenia: perspectives from structural neuroimaging studies. *Schizophr Bull* 37: 504-13

Gonzalez-Burgos G, Fish KN, Lewis DA. 2011. GABA neuron alterations, cortical circuit dysfunction and cognitive deficits in schizophrenia. *Neural Plast* 2011: 723184

Goodell DJ, Zaegel V, Coultrap SJ, Hell JW, Bayer KU. 2017. DAPK1 Mediates LTD by Making CaMKII/GluN2B Binding LTP Specific. *Cell Rep* 19: 2231-43

Grunze HC, Rainnie DG, Hasselmo ME, Barkai E, Hearn EF, et al. 1996. NMDA-dependent modulation of CA1 local circuit inhibition. *J Neurosci* 16: 2034-43

Hagiwara H, Iyo M, Hashimoto K. 2013. Neonatal disruption of serine racemase causes schizophrenia-like behavioral abnormalities in adulthood: clinical rescue by d-serine. *PLoS One* 8: e62438

Haijma SV, Van Haren N, Cahn W, Koolschijn PC, Hulshoff Pol HE, Kahn RS. 2013. Brain volumes in schizophrenia: a meta-analysis in over 18 000 subjects. *Schizophr Bull* 39: 1129-38

Halt AR, Dallapiazza RF, Zhou Y, Stein IS, Qian H, et al. 2012. CaMKII binding to GluN2B is critical during memory consolidation. *EMBO J* 31: 1203-16

Han L, Campanucci VA, Cooke J, Salter MW. 2013. Identification of a single amino acid in GluN1 that is critical for glycine-primed internalization of NMDA receptors. *Mol Brain* 6: 36

Hashimoto K, Fukushima T, Shimizu E, Komatsu N, Watanabe H, et al. 2003a. Decreased serum levels of D-serine in patients with schizophrenia: evidence in support of the N-methyl-D-aspartate receptor hypofunction hypothesis of schizophrenia. *Arch Gen Psychiatry* 60: 572-6

Hashimoto K, Shimizu E, Komatsu N, Watanabe H, Shinoda N, et al. 2005. No changes in serum epidermal growth factor levels in patients with schizophrenia. *Psychiatry Res* 135: 257-60

Hashimoto T, Arion D, Unger T, Maldonado-Aviles JG, Morris HM, et al. 2008. Alterations in GABA-related transcriptome in the dorsolateral prefrontal cortex of subjects with schizophrenia. *Mol Psychiatry* 13: 147-61

Hashimoto T, Volk DW, Eggan SM, Mirnics K, Pierri JN, et al. 2003b. Gene expression deficits in a subclass of GABA neurons in the prefrontal cortex of subjects with schizophrenia. *J Neurosci* 23: 6315-26

Hayama T, Noguchi J, Watanabe S, Takahashi N, Hayashi-Takagi A, et al. 2013. GABA promotes the competitive selection of dendritic spines by controlling local Ca2+ signaling. *Nature neuroscience* 16: 1409-16

Hayashi T, Umemori H, Mishina M, Yamamoto T. 1999. The AMPA receptor interacts with and signals through the protein tyrosine kinase Lyn. *Nature* 397: 72-6

Hayashi-Takagi A, Yagishita S, Nakamura M, Shirai F, Wu YI, et al. 2015. Labelling and optical erasure of synaptic memory traces in the motor cortex. *Nature* 525: 333-8

Heckers S, Heinsen H, Geiger B, Beckmann H. 1991. Hippocampal neuron number in schizophrenia. A stereological study. *Arch Gen Psychiatry* 48: 1002-8

Hedrick NG, Harward SC, Hall CE, Murakoshi H, McNamara JO, Yasuda R. 2016. Rho GTPase complementation underlies BDNF-dependent homo- and heterosynaptic plasticity. *Nature* 538: 104-08

Heresco-Levy U, Javitt DC, Ebstein R, Vass A, Lichtenberg P, et al. 2005. D-serine efficacy as add-on pharmacotherapy to risperidone and olanzapine for treatment-refractory schizophrenia. *Biol Psychiatry* 57: 577-85

Hess P, Lansman JB, Tsien RW. 1984. Different modes of Ca channel gating behaviour favoured by dihydropyridine Ca agonists and antagonists. *Nature* 311: 538-44

Hidaka H, Yokokura H. 1996. Molecular and cellular pharmacology of a calcium/calmodulin-dependent protein kinase II (CaM kinase II) inhibitor, KN-62, and proposal of CaM kinase phosphorylation cascades. *Adv Pharmacol* 36: 193-219

Hill TC, Zito K. 2013. LTP-induced long-term stabilization of individual nascent dendritic spines. *J Neurosci* 33: 678-86

Holtmaat AJ, Trachtenberg JT, Wilbrecht L, Shepherd GM, Zhang X, et al. 2005. Transient and persistent dendritic spines in the neocortex in vivo. *Neuron* 45: 279-91

Homayoun H, Moghaddam B. 2007. NMDA receptor hypofunction produces opposite effects on prefrontal cortex interneurons and pyramidal neurons. *J Neurosci* 27: 11496-500

Honkura N, Matsuzaki M, Noguchi J, Ellis-Davies GC, Kasai H. 2008. The subspine organization of actin fibers regulates the structure and plasticity of dendritic spines. *Neuron* 57: 719-29

Hu R, Chen J, Lujan B, Lei R, Zhang M, et al. 2016. Glycine triggers a non-ionotropic activity of GluN2A-containing NMDA receptors to confer neuroprotection. *Sci Rep* 6: 34459

Jami SA, Cameron S, Wong JM, Daly ER, McAllister AK, Gray JA. 2020. Increased excitation-inhibition balance due to a loss of GABAergic synapses in the serine racemase knockout model of NMDA receptor hypofunction. *bioRxiv*

Javitt DC, Zukin SR. 1991. Recent advances in the phencyclidine model of schizophrenia. *Am J Psychiatry* 148: 1301-8

Job DE, Whalley HC, Johnstone EC, Lawrie SM. 2005. Grey matter changes over time in high risk subjects developing schizophrenia. *Neuroimage* 25: 1023-30

Kannangara TS, Eadie BD, Bostrom CA, Morch K, Brocardo PS, Christie BR. 2015. GluN2A-/- Mice Lack Bidirectional Synaptic Plasticity in the Dentate Gyrus and Perform Poorly on Spatial Pattern Separation Tasks. *Cereb Cortex* 25: 2102-13

Karasawa J, Hashimoto K, Chaki S. 2008. D-Serine and a glycine transporter inhibitor improve MK-801-induced cognitive deficits in a novel object recognition test in rats. *Behav Brain Res* 186: 78-83

Kazi R, Gan Q, Talukder I, Markowitz M, Salussolia CL, Wollmuth LP. 2013. Asynchronous movements prior to pore opening in NMDA receptors. *J Neurosci* 33: 12052-66

Kessels HW, Nabavi S, Malinow R. 2013. Metabotropic NMDA receptor function is required for beta-amyloid-induced synaptic depression. *Proc Natl Acad Sci U S A* 110: 4033-8

Khan MA, Houck DR, Gross AL, Zhang XL, Cearley C, et al. 2018. NYX-2925 Is a Novel NMDA Receptor-Specific Spirocyclic-beta-Lactam That Modulates Synaptic Plasticity Processes Associated with Learning and Memory. *Int J Neuropsychopharmacol* 21: 242-54

Kim IH, Racz B, Wang H, Burianek L, Weinberg R, et al. 2013. Disruption of Arp2/3 results in asymmetric structural plasticity of dendritic spines and progressive synaptic and behavioral abnormalities. *The Journal of neuroscience : the official journal of the Society for Neuroscience* 33: 6081-92

Kim K, Lakhanpal G, Lu HE, Khan M, Suzuki A, et al. 2015. A Temporary Gating of Actin Remodeling during Synaptic Plasticity Consists of the Interplay between the Kinase and Structural Functions of CaMKII. *Neuron* 87: 813-26

Kobrinsky E, Schwartz E, Abernethy DR, Soldatov NM. 2003. Voltage-gated mobility of the Ca2+ channel cytoplasmic tails and its regulatory role. *J Biol Chem* 278: 5021-8

Konopaske GT, Lange N, Coyle JT, Benes FM. 2014. Prefrontal cortical dendritic spine pathology in schizophrenia and bipolar disorder. *JAMA Psychiatry* 71: 1323-31

Kraguljac NV, White DM, Reid MA, Lahti AC. 2013. Increased hippocampal glutamate and volumetric deficits in unmedicated patients with schizophrenia. *JAMA Psychiatry* 70: 1294-302

Krystal JH, Karper LP, Seibyl JP, Freeman GK, Delaney R, et al. 1994. Subanesthetic effects of the noncompetitive NMDA antagonist, ketamine, in humans. Psychotomimetic, perceptual, cognitive, and neuroendocrine responses. *Arch Gen Psychiatry* 51: 199-214

Kwon HB, Sabatini BL. 2011. Glutamate induces de novo growth of functional spines in developing cortex. *Nature* 474: 100-4

Lahti AC, Weiler MA, Tamara Michaelidis BA, Parwani A, Tamminga CA. 2001. Effects of ketamine in normal and schizophrenic volunteers. *Neuropsychopharmacology* 25: 455-67

Lai CSW, Adler A, Gan WB. 2018. Fear extinction reverses dendritic spine formation induced by fear conditioning in the mouse auditory cortex. *Proc Natl Acad Sci U S A* 115: 9306-11

Lane HY, Lin CH, Huang YJ, Liao CH, Chang YC, Tsai GE. 2010. A randomized, double-blind, placebo-controlled comparison study of sarcosine (N-methylglycine) and D-serine add-on treatment for schizophrenia. *Int J Neuropsychopharmacol* 13: 451-60

Latysheva NV, Raevskii KS. 2003. Behavioral analysis of the consequences of chronic blockade of NMDA-type glutamate receptors in the early postnatal period in rats. *Neurosci Behav Physiol* 33: 123-31

Laviv T, Kim BB, Chu J, Lam AJ, Lin MZ, Yasuda R. 2016. Simultaneous dual-color fluorescence lifetime imaging with novel red-shifted fluorescent proteins. *Nat Methods* 13: 989-92

Lee HK, Kameyama K, Huganir RL, Bear MF. 1998. NMDA induces long-term synaptic depression and dephosphorylation of the GluR1 subunit of AMPA receptors in hippocampus. *Neuron* 21: 1151-62

Lee SJ, Escobedo-Lozoya Y, Szatmari EM, Yasuda R. 2009. Activation of CaMKII in single dendritic spines during long-term potentiation. *Nature* 458: 299-304

Leeson PD, Carling RW, Moore KW, Moseley AM, Smith JD, et al. 1992. 4-Amido-2-carboxytetrahydroquinolines. Structure-activity relationships for antagonism at the glycine site of the NMDA receptor. *J Med Chem* 35: 1954-68

Lehmann J, Schneider J, McPherson S, Murphy DE, Bernard P, et al. 1987. CPP, a selective N-methyl-D-aspartate (NMDA)-type receptor antagonist: characterization in vitro and in vivo. *J Pharmacol Exp Ther* 240: 737-46

Leonard AS, Davare MA, Horne MC, Garner CC, Hell JW. 1998. SAP97 is associated with the alpha-amino-3-hydroxy-5-methylisoxazole-4-propionic acid receptor GluR1 subunit. *J Biol Chem* 273: 19518-24

Leonard AS, Lim IA, Hemsworth DE, Horne MC, Hell JW. 1999. Calcium/calmodulin-dependent protein kinase II is associated with the N-methyl-D-aspartate receptor. *Proc Natl Acad Sci U S A* 96: 3239-44

Lesept F, Chevilley A, Jezequel J, Ladepeche L, Macrez R, et al. 2016. Tissue-type plasminogen activator controls neuronal death by raising surface dynamics of extrasynaptic NMDA receptors. *Cell Death Dis* 7: e2466

Lewis DA, Hashimoto T, Morris HM. 2008. Cell and receptor type-specific alterations in markers of GABA neurotransmission in the prefrontal cortex of subjects with schizophrenia. *Neurotox Res* 14: 237-48

Lewis DA, Pierri JN, Volk DW, Melchitzky DS, Woo TU. 1999. Altered GABA neurotransmission and prefrontal cortical dysfunction in schizophrenia. *Biol Psychiatry* 46: 616-26

Li B, Tadross MR, Tsien RW. 2016a. Sequential ionic and conformational signaling by calcium channels drives neuronal gene expression. *Science* 351: 863-7

Li JT, Su YA, Guo CM, Feng Y, Yang Y, et al. 2011. Persisting cognitive deficits induced by low-dose, subchronic treatment with MK-801 in adolescent rats. *Eur J Pharmacol* 652: 65-72

Li LJ, Hu R, Lujan B, Chen J, Zhang JJ, et al. 2016b. Glycine Potentiates AMPA Receptor Function through Metabotropic Activation of GluN2A-Containing NMDA Receptors. *Front Mol Neurosci* 9: 102

Li LL, Ginet V, Liu X, Vergun O, Tuittila M, et al. 2013. The nNOS-p38MAPK pathway is mediated by NOS1AP during neuronal death. *J Neurosci* 33: 8185-201

Li W, Ma L, Yang G, Gan WB. 2017. REM sleep selectively prunes and maintains new synapses in development and learning. *Nat Neurosci* 20: 427-37

Lieberman JA, Girgis RR, Brucato G, Moore H, Provenzano F, et al. 2018. Hippocampal dysfunction in the pathophysiology of schizophrenia: a selective review and hypothesis for early detection and intervention. *Mol Psychiatry* 23: 1764-72

Lin H, Jacobi AA, Anderson SA, Lynch DR. 2016. D-Serine and Serine Racemase Are Associated with PSD-95 and Glutamatergic Synapse Stability. *Front Cell Neurosci* 10: 34

Lorrain DS, Baccei CS, Bristow LJ, Anderson JJ, Varney MA. 2003. Effects of ketamine and N-methyl-D-aspartate on glutamate and dopamine release in the rat prefrontal cortex: modulation by a group II selective metabotropic glutamate receptor agonist LY379268. *Neuroscience* 117: 697-706

Lu Y, Allen M, Halt AR, Weisenhaus M, Dallapiazza RF, et al. 2007. Age-dependent requirement of AKAP150-anchored PKA and GluR2-lacking AMPA receptors in LTP. *EMBO J* 26: 4879-90

Lu YF, Kandel ER, Hawkins RD. 1999. Nitric oxide signaling contributes to late-phase LTP and CREB phosphorylation in the hippocampus. *J Neurosci* 19: 10250-61

Ma TM, Paul BD, Fu C, Hu S, Zhu H, et al. 2014. Serine racemase regulated by binding to stargazin and PSD-95: potential N-methyl-D-aspartate-alpha-amino-3-hydroxy-5-methyl-4-isoxazolepropionic acid (NMDA-AMPA) glutamate neurotransmission cross-talk. *J Biol Chem* 289: 29631-41

Madeira C, Freitas ME, Vargas-Lopes C, Wolosker H, Panizzutti R. 2008. Increased brain D-amino acid oxidase (DAAO) activity in schizophrenia. *Schizophr Res* 101: 76-83

Matsuzaki M, Honkura N, Ellis-Davies GC, Kasai H. 2004. Structural basis of long-term potentiation in single dendritic spines. *Nature* 429: 761-6

Mehra A, Guerit S, Macrez R, Gosselet F, Sevin E, et al. 2020. Nonionotropic Action of Endothelial NMDA Receptors on Blood-Brain Barrier Permeability via Rho/ROCK-Mediated Phosphorylation of Myosin. *J Neurosci* 40: 1778-87

Mellios N, Huang HS, Baker SP, Galdzicka M, Ginns E, Akbarian S. 2009. Molecular determinants of dysregulated GABAergic gene expression in the prefrontal cortex of subjects with schizophrenia. *Biol Psychiatry* 65: 1006-14

Minnella AM, Zhao JX, Jiang X, Jakobsen E, Lu F, et al. 2018. Excitotoxic superoxide production and neuronal death require both ionotropic and non-ionotropic NMDA receptor signaling. *Sci Rep* 8: 17522

Montes de Oca Balderas P, Aguilera P. 2015. A Metabotropic-Like Flux-Independent NMDA Receptor Regulates Ca2+ Exit from Endoplasmic Reticulum and Mitochondrial Membrane Potential in Cultured Astrocytes. *PLoS One* 10: e0126314

Montes de Oca Balderas P, Matus Nunez M, Picones A, Hernandez-Cruz A. 2020. NMDAR in cultured astrocytes: Flux-independent pH sensor and flux-dependent regulator of mitochondria and plasma membrane-mitochondria bridging. *FASEB J* 34: 16622-44

Moyer CE, Shelton MA, Sweet RA. 2015. Dendritic spine alterations in schizophrenia. *Neurosci Lett* 601: 46-53

Murakoshi H, Shin ME, Parra-Bueno P, Szatmari EM, Shibata ACE, Yasuda R. 2017. Kinetics of Endogenous CaMKII Required for Synaptic Plasticity Revealed by Optogenetic Kinase Inhibitor. *Neuron* 94: 37-47 e5

Murakoshi H, Wang H, Yasuda R. 2011. Local, persistent activation of Rho GTPases during plasticity of single dendritic spines. *Nature* 472: 100-4

Mustafa AK, Ahmad AS, Zeynalov E, Gazi SK, Sikka G, et al. 2010. Serine racemase deletion protects against cerebral ischemia and excitotoxicity. *J Neurosci* 30: 1413-6

Nabavi S, Kessels HW, Alfonso S, Aow J, Fox R, Malinow R. 2013. Metabotropic NMDA receptor function is required for NMDA receptor-dependent long-term depression. *Proc Natl Acad Sci U S A* 110: 4027-32

Nakahata Y, Yasuda R. 2018. Plasticity of Spine Structure: Local Signaling, Translation and Cytoskeletal Reorganization. *Front Synaptic Neurosci* 10: 29

Newcomer JW, Farber NB, Jevtovic-Todorovic V, Selke G, Melson AK, et al. 1999. Ketamine-induced NMDA receptor hypofunction as a model of memory impairment and psychosis. *Neuropsychopharmacology* 20: 106-18

Nishiyama J, Yasuda R. 2015. Biochemical Computation for Spine Structural Plasticity. *Neuron* 87: 63-75

Nong Y, Huang YQ, Ju W, Kalia LV, Ahmadian G, et al. 2003. Glycine binding primes NMDA receptor internalization. *Nature* 422: 302-7

O'Dell TJ, Huang PL, Dawson TM, Dinerman JL, Snyder SH, et al. 1994. Endothelial NOS and the blockade of LTP by NOS inhibitors in mice lacking neuronal NOS. *Science* 265: 542-6

Oh WC, Hill TC, Zito K. 2013. Synapse-specific and size-dependent mechanisms of spine structural plasticity accompanying synaptic weakening. *Proc Natl Acad Sci U S A* 110: E305-12

Okamoto K, Nagai T, Miyawaki A, Hayashi Y. 2004. Rapid and persistent modulation of actin dynamics regulates postsynaptic reorganization underlying bidirectional plasticity. *Nature neuroscience* 7: 1104-12

Pantelis C, Velakoulis D, McGorry PD, Wood SJ, Suckling J, et al. 2003. Neuroanatomical abnormalities before and after onset of psychosis: a cross-sectional and longitudinal MRI comparison. *Lancet* 361: 281-8

Paoletti P, Bellone C, Zhou Q. 2013. NMDA receptor subunit diversity: impact on receptor properties, synaptic plasticity and disease. *Nat Rev Neurosci* 14: 383-400

Penzes P, Cahill ME, Jones KA, VanLeeuwen JE, Woolfrey KM. 2011. Dendritic spine pathology in neuropsychiatric disorders. *Nat Neurosci* 14: 285-93

Pi HJ, Otmakhov N, Lemelin D, De Koninck P, Lisman J. 2010. Autonomous CaMKII can promote either long-term potentiation or long-term depression, depending on the state of T305/T306 phosphorylation. *The Journal of neuroscience : the official journal of the Society for Neuroscience* 30: 8704-9

Pigott B, Bartus K, Garthwaite J. 2013. On the selectivity of neuronal NOS inhibitors. *Br J Pharmacol* 168: 1255-65

Plitman E, Iwata Y, Caravaggio F, Nakajima S, Chung JK, et al. 2017. Kynurenic Acid in Schizophrenia: A Systematic Review and Meta-analysis. *Schizophr Bull* 43: 764-77

Ploux E, Bouet V, Radzishevsky I, Wolosker H, Freret T, Billard JM. 2020. Serine Racemase Deletion Affects the Excitatory/Inhibitory Balance of the Hippocampal CA1 Network. *Int J Mol Sci* 21

Pologruto TA, Sabatini BL, Svoboda K. 2003. ScanImage: flexible software for operating laser scanning microscopes. *Biomed Eng Online* 2: 13

Privitera L, Hogg EL, Gaestel M, Wall MJ, Correa SAL. 2019. The MK2 cascade regulates mGluR-dependent synaptic plasticity and reversal learning. *Neuropharmacology* 155: 121-30

Puhl MD, Mintzopoulos D, Jensen JE, Gillis TE, Konopaske GT, et al. 2015. In vivo magnetic resonance studies reveal neuroanatomical and neurochemical abnormalities in the serine racemase knockout mouse model of schizophrenia. *Neurobiol Dis* 73: 269-74

Reif DW, McCreedy SA. 1995. N-nitro-L-arginine and N-monomethyl-L-arginine exhibit a different pattern of inactivation toward the three nitric oxide synthases. *Arch Biochem Biophys* 320: 170-6

Roeske MJ, Konradi C, Heckers S, Lewis AS. 2020. Hippocampal volume and hippocampal neuron density, number and size in schizophrenia: a systematic review and meta-analysis of postmortem studies. *Mol Psychiatry*

Rosoklija G, Toomayan G, Ellis SP, Keilp J, Mann JJ, et al. 2000. Structural abnormalities of subicular dendrites in subjects with schizophrenia and mood disorders: preliminary findings. *Arch Gen Psychiatry* 57: 349-56

Salter MW, Pitcher GM. 2012. Dysregulated Src upregulation of NMDA receptor activity: a common link in chronic pain and schizophrenia. *FEBS J* 279: 2-11

Sanderson JL, Gorski JA, Dell'Acqua ML. 2016. NMDA Receptor-Dependent LTD Requires Transient Synaptic Incorporation of Ca(2)(+)-Permeable AMPARs Mediated by AKAP150-Anchored PKA and Calcineurin. *Neuron* 89: 1000-15

Saneyoshi T, Matsuno H, Suzuki A, Murakoshi H, Hedrick NG, et al. 2019. Reciprocal Activation within a Kinase-Effector Complex Underlying Persistence of Structural LTP. *Neuron* 102: 1199-210 e6

Sanhueza M, Fernandez-Villalobos G, Stein IS, Kasumova G, Zhang P, et al. 2011. Role of the CaMKII/NMDA receptor complex in the maintenance of synaptic strength. *The Journal of neuroscience : the official journal of the Society for Neuroscience* 31: 9170-8

Schobel SA, Chaudhury NH, Khan UA, Paniagua B, Styner MA, et al. 2013. Imaging patients with psychosis and a mouse model establishes a spreading pattern of hippocampal dysfunction and implicates glutamate as a driver. *Neuron* 78: 81-93

Servili E, Trus M, Maayan D, Atlas D. 2018. beta-Subunit of the voltage-gated Ca(2+) channel Cav1.2 drives signaling to the nucleus via H-Ras. *Proc Natl Acad Sci U S A* 115: E8624-E33

Sheardown MJ, Nielsen EO, Hansen AJ, Jacobsen P, Honore T. 1990. 2,3-Dihydroxy-6-nitro-7-sulfamoyl-benzo(F)quinoxaline: a neuroprotectant for cerebral ischemia. *Science* 247: 571-4

Singh SP, Singh V. 2011. Meta-analysis of the efficacy of adjunctive NMDA receptor modulators in chronic schizophrenia. *CNS Drugs* 25: 859-85

Stein IS, Gray JA, Zito K. 2015. Non-Ionotropic NMDA Receptor Signaling Drives Activity-Induced Dendritic Spine Shrinkage. *J Neurosci* 35: 12303-8

Stein IS, Park DK, Claiborne N, Zito K. 2021. Non-ionotropic NMDA receptor signaling gates bidirectional structural plasticity of dendritic spines. *Cell Rep* 34: 108664

Stein IS, Park DK, Flores JC, Jahncke JN, Zito K. 2020. Molecular Mechanisms of Non-ionotropic NMDA Receptor Signaling in Dendritic Spine Shrinkage. *J Neurosci* 40: 3741-50

Stein IS, Zito K. 2019. Dendritic Spine Elimination: Molecular Mechanisms and Implications. *Neuroscientist* 25: 27-47

Steullet P, Cabungcal JH, Coyle J, Didriksen M, Gill K, et al. 2017. Oxidative stress-driven parvalbumin interneuron impairment as a common mechanism in models of schizophrenia. *Mol Psychiatry* 22: 936-43

Stoppini L, Buchs PA, Muller D. 1991. A simple method for organotypic cultures of nervous tissue. *Journal of neuroscience methods* 37: 173-82

Sun W, Wong JM, Gray JA, Carter BC. 2018. Incomplete block of NMDA receptors by intracellular MK-801. *Neuropharmacology* 143: 122-29

Svane KC, Asis EK, Omelchenko A, Kunnath AJ, Brzustowicz LM, et al. 2018. d-Serine administration affects nitric oxide synthase 1 adaptor protein and DISC1 expression in sex-specific manner. *Mol Cell Neurosci* 89: 20-32

Sweet RA, Henteleff RA, Zhang W, Sampson AR, Lewis DA. 2009. Reduced dendritic spine density in auditory cortex of subjects with schizophrenia. *Neuropsychopharmacology* 34: 374-89

Takayanagi Y, Takahashi T, Orikabe L, Mozue Y, Kawasaki Y, et al. 2011. Classification of first-episode schizophrenia patients and healthy subjects by automated MRI measures of regional brain volume and cortical thickness. *PLoS One* 6: e21047

Tamburri A, Dudilot A, Licea S, Bourgeois C, Boehm J. 2013. NMDA-receptor activation but not ion flux is required for amyloid-beta induced synaptic depression. *PLoS One* 8: e65350

Thomazeau A, Bosch M, Essayan-Perez S, Barnes SA, De Jesus-Cortes H, Bear MF. 2020. Dissociation of functional and structural plasticity of dendritic spines during NMDAR and mGluR-dependent long-term synaptic depression in wild-type and fragile X model mice. *Mol Psychiatry*

Thompson PM, Vidal C, Giedd JN, Gochman P, Blumenthal J, et al. 2001. Mapping adolescent brain change reveals dynamic wave of accelerated gray matter loss in very early-onset schizophrenia. *Proc Natl Acad Sci U S A* 98: 11650-5

Tokumitsu H, Chijiwa T, Hagiwara M, Mizutani A, Terasawa M, Hidaka H. 1990. KN-62, 1-[N,O-bis(5-isoquinolinesulfonyl)-N-methyl-L-tyrosyl]-4-phenylpiperazi ne, a specific inhibitor of Ca2+/calmodulin-dependent protein kinase II. *J Biol Chem* 265: 4315-20

Trachtenberg JT, Chen BE, Knott GW, Feng G, Sanes JR, et al. 2002. Long-term in vivo imaging of experience-dependent synaptic plasticity in adult cortex. *Nature* 420: 788-94

Tsai G, Yang P, Chung LC, Lange N, Coyle JT. 1998. D-serine added to antipsychotics for the treatment of schizophrenia. *Biol Psychiatry* 44: 1081-9

Ultanir SK, Kim JE, Hall BJ, Deerinck T, Ellisman M, Ghosh A. 2007. Regulation of spine morphology and spine density by NMDA receptor signaling in vivo. *Proc Natl Acad Sci U S A* 104: 19553-8

van Elst LT, Valerius G, Buchert M, Thiel T, Rusch N, et al. 2005. Increased prefrontal and hippocampal glutamate concentration in schizophrenia: evidence from a magnetic resonance spectroscopy study. *Biol Psychiatry* 58: 724-30

van Erp TG, Hibar DP, Rasmussen JM, Glahn DC, Pearlson GD, et al. 2016. Subcortical brain volume abnormalities in 2028 individuals with schizophrenia and 2540 healthy controls via the ENIGMA consortium. *Mol Psychiatry* 21: 585

van Haren NE, Hulshoff Pol HE, Schnack HG, Cahn W, Brans R, et al. 2008. Progressive brain volume loss in schizophrenia over the course of the illness: evidence of maturational abnormalities in early adulthood. *Biol Psychiatry* 63: 106-13

Verrall L, Walker M, Rawlings N, Benzel I, Kew JN, et al. 2007. d-Amino acid oxidase and serine racemase in human brain: normal distribution and altered expression in schizophrenia. *Eur J Neurosci* 26: 1657-69

Vest RS, Davies KD, O'Leary H, Port JD, Bayer KU. 2007. Dual mechanism of a natural CaMKII inhibitor. *Mol Biol Cell* 18: 5024-33

Vissel B, Krupp JJ, Heinemann SF, Westbrook GL. 2001. A use-dependent tyrosine dephosphorylation of NMDA receptors is independent of ion flux. *Nat Neurosci* 4: 587-96

Volianskis A, France G, Jensen MS, Bortolotto ZA, Jane DE, Collingridge GL. 2015. Long-term potentiation and the role of N-methyl-D-aspartate receptors. *Brain Res* 1621: 5-16

Wang Y, Small DL, Stanimirovic DB, Morley P, Durkin JP. 1997. AMPA receptor-mediated regulation of a Gi-protein in cortical neurons. *Nature* 389: 502-4

Weilinger NL, Lohman AW, Rakai BD, Ma EM, Bialecki J, et al. 2016. Metabotropic NMDA receptor signaling couples Src family kinases to pannexin-1 during excitotoxicity. *Nat Neurosci* 19: 432-42

Wong JM, Folorunso OO, Barragan EV, Berciu C, Harvey TL, et al. 2020. Postsynaptic Serine Racemase Regulates NMDA Receptor Function. *J Neurosci* 40: 9564-75

Wong JM, Gray JA. 2018. Long-Term Depression Is Independent of GluN2 Subunit Composition. *J Neurosci* 38: 4462-70

Woods G, Zito K. 2008. Preparation of gene gun bullets and biolistic transfection of neurons in slice culture. *Journal of visualized experiments : JoVE*

Woods GF, Oh WC, Boudewyn LC, Mikula SK, Zito K. 2011. Loss of PSD-95 enrichment is not a prerequisite for spine retraction. *J Neurosci* 31: 12129-38

Woolfrey KM, O'Leary H, Goodell DJ, Robertson HR, Horne EA, et al. 2018. CaMKII regulates the depalmitoylation and synaptic removal of the scaffold protein AKAP79/150 to mediate structural long-term depression. *J Biol Chem* 293: 1551-67

Wu H, Wang X, Gao Y, Lin F, Song T, et al. 2016. NMDA receptor antagonism by repetitive MK801 administration induces schizophrenia-like structural changes in the rat brain as revealed by voxel-based morphometry and diffusion tensor imaging. *Neuroscience* 322: 221-33

Xu T, Yu X, Perlik AJ, Tobin WF, Zweig JA, et al. 2009. Rapid formation and selective stabilization of synapses for enduring motor memories. *Nature* 462: 915-9

Yang G, Pan F, Gan WB. 2009. Stably maintained dendritic spines are associated with lifelong memories. *Nature* 462: 920-4

Yasuda R, Sabatini BL, Svoboda K. 2003. Plasticity of calcium channels in dendritic spines. *Nature neuroscience* 6: 948-55

Zhang L, Zhang P, Wang G, Zhang H, Zhang Y, et al. 2018. Ras and Rap Signal Bidirectional Synaptic Plasticity via Distinct Subcellular Microdomains. *Neuron* 98: 783-800 e4

Zhang W, Deng W, Yao L, Xiao Y, Li F, et al. 2015. Brain Structural Abnormalities in a Group of Never-Medicated Patients With Long-Term Schizophrenia. *Am J Psychiatry* 172: 995-1003

Zhang ZJ, Reynolds GP. 2002. A selective decrease in the relative density of parvalbumin-immunoreactive neurons in the hippocampus in schizophrenia. *Schizophr Res* 55: 1-10

Zhou Q, Homma KJ, Poo MM. 2004. Shrinkage of dendritic spines associated with long-term depression of hippocampal synapses. *Neuron* 44: 749-57

Zhu JJ, Qin Y, Zhao M, Van Aelst L, Malinow R. 2002. Ras and Rap control AMPA receptor trafficking during synaptic plasticity. *Cell* 110: 443-55

Zhu LJ, Li TY, Luo CX, Jiang N, Chang L, et al. 2014. CAPON-nNOS coupling can serve as a target for developing new anxiolytics. *Nat Med* 20: 1050-4